Dissertation

submitted to the
Combined Faculties for the Natural Sciences and for Mathematics
of the Ruperto-Carola University of Heidelberg, Germany
for the degree of
Doctor of Natural Sciences

Presented by

Camille Lowy, M. Sc. Biology
Born in Vénissieux (France)
Oral examination: 09.12.2016

Tenascin C interacts with integrin receptors to promote breast cancer metastasis to the lungs.

Referees: Prof. Dr. Andreas Trumpp
Prof. Dr. Jonathan Sleeman

The work presented in this thesis was performed from July 2012 until October 2016 in the junior research group ‘Metastatic Niches’ at the German Cancer Research Center (DKFZ), Heidelberg as well as in the Heidelberg Institute for Stem Cell Research and Experimental Medicine (HI-STEM) under the supervision of Dr. Thordur Oskarsson.

To Thomas,
for his faith, his patience and his love,
because he always understood.

Table of Contents

1 Summary

To date, despite significant advances in early detection and treatment of breast cancer, metastatic progression remains a major cause of morbidity and mortality in breast cancer patients. Importantly, patient stratification according to biomarker expression has led to continuous improvement of therapeutic strategies and better understanding of the diseases. However, the aggressive triple-negative subtype of breast cancer is still lacking effective therapeutic options.

The important role of the tumor microenvironment in the formation of metastasis is well recognized. The extracellular matrix glycoprotein tenascin-C (TNC) has been previously described as a functional player of the metastatic niche, supporting the growth of breast cancer cells at the distant site. In this study, we investigated the clinical prognostic value of TNC in breast cancer patient cohorts. We found that TNC predicts poor clinical outcome only in the triple-negative subtype and that these tumors are enriched for TNC expression. Interestingly, while other subtypes rely on the stromal compartment as a source of TNC, triple-negative tumors express TNC in an autocrine manner. In addition, we confirmed that TNC promotes the growth of triple-negative breast cancer cells in the lungs *in vivo*. Therefore, we suggest that triple-negative breast tumors benefit from high, autocrine TNC expression to promote metastasis.

Several cell surface receptors have been suggested to interact with TNC. However, the receptor(s) mediating the pro-metastatic signaling downstream of TNC remained unclear. We identified two integrin receptor subunits, integrin beta 1 (ITGB1) and integrin beta 3 (ITGB3), as TNC receptors. We demonstrated the binding of these molecules to TNC in an endogenous setting and showed that ITGB1 and ITGB3 support the growth of breast cancer cells in the lungs *in vivo*. Furthermore, we observed that the expression of these receptors, similar to TNC, is enriched in the triple-negative subtype. Using a large patient cohort, we showed that the prognostic value of TNC depends on the expression of the identified receptors, underscoring the clinical relevance of our findings. Importantly, ITGB1 and ITGB3 are supporting stem cell properties in triple-negative breast cancer cells.

We found that the TNC knockout phenotype was associated with a decrease in stem cell properties of the normal mammary gland epithelium. In addition, we showed that TNC signaling members are upregulated during stages of the mammary gland development and maturation associated with expansion of the stem cell compartment. More importantly, TNC knockout mice showed an impairment in the formation of alveolar structures during pregnancy. All in all, our data strongly suggest a functional role of the TNC signaling in mammary stem cell biology.

Summary

In this study, we identified two integrin receptors of the mammary gland (ITGB1 and ITGB3) as the receptors mediating the TNC pro-metastatic signaling in triple-negative breast cancer. Furthermore, we showed that TNC supports stem cell properties in the mammary gland. Therefore, we propose that the TNC signaling might play an important role in the mammary stem cell to support its activity and that triple-negative breast cancer cells benefit from high expression of TNC and its receptors to promote metastatic growth in this subtype. Deeper understanding of the mammary stem cell biology might support the development of targeted therapy for triple-negative breast cancer patients.

2 Zusammenfassung

Trotz erheblicher Fortschritte bei der frühen Diagnose und Behandlung von Brustkrebs bleibt die Metastasierung bis heute eine wichtige Ursache für Morbidität und Mortalität bei Patienten mit Brustkrebs. Insbesondere die Stratifizierung von Patienten anhand von Biomarkern hat zu einer kontinuierlichen Anpassung der therapeutischen Strategien sowie zu einem verbesserten Verständnis der Krankheiten geführt. Für den aggressiven triple-negativen Subtyp fehlen jedoch bis heute effektive Therapieoptionen.

Die wichtige Rolle der Mikroumgebung eines Tumors bei der Bildung von Metastasen ist allgemein anerkannt. Das Glykoprotein Tenascin-C (TNC) der extrazellulären Matrix wurde in der Literatur als funktioneller Bestandteil der metastatischen Nische beschrieben, der das Wachstum der Mammakarzinomzellen an entfernten Orten im Körper unterstützt. In der vorliegenden Studie wurde der Wert von TNC für die klinische Prognose anhand von Mammakarzinom-Patientenkohorten untersucht. Dabei zeigte sich, dass TNC ausschließlich im triple-negativen Mammakarzinom ein Prädiktor für eine schlechte klinische Prognose darstellt und dass diese Tumore für TNC Expression angereichert ist. Interessanterweise konnten wir nachweisen, dass diese Tumoren TNC in autokriner Weise exprimieren, während andere Subtypen auf die stromale Komponente als Quelle für TNC zurückgreifen. Weiterhin ließ sich im *in vivo*-Modell bestätigen, dass TNC das Wachstum der triple-negativen Brustkrebszellen in der Lunge fördert. Daher schlagen wir vor, dass triple-negative Tumoren der Brust eine erhöhte autokrine Expression von TNC für eine verstärkte Metastasierung nutzen.

Verschiedene Zelloberflächenrezeptoren wurden als Interaktionspartner von TNC vorgeschlagen. Welche Rezeptoren jedoch das TNC nachgelagerte pro-metastatische Signaling vermitteln, blieb bislang unklar. Mit Integrin-beta-1 (ITGB1) und Integrin-beta-3 (ITGB3) konnten wir zwei neue Integrinrezeptor-Untereinheiten identifizieren, die als TNC-Rezeptoren dienen. Wir zeigten die Bindung dieser Moleküle an TNC innerhalb eines endogenen Modells und konnten im *in vivo*-Modell nachweisen, dass ITGB1 und ITGB3 das Wachstum der Mammakarzinomzellen in der Lunge fördern. Weiterhin beobachteten wir, dass die Expression dieser Rezeptoren, ähnlich wie im Fall von TNC, im triple-negativen Subtyp angereichert ist. Unter Verwendung einer großen Patientenkohorte zeigten wir, dass der prognostische Wert von TNC von der Expression der identifizierten Rezeptoren abhängt, so dass diese Beobachtungen auch klinisch relevant sind. Darüber hinaus vermitteln ITGB1 und ITGB3 Stammzelleigenschaften in triple-negativen Mammakarzinomzellen.

Wir beobachteten, dass der TNC-Knockout-Phänotyp mit einem Rückgang der Stammzelleigenschaften des Brustdrüsenepithels einhergeht. Zudem konnten wir zeigen, dass die Proteine des TNC-Signalweges während Phasen der Brustdrüsenentwicklung, die mit einer Erweiterung des Stammzellkompartimentes assoziiert sind, hochreguliert werden. Darüber hinaus zeigten die Knockout-Mäuse eine beeinträchtigte Ausbildung der alveolären Strukturen

während der Schwangerschaft. In der Gesamtheit legen diese Daten nahe, dass das TNC-Signaweg funktionelle Bedeutung für die Stammzellbiologie der Brust besitzt.

In dieser Studie identifizierten wir zwei Integrin Rezeptoren der Brustdrüse (ITGB1 und ITGB3) als diejenigen Rezeptoren, die das pro-metastatische TNC-Signalweg im triple-negativen Mammakarzinom vermitteln. Weiterhin konnten wir zeigen, dass TNC Stammzellfunktionen in der Brustdrüse unterstützt. Aus diesem Grund schlagen wir vor, dass das TNC-Signalweg in Bruststammzellen deren Aktivität fördert, und dass triple-negative Mammakarzinomzellen die hohen Expressionslevel von TNC und seinen Rezeptoren nutzen, um ihr Wachstum abseits des Primärtumors voranzutreiben. Ein tiefergehendes Verständnis der Stammzellbiologie der Brust könnte die Entwicklung einer zielgerichteten Therapie für Patienten mit triple-negativem Mammakarzinom weiter fördern.

3 Introduction

3.1 Breast Cancer

3.1.1 Epidemiology

In 2016, breast cancer was the most commonly diagnosed cancer among women and the second cause of cancer-related death in the United States (US) [1]. Malignancies of the breast originate in the milk-producing glands called lobes or, more commonly, in the ducts which connect the lobes to the nipple. The normal mammary ducts are tube-like epithelial structures formed by an inner layer of cuboidal luminal cells and an outer layer of basal cells, also called myoepithelial cells. The ducts are separated from the underlying stroma by a basement membrane composed of extracellular matrix (ECM) proteins. When the tumor does not grow beyond the layer of cells where it originated, breast carcinoma is referred to as '*in situ*' or '*ductal carcinoma in situ*' (DCIS). However in most cases, the tumor cells break the basement membrane and infiltrate the surrounding fatty, connective and lymphatic tissues. In that case, breast carcinoma is termed '*invasive carcinoma*'. If the tumor cells leave the breast tissue and spread throughout the body to distant organs, breast cancer is referred to as '*metastatic carcinoma*' **(Figure 1)**. In 2015, 292,130 new cases of breast cancer were diagnosed in the US, among which 80% were invasive or metastatic [2].

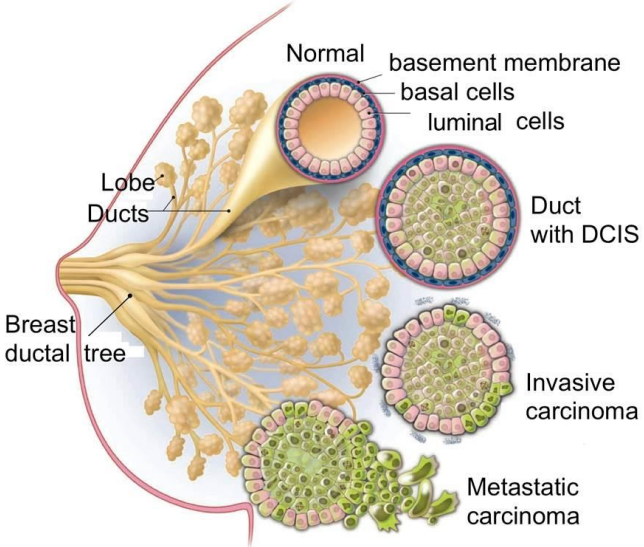

Figure 1 Anatomy of the breast and associated malignancies.

The female breast is composed of 15 – 20 ducts, which begin at the nipple, branch into smaller ducts and end in the terminal milk-producing units called lobes. Breast cancer malignancies typically arise in the ducts and can be categorized as 'in situ', 'invasive' or 'metastatic' depending on the degree of invasion of the surrounding healthy tissue. Figure was adapted from from www.caperay.com.

3.1.2 Staging

The clinical prognosis of invasive breast cancer strongly depends on the extent of the disease at the time of diagnosis. Clinicians routinely describe the spread of breast cancer using the TNM staging system of the American Joint Committee on Cancer (AJCC). In this system, three parameters are assessed and described with the letters 'T', 'N' and 'M':

- 'T' describes the size of the tumor and whether it has invaded nearby tissues or not;
- 'N' indicates the degree of spread to the regional lymph nodes;
- 'M' corresponds to the presence or the absence of distant metastasis [2, 3].

The TNM staging is then expanded by the assignment of a roman number ranging from 0 to IV. Briefly, the stages 0, I and some stage II breast cancer refer to *in situ* carcinomas, while tumors that have spread to surrounding tissues or nearby lymph nodes generally correspond to stage II and III. The last stage of the system, stage IV, is the distant stage referring to breast cancers that have spread to distant organs [2, 3]. The prognostic value of the TNM classification is well recognized: In most of the cases, lower stages of breast cancer are associated with longer patient survival, while the 5-year survival rate decreases in higher stages. Importantly, the stage IV of the disease represents a threshold in term of patient survival. Indeed, according to the National Cancer Institute's surveillance, epidemiology and end results (SEER) database, the 5-year relative survival rate dramatically drops from 72% when a patient is diagnosed at stage III to 22% when the disease has already reached stage IV [4] **(Figure 2)**.

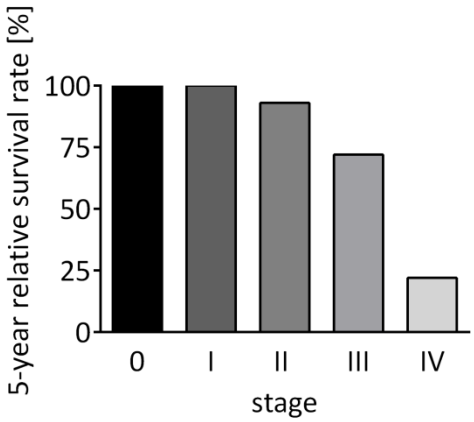

Figure 2 Female breast cancer relative 5-year survival according to stage.
The 5-year survival rate of stage 0, I and II are close to 100% and slightly decreases to 72% in stage III. Stage IV of breast cancer corresponds to a 5-year survival rate of only 22%. The rates are based on patients diagnosed between 2006 and 2012 in the US according to the National Cancer Institute's SEER database [4].

It has been recognized for a long time that breast cancer cannot be managed as a single disease. In fact, breast cancer is rather a collection of malignancies arising in the same tissue but differing greatly in term of biology, response to treatment and outcome. To date, there are mainly two classification systems for breast cancer patients. The first classification system is a routine clinical procedure based the expression of biomarkers. Importantly, biomarker-based stratification of breast cancer patients is used to determine therapeutic options and treatment plans. The second classification system arose with the development of microarray techniques and uses global gene expression profiling to stratify breast cancer patients into so called 'intrinsic subtypes'.

3.1.3 Stratification according to biomarkers

Upon clinical diagnosis of invasive breast cancer, patients are typically stratified based on four different subtypes. This classification is highly important as it has both a prognostic value and it determines treatment options. Currently, three biomarkers are routinely used for stratification of breast cancer patients. Those are, on one hand, the presence or absence of the hormone receptors (HR) for estrogen and progesterone (ER and PR) and, on the other hand, excess levels of the growth-promoting human epidermal growth factor receptor 2 (HER2). Typically, the scoring of the three membrane proteins is performed on paraffin-embedded needle-biopsies or surgical tissue samples stained by immunohistochemistry (IHC). However, receptor status can also be determined by gene expression quantification based on microarrays in a reliable

manner [5, 6]. In addition to the HR and HER2, the proliferation marker Ki-67 is used to refine the classification. Ki67 is strictly associated with proliferating cells as it is expressed during the all active phases of cell cycle (G_1, S, G_2 and mitosis) but it absent in quiescent cells (G_0) [7]. Scoring of the described biomarkers (ER, PR, HER2 and Ki67) results in four clinical subtypes of breast cancer, which are termed luminal A, luminal B, HER2-enriched and triple-negative. The luminal subtypes are characterized by expression of the ER and/or PR biomarkers and are therefore described as 'HR positive'. The two luminal subtypes differ in Ki-67 expression and/or HER2 levels. More precisely, tumors which are positive for HR, negative for HER2 and with a low Ki-67 score are classified as luminal A, while the luminal B subtype is also positive for HR but displays either a high Ki-67 score or an enrichment in HER2 expression. Breast cancer tumors showing negative staining for HR and abnormal expression of HER2 are classified into a third subtype, termed 'HER2-enriched'. Finally, the last subtype is characterized by negativity for all three marker receptors (ER, PR and HER2) and is therefore called 'triple-negative' **(Table 1)** [8].

Table 1 Clinical subtypes of breast cancer.
Breast cancer patients are stratified into four clinical subtypes according to HR presence or absence, expression level of HER2 and Ki-67 score. Table was adapted from [8].

Clinical subtype	Biomarker expression
Luminal A	HR positive HER2 negative Ki-67 low
Luminal B	HR positive Ki-67 high or HER2 enrichment
HER2-enriched	HR negative HER2 enrichment
Triple-negative	HR negative HER2 negative

3.1.4 Stratification according to gene expression profiling

In the last two decades, human breast cancer has been as well analyzed by gene expression profiling and hierarchical clustering regardless of disease stage or biomarker expression. In 2000, Perou *et al.* used DNA microarray to characterize variations in global gene expression patterns in 65 frozen surgical samples from 42 breast cancer patients [9]. Unsupervised clustering analysis revealed the existence of different subtypes termed 'intrinsic subtypes'. The adjective 'intrinsic' refers to the fact that the model is built on genes showing minimal variations within a tumor sample but maximal variations between different patients. The

identified subtypes were refined and validated in further patient cohorts and more recently this classification has been validated by the Cancer Genome Atlas Network [10-12]. Four major clusters were consistently described and named after their major characteristics. The luminal subtypes (A and B) are characterized by an enrichment in genes typically expressed by normal luminal epithelial cells of the mammary gland and genes associated with the ER signaling. Compared to the luminal A subtype, the luminal B subtype shows lower ER levels but higher expression of proliferation-associated genes. The basal-like subtype resembles the second epithelial lineage of the breast, the basal epithelial cells, and does not express genes associated with the luminal lineage. The HER2-enriched subtype is characterized by high expression level of a subset of genes which are associated with overexpression of the *HER2* oncogene and the absence of almost all genes associated with ER expression [9, 13]. Subsequent studies have revealed heterogeneity within the subtypes themselves. Particularly basal-like breast cancer is likely to represent different molecular tumor types rather than a single phenotype [14]. In 2007, a novel intrinsic subtype was described both in human and murine breast tumor data sets [15]. This group of tumors is characterized by low gene expression of the tight junction proteins claudin 3, 4 and 7 as well as E-cadherin, a calcium dependent cell-cell adhesion glycoprotein. Therefore, it was termed 'claudin-low'. Subsequently, the claudin-low subtype was shown to be characterized by strong epithelial-to-mesenchymal transition (EMT), high tumor initiation capacity and enrichment in stem cell characteristics [16-19].

3.1.5 Concordance between biomarker-based stratification and intrinsic subtypes

Importantly, the classification according to intrinsic subtypes not only provides comprehensive biological understanding of breast cancer but it also revealed critical differences in term of clinical parameters such as incidence, survival and response to treatment [9, 10, 17, 20-27]. Therefore, the question of concordance between the routinely used biomarker-based stratification and the newly defined intrinsic subtypes rapidly arose.

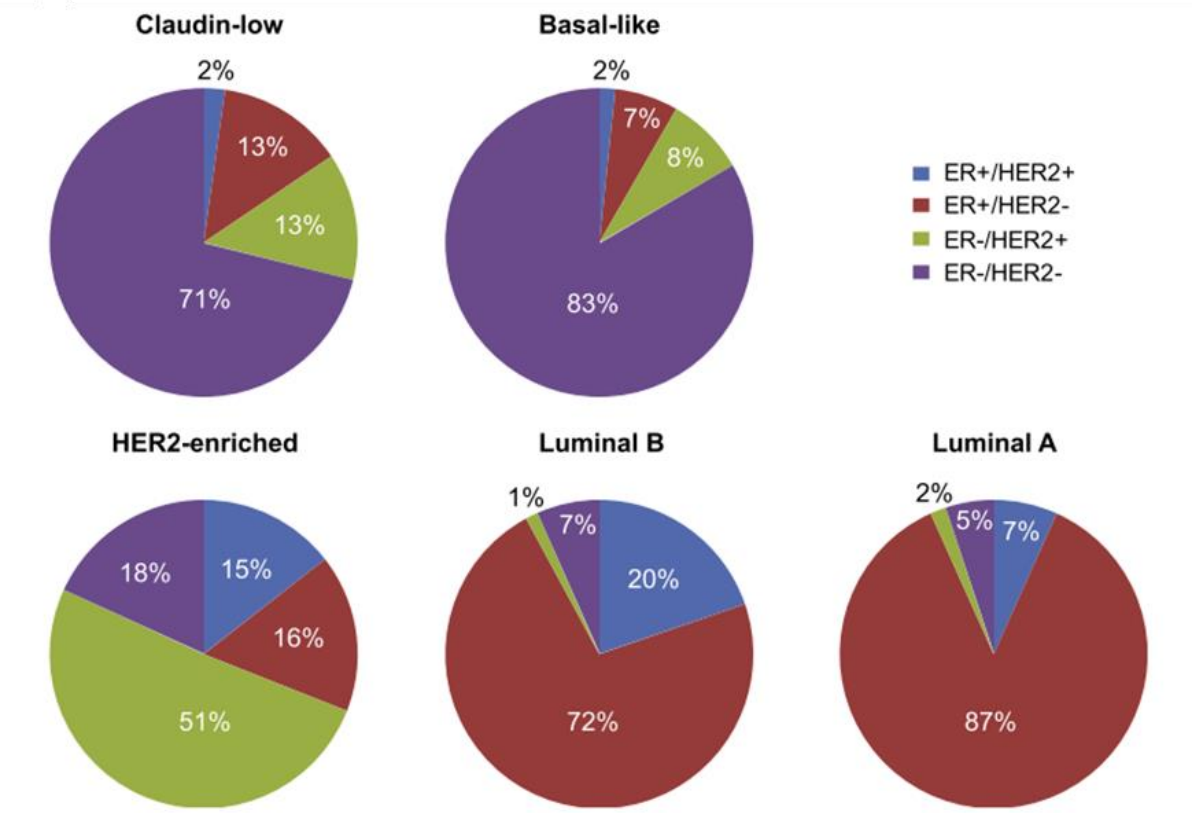

Figure 3 Distribution of the clinical subtypes of breast cancer within each intrinsic subtype. 71% and 83% of claudin-low and basal-like tumors, respectively, are negative for expression of ER and HER2. In tumors classified as HER2-enriched according to the intrinsic subtypes, 66% display an enrichment for the HER2 biomarker. 92% of tumors classified as luminal B are positive for ER biomarker expression, with or without overexpression of HER2. Finally, 87% of luminal A tumors are positive for ER biomarker expression and negative for HER2. Figure was adapted from [28].

The distribution of the intrinsic subtypes according to the biomarkers ER, PR and HER2 revealed a broad overlap between the different classification strategies. As an example, 87% of the luminal A intrinsic subtype is positive for ER and negative for HER2 enrichment. The majority of the HER2-enriched intrinsic subtype scores positive for HER2 overexpression by biomarker analysis, although the correlation is not 100%. Regarding the basal-like subtype, 83% is negative for both ER and HER2. Therefore, despite transcriptomic and histological differences between the two groups and although the terms ‘triple-negative’ and ‘basal-like’ cannot be used in an interchangeable manner, there is assuredly a strong overlap between the basal-like intrinsic subtype and the triple-negative phenotype. To date, the claudin-low intrinsic subtype is not considered in the biomarker-based clinical stratification of breast cancer patients. However, it is remarkable that 71% of the claudin-low subtype is negative for both ER expression and HER2 overexpression [28-30] **(Figure 3)**.

3.1.6 The PAM50 stratification

In order to improve the concordance between laboratories and to increase the clinical feasibility of intrinsic classification, a standardized gene set for intrinsic classification was designed. The PAM50 assay uses a 50-gene set to stratify patients according to the intrinsic subtypes [25, 31]. Expression of the defined genes can be assessed on RNA isolated from formalin-fixed, paraffin embedded tissue, which are more commonly available than frozen tissue. A satisfying concordance with the original intrinsic subtypes and between laboratories has been established for the PAM50 assay [32]. Importantly PAM50 has shown potential for treatment prediction and general prognostic according to subtype [25]. Therefore, the use of the PAM50 gene expression signature is implemented in certain pathological institutes in the form of the Prosigna assay, a multiplexed gene expression profiling method, which has been approved by the US Food and Drug Administration (FDA). Prosigma is based on the NanoString Technolgy, which allows direct quantification of mRNA transcripts [33].

3.1.7 Clinical prognosis and prevalence of the intrinsic breast cancer subtypes

Stratification of breast cancer patients according to the intrinsic subtypes allows efficient prediction of relapse and survival rates. Although the luminal A subtype is the most frequent subtype (prevalence ~ 28-31%), the patients show the best relapse-free and overall survival with 80-90% of the patients surviving the first 120 months without relapsing. The claudin-low, basal-like and HER2-enriched subtypes are less frequent (prevalence ~ 7-14%, ~ 14-23% and ~ 12-17%, respectively) but the relapse-free and overall survival rate are dramatically diminished compared to the luminal A subtype. Accordingly, 50% of the basal-like and claudin-low patients will relapse after 50 and 75 months, respectively. Even more dramatic, 50% of the basal-like and claudin-low patients will not survive the first 50 and 95 months, respectively. The patients belonging to the luminal B subtype (prevalence ~ 19-23%) have a slightly better overall survival prognosis with 50% of them surviving the first 150 months [28] **(Figure 4)**. In sum, patients belonging to the luminal A subtype are have an overall good clinical prognosis, while the basal-like, claudin-low and HER2-enriched subtypes are characterized by shorter relapse-free and overall survival rates.

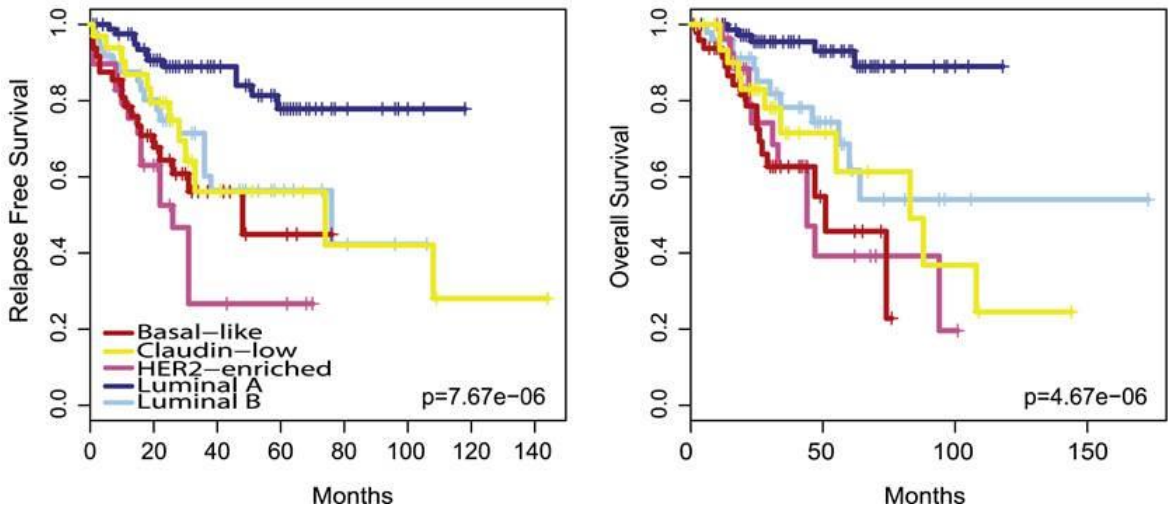

Figure 4 Kaplan-Meier analysis of relapse-free and overall survival of breast cancer patients. The patients were stratified according to the intrinsic subtypes (basal-like, claudin-low, HER2 enriched and luminal A and B) in the UNC337 dataset (*n* = 320). Figure was adapted from [28].

3.1.8 Treatment

Surgery

To date, surgery is routinely performed as part of the treatment plan of breast cancer. Surgical procedures can involve mastectomy or breast-conserving surgery (BCS), which consists in removing only the cancerous tissues and a rim of normal tissue (tumor margin). The more advanced the cancer is at time of diagnosis, the more aggressive the surgical procedure generally is. As an example, 36% of young women diagnosed with early stage breast cancer (stage I and II) have BCS, against 14% among woman with more advanced breast cancer (Stage III and IV) [2, 34]. Both BCS and mastectomy usually involve the removal of one or more axillary lymph node in order to determine the stage of the disease and the course of treatment.

Radiation therapy

Radiation therapy, which is the use of ionization radiation in order to induce DNA damage and cell death, is typically part of adjuvant therapy in breast cancer. Indeed, it was shown that the combination of surgery followed by radiation therapy decreases the risk of breast cancer recurrence by about 50% and the relative risk of breast cancer death by about 20% in most patients [35]. In late stage breast cancer, radiation therapy accompanies mastectomy and chemotherapy in 34% of all cases [2].

Systemic therapy: chemotherapy and endocrine therapy

Chemotherapy is administered to breast cancer patients in three different therapeutic settings. First, chemotherapy is recommended in an adjuvant setting, i.e. after surgery, in order to avoid local relapse and to target distant micrometastasis. Second, locally advanced cancers might be treated by neoadjuvant chemotherapy, i.e. before surgery, to reduce the tumor size and to make surgery less extensive or possible at all. Finally, chemotherapy is used to manage late stage breast cancer patients for whom surgery is not an option due to the spread of the disease. Indeed, 17% of late stage breast cancer patients receive only chemotherapy and/or radiation without surgery [2]. The benefit of chemotherapy depends on several clinical parameters, which are mainly assessed by staging and biomarker-based stratification. While triple-negative and HER2-enriched breast cancer patients tend to be more sensitive to chemotherapy, it is less likely to be beneficial for ER and/or PR positive breast cancer patients [36, 37]. Neoadjuvant and adjuvant chemotherapy regimen mostly involves a combination of drugs rather than a single agent. Typical chemotherapeutic drugs for these patients are anthracyclines such as doxorubicin or epirubicin, taxanes such as paclitaxel or docetaxel, 5-fluorouracil, cyclophosphamide and carboplatin [38, 39]. The same agents and others, such as gemcitabine, are used in the treatment of metastatic breast cancer, although there is a general consensus that the efficacy is uniformly poor [40].

Endocrine therapy is strongly recommended for treatment of HR positive tumors. The aim of such a treatment is to lower the overall estrogen levels or to block the pro-proliferative effect of estrogen on the tumor cells. Tamoxifen is a pro-drug, which metabolites can bind to ER and block its downstream signaling. Long-term treatment of HR positive breast cancer patients with tamoxifen have be shown to significantly reduce the risk of recurrence and mortality of these patients [41, 42]. Another class of drugs used to successfully treat HR positive tumors are aromatase inhibitors (AI), which interfere with the production of estrogen [43].

Commercially available assays based on gene panels such as ProSigna / PAM50, Oncotype DX or MammaPrint may also help to identify patients who will benefit from chemotherapy and endocrine therapy [44-47]. Indeed, stratification of breast cancer patients according to PAM50 assay was shown to predict the benefit of adjuvant tamoxifen treatment in luminal A patients [47]. Both MammaPrint and Oncotype DX tests were originally designed to predict the probability of metastatic relapse in breast cancer patients. The Oncotype DX test is based on the expression of 21 ER-related genes and is used for patients with early stage of HR positive breast cancer in order to assess the potential benefit of adjuvant chemotherapy [45, 46]. The 70 tested genes of the MammaPrint assay are related to the hallmarks of cancer and efficiently predict beneficial effects of chemotherapy [44, 48].

Targeted therapy: Anti-HER2 therapy

A well-established targeted therapy in breast cancer is directed against the proliferation promoting receptor tyrosine-protein kinase HER2. Trastuzumab (Herceptin) is a monoclonal antibody that directly targets the HER2 protein. The combination of trastuzumab and chemotherapy in early-stage breast cancer overexpressing HER2 shows significant improvement with respect to both recurrence and death rates [49]. Trastuzumab is also used in the treatment of metastatic breast cancer patients overexpressing HER2 [2]. More recently, a second monoclonal antibody binding to another site of HER2, Pertuzumab (Perjeta), was approved for neoadjuvant and late stage treatment of HER2 positive breast cancer [50]. This drug is used in combination with chemotherapy and trastuzumab and was shown to prolong the survival of patients [51]. Additional drugs for treatment of HER2 overexpressing breast cancer malignancies, especially metastatic disease, are ado-trastuzumab emtansine (Kadcyla, formerly called TDM-1) and lapatinib (Tykerb) [52, 53].

Other approved targeted therapies in breast cancer are Palbociclib (Ibrance) and Everolimus (Afinitor). These drugs are recommended for HR positive, HER2 negative postmenopausal patients. Palbociclib is a cyclin dependent kinase (CDK) 4 and 6 inhibitor showing good results in patients with advanced breast cancer [54, 55]. Everolimus is an mTOR inhibitor, which can improve the effectiveness of endocrine therapy in advanced HR positive, HER2 negative post-menopausal breast cancer patients [56, 57].

3.1.9 Therapeutic challenges

In the last 40 years, the mortality rate of breast cancer patients in the US declined by 36%, while the 5-year survival rate increased by 20% [4]. This is the encouraging consequence of constant improvement in patient stratification and the use of targeted therapies. However, one has to keep in mind that chemotherapy remains the only option for triple-negative breast cancer patients to date and that while it might be effective initially, long-term chemotherapy treatment is often associated with the development of resistance mechanisms [58]. Therefore, an improved understanding of the triple-negative phenotype and development of targeted therapy is urgently needed.

The most demanding clinical challenge in breast cancer treatment is the management of metastatic diseases. Indeed, breast cancer remains the second cause of cancer-related death among women, mainly as a consequence of metastatic progression [2]. As described above, targeted therapy against advanced disease in HR positive and HER2 overexpressing breast cancer has been approved. Especially trastuzumab improves overall survival and progression-

free survival of HER2-enriched breast cancer patients, although not without side effects which can be as severe as lung toxicity or cardiac failure [59]. However, due to the absence of known target, triple-negative metastatic breast cancer does not benefit from any targeted therapy and is also associated to broad chemoresistance [60].

3.2 Metastasis

Tumor metastasis refers to the spread of the cancer cells from the primary site to progressively colonize distant organs. To date, metastasis is the major contributor to cancer-related deaths, regardless of the cancer entity. In the context of breast malignancies, metastasis at time of diagnosis is uncommon, accounting for only 6% of breast cancer patients [4]. However, every third breast cancer patient will develop metastatic disease during his life and the progression of the disease is associated with very poor survival rates [61].

3.2.1 The metastatic cascade

At the cellular level, metastasis represents the end product of a multistep cascade and an evolutionary process [62] **(Figure 5, A)**. In order to colonize a distant organ, a cancer cell has to go through the following steps:

1. *Local invasion* - Upon transformation of epithelial cells and formation of a primary tumor, the cancer cells break through the basement membrane and invade the surrounding stroma. The acquisition of a mesenchymal signaling program and phenotype in a process called epithelial to mesenchymal transition (EMT) is widely believed to be a pre-requisite for cell mobility and invasion [63].

2. *Intravasation* – At the primary site, tumor cells stimulate the formation of new blood vessels in a process termed neoangiogenesis. In contrast to blood vessels present in healthy tissues, the tumor-associated vasculature is leaky, which facilitates intravasation of the cancer cells into the lumen of blood vessels.

3. *Survival in circulation* - Cancer cells use the vascular and lymphatic networks in order to spread throughout the body and must resist anoikis triggered by the lack of adhesion in circulation.

4. *Arrest at the distant site* - The cancer cells arrest in the microvasculature of a distant organ.

5. *Extravasation* - The cancer cells exit the vasculature and enter the parenchyma of a distant organ, either as micro-colony or as a single cell.

6. *Formation of micrometastasis* – In order to form micrometastasis, the cancer cells have to survive the strong negative pressure exerted by the foreign microenvironment at the distant site.

7. *Formation of macrometastasis* - The cancer cells reactivate their proliferative capacities and corrupt the microenvironment to promote their own survival and form clinically detectable macrometastasis.

Importantly, the efficiency of the different steps varies greatly, as determined by experimental studies. To be more specific, step 3 to 5 display a high efficiency rate with 80% of the cells implanted intravenously successfully extravasating the microvasculature. In contrast, the efficiency dramatically drops in the last steps of the metastatic cascade, with only 3% of the cells forming micrometastasis and 0.02% of the cells generating overt metastasis [64, 65]. In summary, the last two steps of the metastatic cascade, commonly called metastatic colonization, represent the rate limiting steps of the disease. Importantly, carcinomas originating from a particular organ only form metastasis in a subset of theoretically possible distant organs. This has been described as the 'seed and soil' hypothesis more than 120 years ago. Paget's theory describes the phenomenon according to which even if the cancer cells, the 'seeds', broadly disseminated throughout the body, they can only form metastasis in specific organs, referred to as the 'soils', i.e. the soil has to fit the seed [66]. In the case of breast cancer, the organs prone to metastasis formation are the bone, the lung, the liver and the brain, in order of prevalence [62] **(Figure 5, B)**.

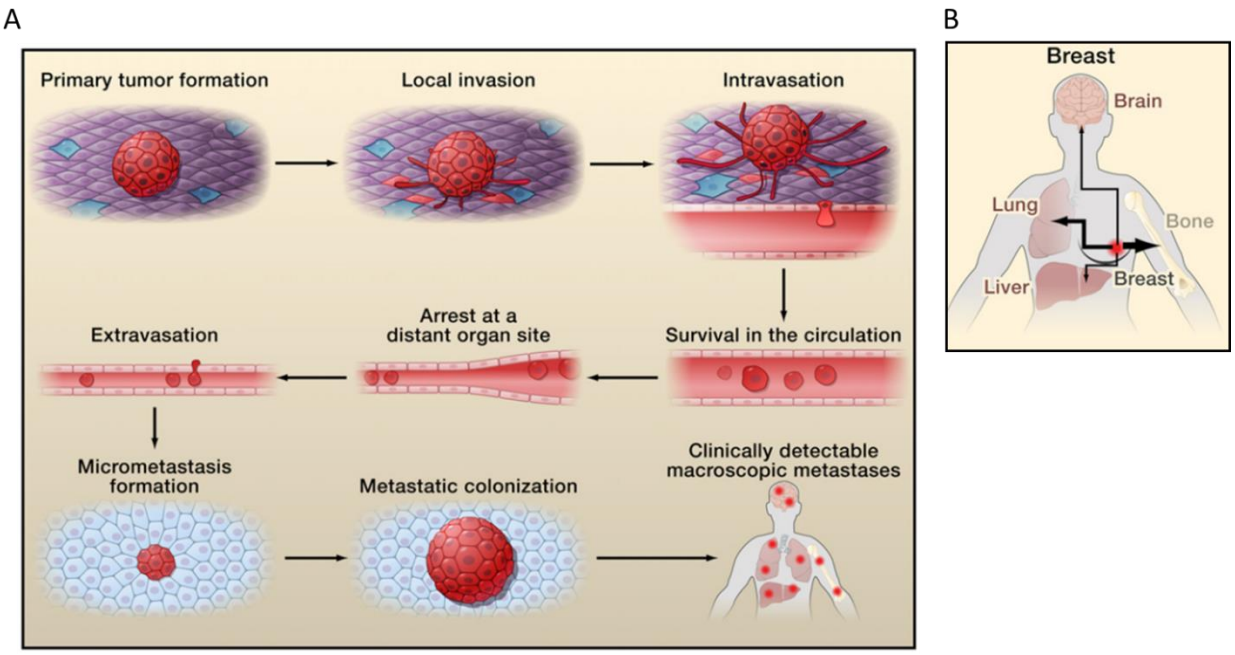

Figure 5 The metastatic cascade and the sites of colonization in breast cancer.
(A) Metastasis is a multistep process starting with the formation of a primary tumor, the invasion of the local tissue and the intravasation into the blood circulation. Once in circulation, cancer cells have to survive before arresting in a distant organ and extravasating into its parenchyma. The metastatic colonization comprises the formation of micro- and macrometastasis, leading to clinically detectable lesions. **(B)** Although broadly spread by the vascular system, breast cancer cells typically form overt metastasis only in the bone, the lung, the liver and the brain. Thickness of black lines is proportional to the relative frequencies of metastasis in a specific organ. Figures were adapted from [62].

3.2.2 The metastatic niche

At the distant site, the cancer cells are facing a microenvironment which typically differs greatly from that present at the site of primary tumor formation. This microenvironment is composed of stromal cells (e.g. fibroblasts, endothelial cells, pericytes, adipocytes…), immune cells (e.g. macrophages, neutrophils, lymphocytes…), soluble factors (growth factors and cytokines), nutrients and metabolic components and ECM **(Figure 6)**. The formation of overt metastasis is accompanied by the establishment of a so-called 'metastatic niche', referring to microenvironment corrupted by the cancer cells and which is favorable to tumor growth.

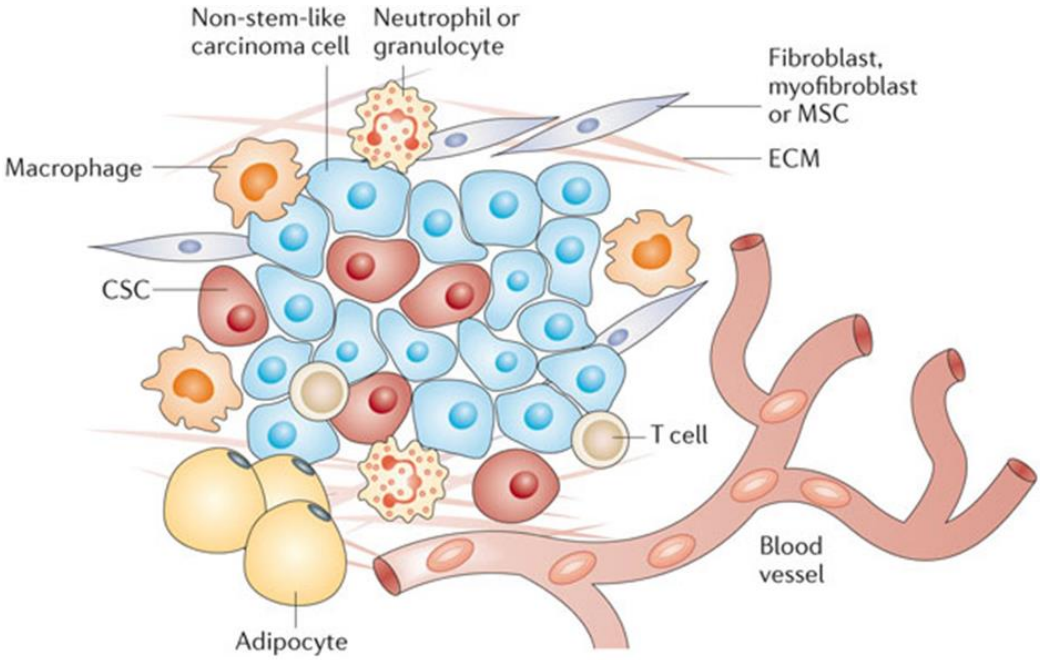

Figure 6 The tumor associated microenvironment.
The microenvironment of cancer cells is typically composed of fibroblasts, immune cells, a vascular network and ECM components. Figure was adapted from [67].

Recent studies have shown that cancer cells at the distant site may occupy native stem cell niches of the host tissue, as in the case of prostate cancer, where disseminated cancer cells exhibit preference for lodging in hematopoietic niches of the bone [68]. Indeed stem cell niches show activation of several pathways promoting tumor growth. These are for example the Wnt, Notch, transforming growth factor (TGF) beta, hedgehog, phosphoinositide-3 kinase (PI3K) and the janus kinase / signal transduced and activator of transcription (JAK/STAT) pathways [69]. In breast cancer embryonic signaling pathways are known to promote an invasive phenotype [70]. Another location of choice for the cancer cells to establish a metastatic niche is the perivascular microenvironment, as for example in breast or renal cancer metastasis to the brain [71, 72]. Activated endothelium might support the growth of cancer cells at the distant site by paracrine factors, such as the Notch ligand Jagged-1 (JAG1) and TGF beta 1 [73, 74]. Noteworthy, endothelial cells also provide the cancer cells with specific ECM proteins as for example periostin (POSTN), which has been suggested to promote the formation of micrometastasis upon exit of dormancy [74].

Fibroblasts are associated with cancer cells at all stages of the disease and are important cellular components of the metastatic niche. Upon arrival of cancer cells at the distant site, fibroblasts become activated by growth factors and cytokines present in the milieu and elicit pleiotropic functions. Activated fibroblasts, also called myofibroblasts, are the most prominent

source of ECM molecules and secreted growth factors at the distant site. Thereby they drive recruitment of endothelial cells and pericytes, regulate immune and metabolic functions and directly promote the growth of tumor cells through paracrine signaling [75-77].

3.2.3 The extracellular matrix

The ECM is a highly diverse collection of glycoproteins, proteoglycans and polysaccharides [78]. In healthy tissue, the ECM makes up both the basement membrane, which is compact and primarily composed of collagen type IV, laminins and fibronectin, and the more porous interstitial matrix, which is rich in fibrillary collagen type I, proteoglycans and various glycoproteins [79]. The functions of the ECM are as diverse and versatile as its components are. First, the ECM plays a physical role for the cells by functioning as an anchorage site for cell surface receptors and by forming a migration barrier or, alternatively, migration tracks **(Figure 7, function 1 – 3)**. Second, the ECM display biochemical properties referring to its ability to modulate cell signaling. Binding of soluble growth factors allows the ECM to act as a reservoir for these signals and to present them specifically to co-receptors or receptors on adjacent cells, thereby triggering a signaling cascade **(Figure 7, function 4 – 6)**. The ECM can also trigger signaling by itself via endogenous growth factor domains or functional domains requiring processing by proteases such as thrombin or matrix metalloproteinases (MMPs) **(Figure 7, function 7)**. Finally, the biomechanical force resulting from ECM composition can be translated into signaling activities via focal adhesion complex and the actin cytoskeleton **(Figure 7, function 8)** [79]. Importantly, all these functions are interconnected. As an example, a stiff matrix can exert biomechanical force, thereby triggering changes in gene expression, and at the same time it can impact the motility of a cell.

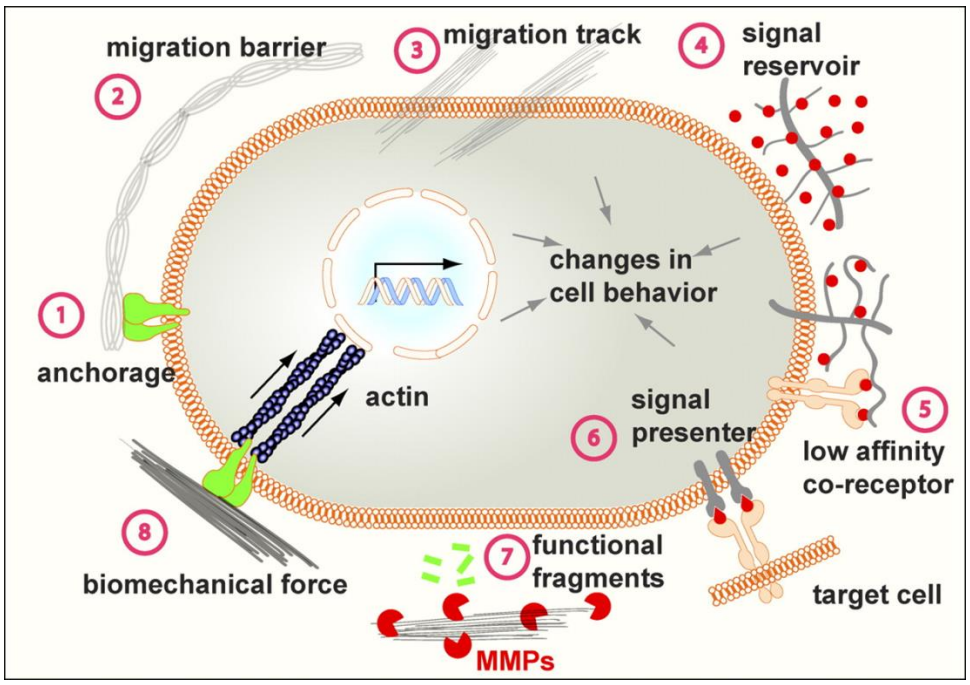

Figure 7 Functions of the ECM.
The ECM is functionally versatile and exerts physical (1 – 3), biochemical (4 -7) and biomechanical (8) cues. Figure was adapted from [79].

Although ECM-dependent activities are tightly controlled in healthy tissues, its quantity, composition and dynamics become abnormal in cancer. Among the alterations of the ECM in the tumor microenvironment, increased deposition of collagens is well studied and recognized [80]. Moreover, many other ECM components and their receptors are frequently overexpressed in cancer. This is the case for heparan sulfates proteoglycans and CD44, fibronectin (FN), fibrillin, fibulin, hyaluronan as well as matricellular proteins [79-81]. Consistent with these changes, expression of matrix remodeling enzymes such as MMPs, cathepsins and urokinases is often deregulated in cancer [79]. In addition, the collagen crosslinker enzymes lysyl oxidase (LOX) are upregulated in several types of cancer, leading to an increased ECM stiffness [82].

Remodeling of the ECM impacts both the tumor cells themselves and the stromal cells. For example, deregulated ECM has been associated with EMT and enhanced migration of the tumor cells due to thickening and linearization of collagen fibers and MMPs activity [83-85]. On the other hand, abnormal ECM in tumors can promote tumor angiogenesis and lymphangiogenesis as well as tumor-associated inflammation [79]. In summary, cancer-associated ECM not only promotes cancer-cell transformation and invasion but it also supports the formation of a niche further supporting cancer progression.

In recent years, a concept of pre-metastatic niche has emerged. According to some studies, tumor cells induce changes in the microenvironment at distant sites through secretion of soluble molecules, thereby facilitating metastatic colonization. Particularly homing of bone marrow-derived hematopoietic cells has been shown to facilitate tumor metastasis. In this process, the ECM might play an important role. For example, vascular endothelial growth factor receptor (VEGFR) positive myeloid cell, which are recruited at pre-metastatic sites, express the FN receptor integrin alpha 4 beta 1 (ITGA4-ITGB1), thereby providing a permissive niche for incoming tumor cells [86]. Another example is the recruitment of CD11b+ myeloid cells to the lungs by LOX, which are secreted by hypoxic breast tumor cells. CD11b+ cells adhere to crosslinked collagen IV and produce MMP2, thereby enhancing the invasion and the recruitment of bone marrow-derived hematopoietic cells and metastasizing tumor cells to the lungs. [87].

Many of the cited ECM components were also shown to support the growth of cancer cells in the metastatic niche. For example, binding of the ECM glycosaminoglycan hyaluronan to its receptor CD44 at the distant site drives metastasis in colon and breast cancer [88, 89]. In addition, a specific subgroup of ECM molecules, matricellular proteins, is of particular interest in the context of the metastatic niche due to their expression in normal stem cell niches.

3.2.4 Matricellular proteins

Within the ECM, matricellular proteins form a family of non-structural molecules often expressed in normal stem cell niches and frequently upregulated in cancer [90]. Tenascin C (TNC) and periostin (POSTN) are two matricellular proteins playing an important role in the metastatic niche in mouse models for breast cancer. TNC and POSTN are both expressed in normal adult stem cell niches and their functions at the distant site show a significant overlap [91-94]. Indeed, TNC promotes the expression of the Wnt target gene leucine-rich repeat-containing G protein-coupled receptor 5 (LGR5) and POSTN binds and presents Wnt ligands to the cancer cells. As a consequence of this signaling modulation, both TNC and POSTN are required for the initiation of lung metastasis in mouse models for breast cancer [91, 94, 95]. In addition, overexpressed TNC and POSTN were shown to bind to each other in an *in vitro* setting [96]. Together, this data suggest a putative cooperation of TNC and POSTN that may play a role in metastasis. Furthermore, matricellular proteins have been linked to several cellular processes of the metastatic cascade such as EMT, angiogenesis, migration, proliferation, evasion of immune surveillance and survival of anoikis [90]. In addition of promoting a cancer stem cell phenotype and aggressiveness in glioma, the glycoprotein osteopontin (SPP1) was shown to support mammary tumor growth and metastasis [97-99]. Secreted protein acidic and rich in cysteine (SPARC) was shown to promote EMT and its expression is associated with invasion and

metastasis of several cancer entities [90]. Overexpression of SPARC promotes metastasis to the lung in a mouse model for breast cancer [100]. Although originally known for its anti-angiogenic properties, thrombospondin-1 (THBS1) is a glycoprotein of the ECM displaying a differential role in primary tumor growth and metastasis. Indeed, in a transgenic mouse model primary tumor formation was repressed by THBS1 while it promoted metastasis to the lung [101]. Importantly, the expression of many matricellular proteins in tumors is associated with metastatic progression in cancer patients [81].

3.3 Tenascin C

3.3.1 Structure and cellular receptors

TNC is a glycoprotein of the ECM originally described in the 1980's for its anti-adhesive properties and its ability to inhibit attachment of fibroblasts to FN [102-105] **(Figure 8, A)**. Its structure was rapidly characterized as a 'hexabrachion', i.e. a disulfide-linked hexamer which subunits range from 190 to 300 kDa [106] **(Figure 8, B)**. Each arm emanates from a central globular particle, called assembly domain (AD), which is followed by 14 ½ epidermal growth factor (EGF) -like repeats, 8 constant and up to 9 alternatively spliced FN type III repeat domains and a carboxyl terminal fibrinogen globe (FG) **(Figure 8, C)**. The central part of the FN type III repeat domain is alternatively spliced, giving rise to numerous TNC isoforms expressed in different contexts [107, 108].

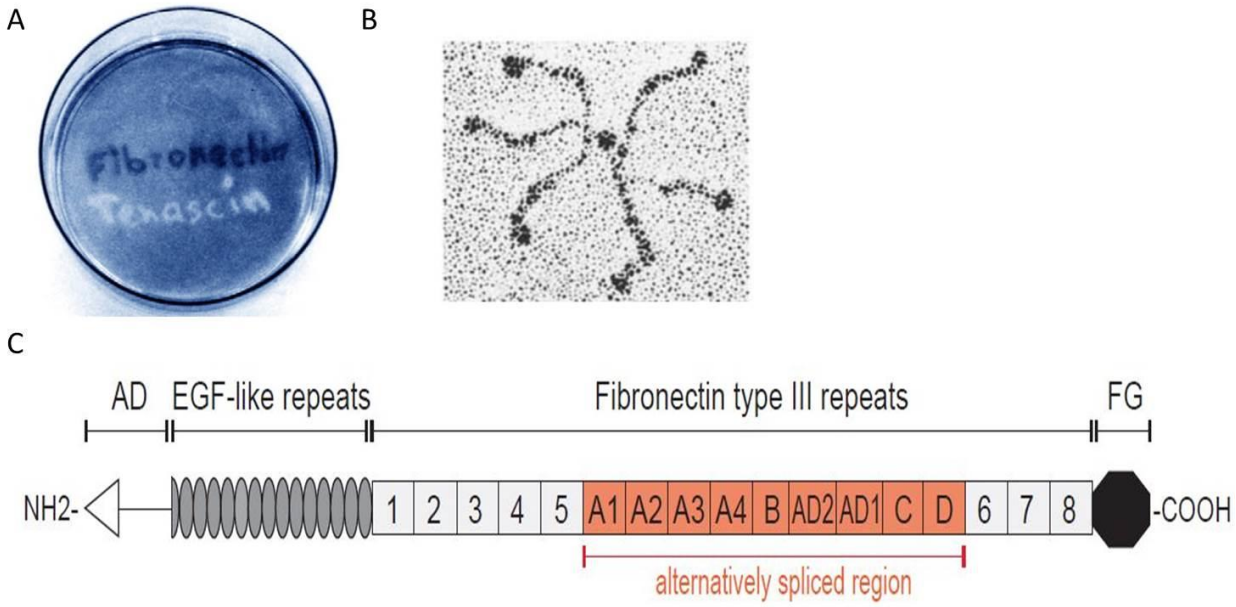

Figure 8 Structure of the matricellular protein TNC.

(A) Illustration of the adhesive / antiadhesive properties of TNC compared to FN. Mouse fibroblasts were plated on plastic coated with FN or TNC. Noteworthy, the cells attached more on FN coating compared to plastic while they do not attach at all on TNC coating. Figure was adapted from [105]. **(B)** Electromicrograph of TNC forming a hexabrachion. Figure was adapted from [109]. **(C)** TNC monomers comprise four distinct domains: an N-terminal assembly domain, 14 ½ EGF-like repeats, 8 constant and up to 9 alternatively spliced FN type III repeats and a C-terminal FG domain. Figure was adapted from [107].

By virtue of its multiple domains, TNC was shown to interact with a variety of molecules, among which are many cell surface receptors [108]. TNC binding receptors include annexin II (ANXA2) [110], epidermal growth factor receptor (EGFR) [111], glypican 1 (GPC1) [112], phosphacan (PTPRZ1) [113], sodium channel Xia (NaN) [114], syndecan 4 (SDC4) [115-117], toll-like receptor 4 (TLR4) [118], integrin alpha (ITGA) 2, 7, 8, 9, V, integrin beta (ITGB) 1, 3, 6 [119-124] and contactin 1 (CNTN1) [125]. To note is that only the heterodimers ITGA2/9-ITGB1 and ITGAV-ITGB1/3/6 are known to be expressed on epithelial cells [126]. All these heterodimers are binding to the FNIII3 domain of TNC, except for ITGAV-ITGB3 which binds to the C-terminal FG domain and the ITGA2-ITGB1 which binding site is not known to date [127]. It is important to point out that the various cellular receptors of TNC were identified in different biological contexts using different approaches.

Alternative splicing and binding to multiple cell surface receptors and ECM molecules (e.g. FN and POSTN [96, 128]) confer pleiotropic functions to TNC, in homeostasis (stem cell niches and tissue remodeling) and pathological stress (vascular disease, cardiac disease, atherosclerosis and cancer) [129].

3.3.2 Expression pattern and association with stem cell niches

TNC has a tightly regulated pattern of expression throughout life, both in healthy and pathological conditions. During embryogenesis, TNC expression is first observed during gastrulation and somites' formation and later during invasion of neural crest cells. TNC is then highly expressed in the developing central nervous system by glia cells, particularly during neuronal differentiation and migration in the cortex and cerebellum [130-132].

In adult tissues, TNC is mostly repressed with the exception of some connective tissues such as dense connective tissues (ligaments and tendons), bone periosteum and smooth muscle [129, 133]. Interestingly, TNC is expressed in a number of the stem cell niches, such as the neural

stem cell niche, the epithelial niches of hair and whisker follicles or the osteogenic stem cell niche [92]. In the mammary gland, TNC is expressed during embryonic development and in regenerative regions upon mammary transplantation assay. In addition, TNC is also expressed during involution of the mammary gland upon lactation. [134, 135]. This is part of a striking aspect of the TNC biology, which is its association with tissue remodeling and regeneration. Further examples are pathological conditions such as wound healing or inflammation, which are also accompanied by upregulation of TNC [133, 136]. The expression pattern of TNC is in line with the described phenotype of mice lacking TNC. In 1992 and 1996, two groups independently generated TNC knockout mice [137, 138]. Although in both cases the mice were phenotypically normal when compared to wildtype animals, the TNC knockout mice showed several defects upon stress or injury. These defects become then apparent in the peripheral nerves, the cornea or in the hematopoietic compartment [139]. This tissue remodeling-associated phenotype suggests a role for TNC in adult stem cell niches.

3.3.3 Clinical association with cancer progression

Another pathological condition where the expression of TNC is markedly increased is cancer [140]. TNC is highly expressed in most of the solid tumor tissues, including brain, breast, ovaries, prostate, pancreas, head and neck, colon, stomach, lung, liver, kidney, bladder, skin, bone as well as lymphomas [108]. The main source of TNC is the cancer-associated stroma, particularly myofibroblasts and endothelial cells. However, there is strong evidence that cancer cell can also express TNC in an autocrine manner, as in the case of breast and colon cancer [141, 142]. Accordingly, various cancer cells lines (melanoma, breast and colon) do express TNC [143-146]. Studies on diverse malignancies have revealed a clinical association between TNC expression and patients' survival. In breast cancer, accumulating evidences show a prognostic value for TNC. Indeed, high expression of TNC in early stage of breast cancer is associated with invasive behavior and progression of the disease [147, 148]. In addition, several independent studies have shown that high expression of TNC in the primary tumor or in metastatic nodules correlates with disease recurrence and overall poor patient outcome [94, 149, 150]. Moreover, TNC was identified within a gene expression signature predicting clinical relapse in breast cancer patients [100]. Interestingly, studies showing a prognostic value for TNC also showed an inversed correlation between TNC expression and ER expression [145, 151]. In non-small cell lung carcinoma (NSCLC), high expression of TNC is associated with disease recurrence [152]. Similarly in head and neck cancer, evidence are accumulating that TNC represents a prognostic factor for relapse and poor overall survival [153, 154]. In melanoma and colon cancer, TNC expression in the lesions has been associated with advanced stage of the disease and poor clinical outcome [155-157]. This suggests that TNC might play a functional role in cancer progression and metastasis.

3.3.4 Molecular roles of TNC in cancer progression

As a highly pleiotropic molecule, TNC indeed promotes various cellular mechanisms that can support the metastatic cascade. These range from adhesion and migration, angiogenesis, modulation of immune response to survival in a foreign microenvironment [107] **(Figure 9)**.

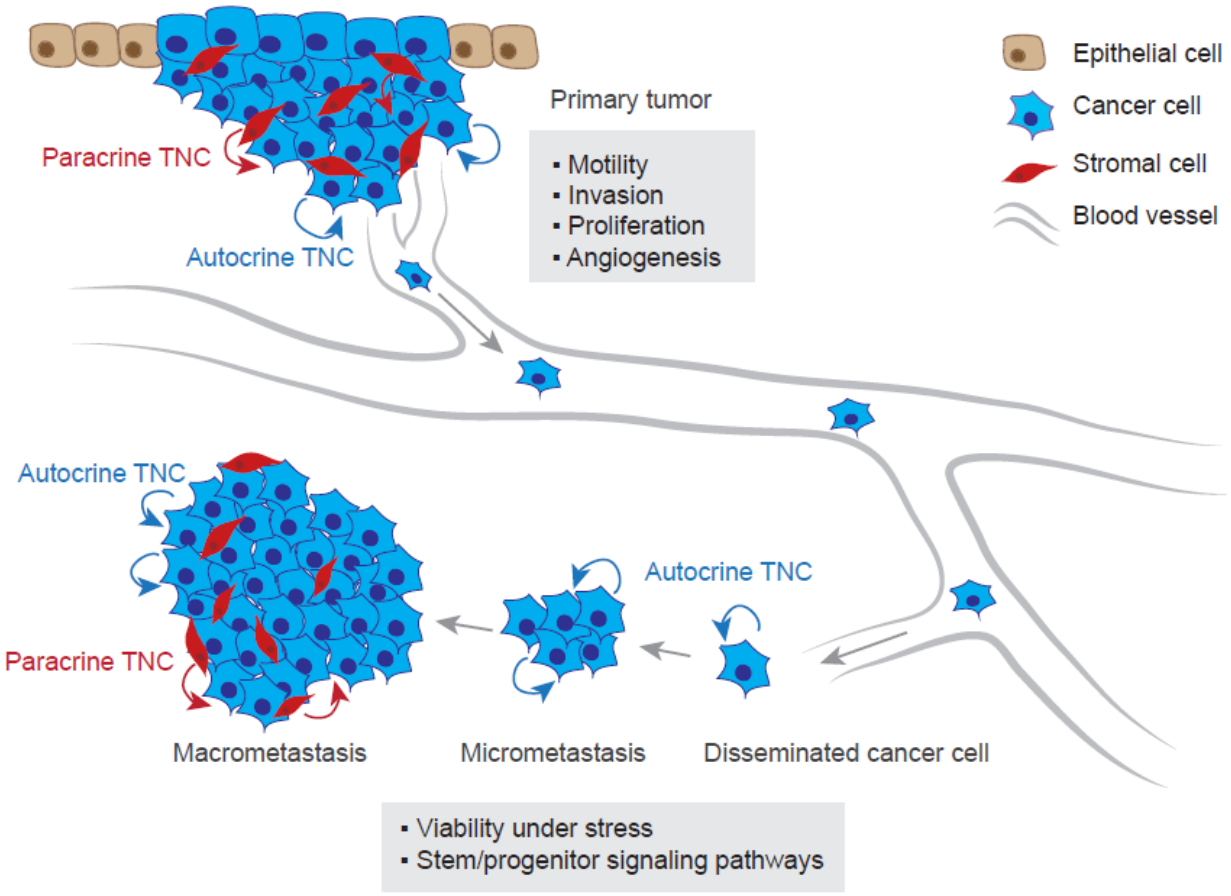

Figure 9 Function of paracrine and autocrine TNC in the metastatic cascade.
At the primary site, TNC promotes proliferation and migration of the cancer cells, thereby supporting the invasive phenotype. In addition, it also promotes the formation of new blood vessels. At the distant site, primarily autocrine TNC supports viability of the cancer cells through stem and progenitor signaling molecules. Figure was adapted from [107].

Modulation of adhesion and migration

The anti-adhesive properties of TNC have been recognized for a long time [104, 105]. At the molecular level, TNC was shown to interfere with the binding of FN to its co-receptor SDC4, thereby altering the FN-induced ITGB1-ITGA5 signaling. As a result, formation of actin stress fibers and focal adhesion was inhibited and migration, as well as proliferation, was induced in glioblastoma and breast cancer cells [116]. Further studies in breast cancer and a study on melanoma have confirmed a role of TNC in promoting migration and invasion of cancer cells at the primary site [144, 158, 159].

Role in angiogenesis

TNC expression is associated with angiogenic processes during development and in adult tissue regeneration, as well as in pathological angiogenesis [160]. Evidences suggest that the pro-angiogenic role of TNC plays a role in tumorigenesis. When human melanoma cells were injected into TNC knockout mice, the resulting tumors showed a decreased vascularization compared to control mice. Molecularly, stromal TNC was shown to promote the expression of vascular endothelial growth factor (VEGF), a key signaling molecule in angiogenesis [161]. Additionally, TNC was shown to induce an angiogenic switch in a transgenic mouse model for neuroendocrine pancreas carcinoma through Wnt signaling. In this model, TNC promotes the Wnt signaling by repressing its antagonist dickkopf-related protein 1 (DKK1) in endothelial and tumor cells [162].

Role in inflammation

TNC is an important player of innate and adaptive immune surveillance through modulation of the production of inflammatory cytokines and recruitment of immune cells. This has been demonstrated in particular for chronic inflammatory diseases such as arthritis [118, 136]. In a mouse model for mammary carcinoma driven by the polyoma middle T (PyMT) oncogene, knockout of TNC resulted in less macrophages and monocytes infiltration when compared to control mice, suggesting a role for TNC in tumor-associated inflammation [163]. TNC was also suggested to modulate adaptive immunity in cancer. Indeed, in human lung cancer, TNC inhibited proliferation and interferon (IFN) gamma secretion of tumor-infiltrating lymphocytes [152]. Taken together, these findings suggest a role for TNC in cancer-associated inflammation.

Role in the metastatic niche

Interestingly, TNC shows a heterogeneous expression pattern in many tumors, with the strongest expression often observed at the invasive front of the tumor nodules [108]. This

phenomenon has been observed in breast cancer, melanoma, malignant pleural mesothelioma and intrahepatic cholangiocarcinoma and it is associated with higher risk of metastasis [107]. Importantly, expression of TNC at the invasive front was also observed in metastatic lesions of breast cancer [94].

In the past years, *in vivo* studies have demonstrated a functional role of TNC in the colonization of distant organs. The analysis of *in vivo* xenograft model for breast cancer metastasis demonstrated that TNC is required for lung and bone metastasis in breast cancer but not for mammary tumor growth. TNC deficient breast cancer cells showed a decreased ability to colonize the lung and the bone due to increased apoptosis as demonstrated by a marked expression of the apoptosis marker cleaved caspase 3 at the distant site. [94, 159]. In a syngeneic mouse model, the role of stromal TNC in breast cancer metastasis to the lung was addressed. Together with VEGF-A, stromal TNC was shown to promote metastasis to the lung [164]. Importantly, expression of TNC by the cancer cells themselves represents a considerable survival advantage at the distant site. Indeed, initially the stromal cells are not able to compensate for autocrine loss of TNC, as attested by the decreased metastatic burden when $TNC^{+/+}$ mice are injected by TNC deficient cancer cells or control cells. However, once the metastatic lesions have reached significant size and upon activation of the stroma, as attested by the expression of alpha smooth muscle actin (αSMA) by myofibroblasts, autocrine TNC is no longer required [94]. Therefore, cancer cells expressing TNC in an autocrine manner might be able to proliferate at the distant site more readily compared to cells relying on the stromal activation as a source of TNC.

In breast cancer metastasis to the lung, survival at the distant site was shown to rely on two adult stemness markers. TNC supports on one hand the expression of the Wnt target gene leucine-rich repeat-containing G protein-coupled receptor (*LGR5*) and on the other side the positive regulator of the Notch signaling musashi homolog 1 (*MSI1*). Thereby TNC promotes the Notch signaling, as attested by the TNC-dependency of the Notch target genes hairy/Enhancer-Of-Split Related With YRPW Motif 2 (*HEY2)* and protein deltex 1 (*DTX1)*, while it does not control the Wnt signaling as a whole. Indeed, the expression of the Wnt target genes *AXIN2* and lymphoid enhancer-binding factor 1 (*LEF1*) is not affected upon knockdown of TNC **(Figure 10)**. The pro-metastatic function of both adult stem cell markers, LGR5 and MSI1, was validated experimentally [94].

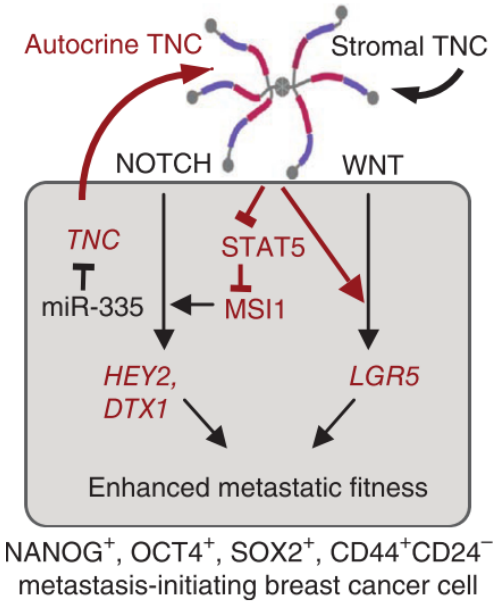

Figure 10 TNC signaling in breast cancer metastasis to the lungs.
Autocrine TNC enhances metastatic fitness of breast cancer cells at the distant site through de-repression of the Notch positive regulator *MSI1*, and through the Wnt target gene and adult stem cell marker *LGR5*. Figure was adapted from [94].

MSI1 is an RNA-binding protein, which main target is the transcript of the Notch inhibitor *NUMB* [165] **(Figure 11, A)**. MSI1 was originally described for its role in the central nervous system of *Drosophila*, where it is required for the development of adult external sensory organs [166, 167]. Subsequently, the MSI1 function was shown to play a crucial role in the maintenance of neural, intestinal epithelial and mammary stem cells [166, 168, 169]. In the last years, MSI1 has been reported to promote the growth of several cancer entities such as colon, pancreatic or cervival cancer and may represent a promising therapeutic target [170-172].

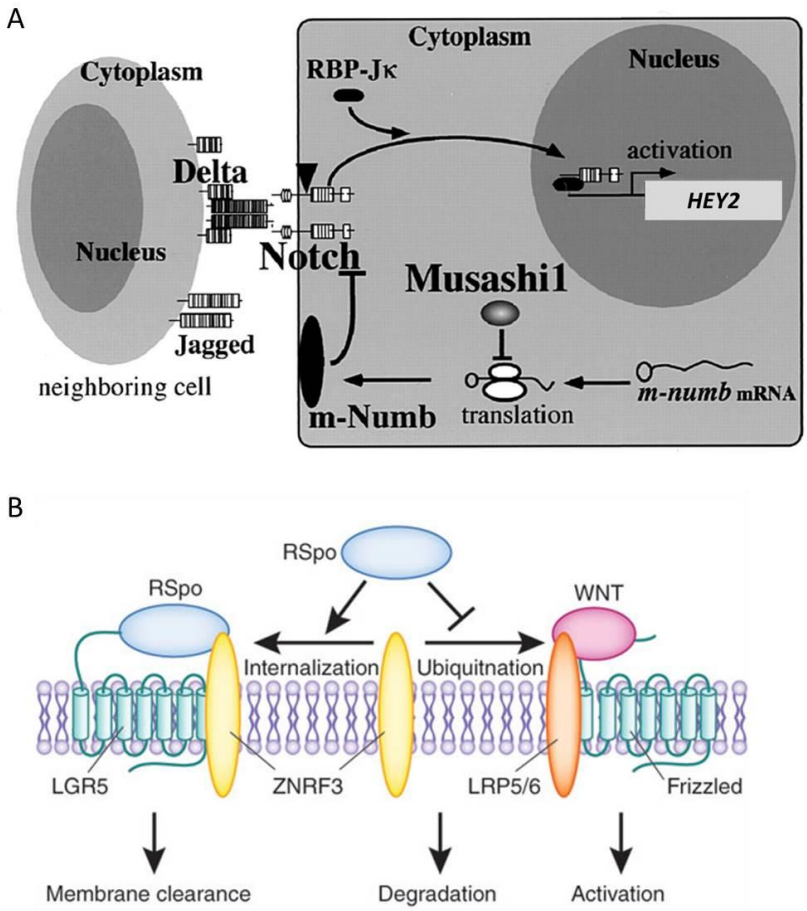

Figure 11 Notch and Wnt signaling regulation by MSI1 and LGR5, respectively.
(A) Binding of Delta-like 1 protein (DLL1) or Jagged (JAG) ligand to active Notch receptor leads to cleavage of the intracellular part of the Notch receptor and activation of translational activity, i.e. expression of the Notch target HEY2. Notch signal activation can be blocked by NUMB. By binding to the Numb mRNA, MSI1 impedes repression of the pathway and potentiates the Notch signaling. Figure was adapted from [173]. **(B)** In the absence of RSpo proteins, the ZNRF3 receptor ubiquitinates the Wnt receptor Frizzled, leading to its degradation and inhibition of the pathway. Upon binding of RSPOs to LGR5, ZNRF3 dimerizes with LGR5 receptor, leading to membrane clearance of ZNRF3 from the cell surface and enhancement of Wnt signaling. Figure was adapted from [174].

The Wnt target gene *LGR5* was originally discovered as a marker of cycling stem cells of the adult small intestine and colon [175]. Previously, the biology of adult stem cells had been linked to activation of the Wnt signaling [176]. Subsequently, LGR5 was shown to associate with the Frizzled/Lrp Wnt receptor complex and to bind the functional markers of adult stem cells R-spondins (RSPOs). The four members of the R-spondin family are secreted molecules which potentiate the Wnt signaling by enhancing the response to low-dose Wnt ligand [177]. At the

molecular level, the R-spondin / LGR5 complex captures and neutralizes Rnf43 and Znrf3, two transmembrane E3 ligases that remove the Wnt receptors from the surface of stem cells, thereby representing a positive feedback loop of the Wnt signaling [178, 179] **(Figure 11, B)**. Originally restricted to the small intestine and the colon, the definition of LGR5 as an adult stem cell marker has now expanded to further tissues such as the stomach and the hair follicle [180-183]. In the mammary gland, a role for LGR5 in the stem cell biology has been suggested by a study showing that LGR5+ cells display enriched repopulating capacity upon transplantation compared to LGR5- cells [184]. However, the functional role of LGR5 in mammary stem cells needs to be confirmed [185]. In cancer, LGR5 has been functionally linked to tumor initiation and the cancer stem cell phenotype in colorectal malignancies [186, 187]. In addition, a recent study in breast cancer showed that LGR5 promotes tumor formation and the maintenance of stemness properties through the Wnt pathway [188].

3.4 General biology of integrin receptors

Integrins are heterodimeric cell surface receptors acting as the main receptors for ECM molecules. In human, the integrin family comprises 18 alpha subunits and 8 beta subunits pairing in order to form at least 24 different functional heterodimeric receptors. It is noteworthy that ITGB1 can bind to most of the alpha subunits [189] **(Figure 12)**.

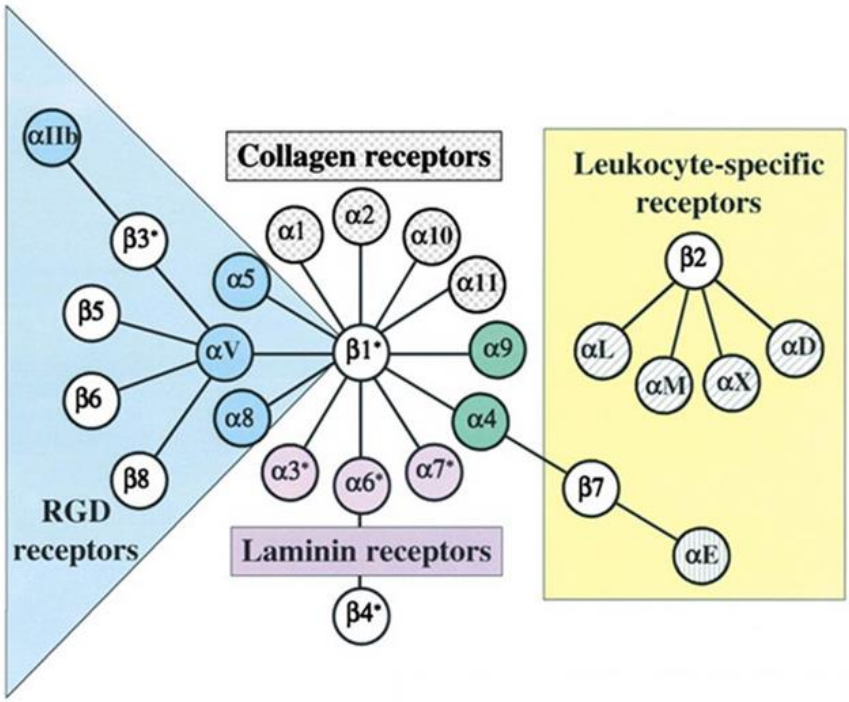

Figure 12 Mammalian integrin subunits and their alpha to beta association.

Here, integrin subunits were classified in several subfamilies based on ligand specificity (collagen receptors, laminin receptors and RGD domain receptors) and restricted expression (leukocyte-specific receptors). Figure was adapted from [189].

Each integrin can bind to multiple ECM molecules and a single ECM molecule often recognizes several heterodimers. Upon binding of a ligand, inactive bent integrin heterodimers undergo conformational changes, which culminate in the separation of the short cytoplasmic alpha and beta domain. This allows the binding of the linker molecule talin to the beta cytoplasmic domain and the stimulation of local actin polymerization. The separated integrin cytoplasmic domains and talin form a recruitment platform for focal-adhesion proteins such as vinculin, FAK and paxilin, which are recruited sequentially. Autophosphorylation of FAK leads to the recruitment of SRC resulting in activation of both kinases. The FAK/Src complex is the starting point of signal transduction to various signaling pathways, triggering changes in gene expression. The typical signaling machinery downstream of integrins involves the JNK pathway, the NFκB pathway and the MAPK pathway [190]. This signaling cascade, starting upon ligand binding, is termed ‘outside-to-inside’ signaling [191]. Conversely, the ‘inside-to-outisde’ signaling describes how integrins become activated by intracellular signals [192].

4 Aim of the study

In breast cancer, expression TNC has been suggested to predict poor clinical outcome. Importantly, breast cancer is a very heterogeneous collection of diseases reflected in the different subtypes. In this study, we aimed to investigate the prognostic value of TNC in the different subtypes of breast cancer using gene expression profiling and tissue-microarray of breast cancer patients.

TNC has been shown to promote breast cancer metastasis. However, the receptors mediating this effect remained unknown. Therefore, this project was geared towards the identification of the receptor(s) mediating the TNC pro-metastatic signaling in breast cancer using various *in vitro* and *in vivo* assays.

The identification of the receptors mediating the TNC signaling led us to the investigation of a putative functional role of TNC in the context of the mammary stem cell biology. Therefore, we finally aimed to address the role of TNC in the mammary gland development and maturation.

5 Materials & Methods

5.1 Tissue culture

5.1.1 Culture of cell lines

Adherent, monolayer cultures were maintained at 37 °C and 5% CO_2 in appropriate medium. Medium composition is specified below **(Table 2)**. For comparison of gene expression between different cell lines, the cells were cultured in identical medium (DMEM complete) for at least two passages prior analysis.

Table 2 Cell lines and media.

Cell line	Medium
BT474	DMEM/F12 complete
HCC1937	RPMI-1640 complete
HEK 293T	DMEM complete
MCF7	DMEM complete
MDA157	DMEM complete
MDA231	DMEM complete
MDA231 LM2	DMEM complete
MDA436	DMEM complete
MDA468	DMEM complete
SKBR3	McCoy's 5a complete
SUM159	DMEM/F12 complete with insulin
SUM159 LM1	DMEM/F12 complete with insulin
T47D	RPMI-1640 complete
WMPY1	DMEM complete

DMEM complete
DMEM, GlutaMAX™ (Thermo)
10% (vol/vol) Fetal Bovine Serum (FBS) (Thermo)
1% (vol/vol) Penicillin-Streptomycin (10,000 U/ml) (Thermo)
1% (vol/vol) Amphotericin B (US Biological)

DMEM/F12 complete with insulin
DMEM/F12, GlutaMAX™ (Thermo)
5% FBS (Thermo)
1 µg/ml hydrocortisone (Sigma)
5 µg/ml insulin (Sigma)
1% (vol/vol) Penicillin-Streptomycin (10,000 U/ml) (Thermo)
1% (vol/vol) Amphotericin B (US Biological)

RPMI-1640 complete
RPMI 1640 Medium, GlutaMAX™ (Thermo)
10% FBS (Thermo)
1% (vol/vol) Penicillin-Streptomycin (10,000 U/ml) (Thermo)
1% (vol/vol) Amphotericin B (US Biological)

DMEM/F12 complete
DMEM/F12 GlutaMAX™ (Thermo)
10% FBS (Thermo)
1% (vol/vol) Penicillin-Streptomycin (10,000 U/ml) (Thermo)
1% (vol/vol) Amphotericin B (US Biological)

McCoy's 5a complete
McCoy's 5a Medium (Thermo)
10% FBS (10,000 U/ml) (Thermo)
1% (vol/vol) Penicillin-Streptomycin (10,000 U/ml) (Thermo)
1% (vol/vol) Amphotericin B (US Biological)

Cell lines were passaged by addition of Trypsin-EDTA, 0.25% (Thermo). Once cells detached, appropriate medium was added. Splitting ratios were 1:2 – 1:10 depending on the cell line. Vi-CELL XR (Beckman Coulter) was used for cell counting. For cryopreservation, the cells were pelleted (1200 rpm, 5 min, 4 °C), re-suspended in appropriate medium supplemented with 10% Dimethyl Sulfoxide (DMSO) Hybri-Max® (Sigma) and aliquoted in cryovials. Cryovials were progressively frozen down to -80 °C using a freezing container filled with propan-2-ol (Sigma) and transferred to a liquid nitrogen tank for long-term storage. For retrieval of frozen cells, the vial was thawed in a water bath at 37 °C. The cells were resuspended in appropriate medium and 12-24h after thawing the medium was exchanged for fresh medium.

5.1.2 Culture of primary patient material

The effusion sample was obtained from a patient admitted to the gynecological clinic at the University Hospital of Mannheim by Prof. Dr. Med. Marc Sütterlin and Dr. Med. Saskia Speck in

August 2013. The study was approved by the ethical committee of the University of Mannheim (case number 2011-380N-MA) and conducted in accordance with the Helsinki Declaration. Written informed consent was obtained from the patient.

For preparation of the sample, the cells were pelleted (1200 rpm, 5 min, 4 °C) and red blood cell lysis was achieved using ACK Lysing Buffer (Lonza). Breast patient effusion 16 (BPE16) cells were cultured in adherent conditions in M199 medium at 37 °C and 5% CO_2 and passaged by the addition of StemPro® Accutase® Cell Dissociation Reagent (Thermo).

M199 complete
Medium 199 (Thermo)
2.5% FBS (10,000 U/ml) (Thermo)
1% (vol/vol) Penicillin-Streptomycin (10,000 U/ml) (Thermo)
1% (vol/vol) Amphotericin B
10% (vol/vol) L-Glutamine (200 mM) (Thermo)
10 µg/ml Insulin (Sigma)
0.5 µg/ml Hydrocortisone (Sigma)
100 µg/ml Epidermal Growth Factor (EGF; Sigma)
100 ng/ml Cholera toxin (Sigma)

5.1.3 Mammosphere assay

Mammary fat pats (3^{rd} and 4^{th}) were dissected from age-matched 8- to 16 week old virgin NOD/SCID interleukin-2 receptor gamma chain null (NSG) $TNC^{-/+}$ and NSG $TNC^{-/-}$ mice. The fat pads were finely minced using scalpels and digested at 37 °C for 1h in 0.3 % collagenase III (Worthington) and 0.1 % trypsin (Sigma) in CO_2 independent medium without additives (Thermo). Upon complete digestion, the fatty tissue was removed by two rounds of centrifugation and the pellet consisting of epithelial organoids, red blood cells, fragment of vessels and fibroblasts was resuspended in CO_2 independent medium / 10% FBS (Thermo). Red blood cell lysis was achieved using ACK Lysing Buffer (Lonza) and organoids were resuspended in DMEM / 5% FBS (Thermo) in a cell culture flask and incubated for 1h at 37 °C and 5% CO_2. After incubation, the flask was shaken horizontally with moderate vigor and the floating organoids were collected, while the attached fibroblasts were discarded. Preparation of single cell suspension from mammary epithelial organoids was achieved by incubating the organoids in 1:1 vol/vol versene (Sigma) / 0.25% trypsin (Sigma) 0.02% EDTA (Sigma) for 2 min in a 37 °C water bath. DNase 1 (5 µg/ml in CO_2 independent medium without additives) was added to the sample and incubated for further 5 min at 37 °C. Inactivation of trypsin enzymatic reaction was achieved by the addition of CO_2 independent medium / 10% FBS (Thermo) and the sample was

filtered through a 35 µm cell strainer to obtain single cell suspension. The cells were seeded in Ultra-low attachment cell culture flasks (Corning) at a density of 0.25 x 10^6 cells/ml and grown in mammosphere medium at 37 °C and 5% CO2. After 14 days, the mammospheres were passaged by the addition of StemPro® Accutase® Cell Dissociation Reagent (Thermo) and re-seeded at the same cell density. After additional 14 days, the AxioVision LE64 software was used for image acquisition and area quantification of mammospheres.

Mammosphere medium
HUMEC Basal Serum-Free Medium (Thermo)
0.25% (vol/vol) Penicillin-Streptomycin (10,000 U/ml) (Thermo)
5 µg/ml hydrocortisone (Sigma)
5 µg/ml insulin (Sigma)
20 ng/ml EGF (Sigma)
20 ng/ml Basic Fibroblast Growth Factor (bFGF; Invitrogen)
2% (vol/vol) B27® Supplement (Thermo)

5.1.4 Oncosphere assay

The breast cancer cells were seeded in Ultra-low attachment cell culture flasks (Corning) at a density of 0.25 x 10^6 cells/ml and grown in oncosphere medium at 37 °C and 5% CO_2 for 7 days. For harvesting, the cells were pelleted by centrifugation (1200 rpm, 5 min, 4 °C) and re-suspended in the appropriate buffer.

For quantitative analysis, the AxioVision LE64 software was used for image acquisition and area quantification of oncospheres with a minimum area of 15,000 µm^2.

Oncosphere medium
HUMEC Basal Serum-Free Medium (Thermo)
0.25% (vol/vol) Penicillin-Streptomycin (10,000 U/ml) (Thermo)
5 µg/ml insulin (Sigma)
20 ng/ml EGF (Sigma)
10 ng/ml bFGF (Invitrogen)
2% (vol/vol) B27® Supplement (Thermo)

5.1.5 Lentiviral production

Lentiviral particles were produced in HEK 293T cells, which were transfected at a confluency of 70%. 2.6 µg lentiviral plasmid, 2 µg envelope plasmid (pMD2G) and 5.4 µg packaging plasmid (psPAX2) were mixed in 850 µl Opti-MEM® Reduced Serum Medium (Thermo). In a second tube, 40.8 µl Lipofectamine® 2000 Transfection reagent (Thermo) were diluted in 809.2 µl Opti-MEM® Reduced Serum Medium. After 15 min incubation, the plasmid DNA mix was added to the Lipofectamine mix and incubated for further 30 min at room temperature. The HEK 293T cells were washed with phosphate-buffered saline (PBS; Sigma) and supplied with 5.1 ml transfection medium before adding the DNA-Lipofectamine mix. After 24 h, the medium was replaced by 7 ml fresh transfection medium. The viral supernatants were collected 48 h and 72 h after transfection and filtered through a 0.2 µm mesh to remove cellular debris. The viral particles were stored at -80 °C and thaed on ice prior infection.

Transfection medium
DMEM, GlutaMAX™ (Thermo)
10% Fetal Bovine Serum (10,000 U/ml) (Thermo)
1% (vol/vol) Sodium Pyruvate (100 mM) (Thermo)

5.1.6 Lentiviral infection

Target cells were transduced at a confluency of 70% by adding 600 µl non-concentrated viral particles and 600 µl appropriate medium supplemented with 8 µg/ml polybrene (Sigma). Successfully transduced cells were selected by Puromycin (2-3 µg/ml, Thermo) or Zeocin™ (800 µg/ml, Thermo) antibiotic selection (all) and sorted for fluorescent proteins (only miRE system). The lentiviral constructs are described below **(Table 3)**

Table 3 Short-hairpin RNA (shRNA) sequences, backbone vectors and origin.
The miRE shRNA were cloned in our laboratory as described below. Therefore no company or catalogue number is indicated.

Vector	Oligonuclotides	Antisense sequence (5'-3')	Company	Catalogue number
miRE-puromycin-BFP	ITGB3_1	TTTCATCACAGACTGTAGCCT		
miRE-puromycin-BFP	ITGB3_3	TAAGCATCAACAATGAGCTGG		
miRE-puromycin-BFP	REN713	TAGATAAGCATTATAATTCCT		
miRE-zeocin-tdTomato	ITGB1_1	TCAGTTGAAATTATCACACTC		
miRE-zeocin-tdTomato	ITGB1_3	TTAAACATCTATTTTCATCTG		
miRE-zeocin-tdTomato	TNC_1	TTTGGTAGAAGTTCTCGCGTC		
miRE-zeocin-tdTomato	TNC_2	TTGTCTGAGAAAATGACTTCC		
miRE-zeocin-tdTomato	REN713	TAGATAAGCATTATAATTCCT		
GIPZ-puromycin	ANXA2_3	TAATAGTACAGGGACTTGC	Open biosystem	V2LHS_190394
GIPZ-puromycin	EGFR_1	TTCCGTTACACACTTTGCG	Open biosystem	V2LHS_200678
GIPZ-puromycin	EGFR_2	TTTCCAAATTCCCAAGGAC	Open biosystem	V2LHS_201187
GIPZ-puromycin	GPC1_2	TGGTCATGATCTTCAGCTG	Open biosystem	V3LHS_307212
GIPZ-puromycin	GPC1_4	AGATCTGGCGGACCTCGCC	Open biosystem	V3LHS_307210
GIPZ-puromycin	ITGA2_4	GAACTGTGATTTCTGTCCT	Open biosystem	V3LHS_376868
GIPZ-puromycin	ITGAV_2	TTCTCAAAGGGTTGATCTC	Open biosystem	V2LHS_133468
GIPZ-puromycin	ITGAV_3	AAAACAGCAAGATCAACTT	Open biosystem	V3LHS_365150
GIPZ-puromycin	SDC4_1	ATACCACAGAGATTCCCGT	Open biosystem	V2LHS_30982
GIPZ-puromycin	SDC4_2	TCCATTTCAGCATAAACTC	Open biosystem	V2LHS_30985
GIPZ-puromycin	TLR4_1	TTTGTTTCAAATTGGAATG	Open biosystem	V2LHS_221582
GIPZ-puromycin	TLR4_2	TATTAAGGTAGAGAGGTGG	Open biosystem	V2LHS_171350
GIPZ-puromycin	non-target control	CTTACTCTCGCCCAAGCGAGAG	Open biosystem	RHS4348

5.2 Molecular cloning

For generation of miRE lentiviral shRNA vectors, 10 ng desalted oligomers (Sigma; **Table 3**) were amplified by polymerase-chain reaction (PCR) using Q5® High-Fidelity DNA Polymerase (NEB). Amplification primers are listed in **Table 4**. The PCR product was resolved by gel electrophoresis (2% agarose, Sigma) and extracted using the QIAquick gel extraction kit (Qiagen) according to manufacturer's instructions. Subsequently, the PCR product was digested with EcoRI-HF (NEB) and XhoI (NEB) restriction enzymes and purified using the QIAquick PCR purification kit (Qiagen) according to manufacturer's instructions. In parallel, 10 µg of vector was digested with EcoRI-HF (NEB) and XhoI (NEB) restriction enzymes and dephosphorylated using Antarctic Phosphatase (NEB) **(Figure 13)**. The reaction product was resolved by gel electrophoresis (1% agarose, Sigma) and extracted using the QIAquick gel extraction kit (Qiagen) according to manufacturer's instructions. Ligation was performed at 16 °C overnight in a 1:3 molar ratio using T4-Ligase (NEB). ElectroMAX Stbl4 Competent Cells (Invitrogen) were used for transformation. Positive clones were verified by Sanger sequencing (GATC Biotech) using the sequencing primer (**Table 4**).

Table 4 Primers for molecular cloning.

Oligonucleotide	Sequence (5'-3')
amplification primer (forward)	TGAACTCGAGAAGGTATATTGCTGTTGACAGTGAGCG
amplification primer (reverse)	TCTCGAATTCTAGCCCCTTGAAGTCCGAGGCAGTAGGC
sequencing primer	GCCACCAAAGAACGGAGCC

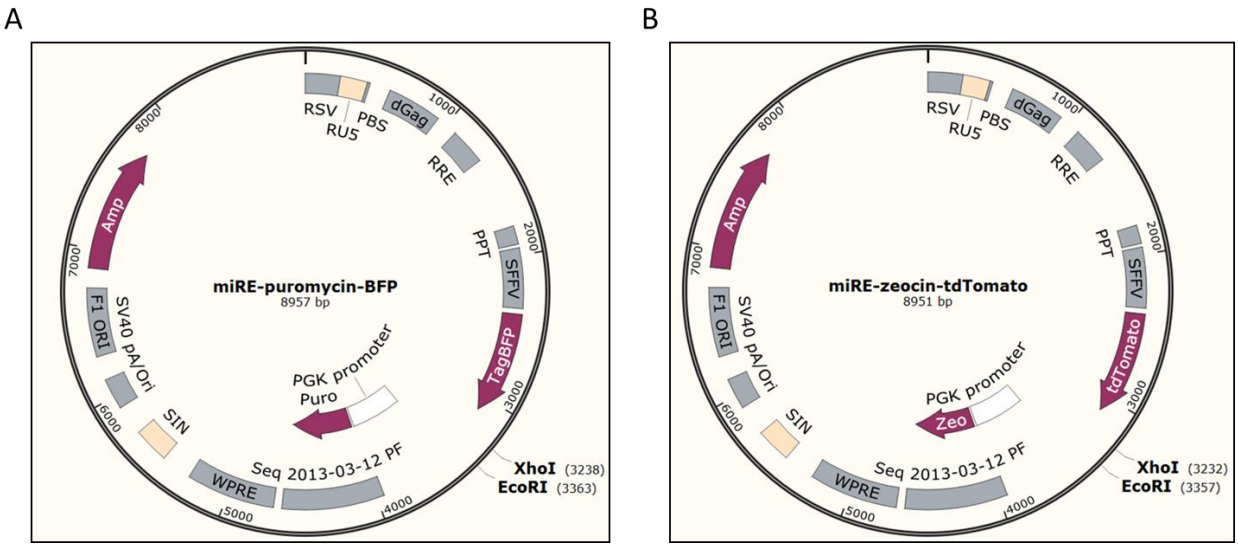

Figure 13 miRE-puromycin-BFP (A) and miRE-zeocin-tdTomato (B) vector map.
The restriction sites XhoI and EcoRI were used for molecular cloning as described in 5.2. The vectors were mapped using the SnapGene software.

5.3 Gene expression analysis

5.3.1 RNA extraction

Total RNA was isolated from different cell lines and from mouse mammary glands (four per mouse) using the RNeasy Mini Kit (Quiagen) according to manufacturer's instructions. Cells lines were lysed directly in RLT buffer supplemented with 1% β-mercaptoethanol (Sigma) and mammary glands were dissociated in the same buffer using the GentleMACS Dissociator (Miltenyi Biotec) according to manufacturer's instructions. RNA concentration and quality was determined using the NanoDrop (Thermo). RNA samples were stored at -80 °C.

5.3.2 Quantitative real-time PCR

Total RNA was reverse-transcribed using the High-Capacity cDNA Reverse Transcription Kit (Thermo) according to manufacturer's instructions. cDNA corresponding to 40 ng of starting RNA was used for quantitative real-time PCR (qRT-PCR). qRT-PCR was performed on the ViiA ™ 7 Real-Time PCR System (Applied Biosystems) according to the following program: 50 °C for 2 min, 95 °C for 10 min (enzyme activation phase), 95 °C for 15 sec, 60 °C for 1 min (40 cycles, amplification phase), 95 °C for 15 sec, 60 °C for 1 min, 95 °C for 15 sec (enzyme inaction and dissociation phase). SYBR® Green PCR Master Mix (Thermo) was used for detection of double-stranded PCR products. Data acquisition and analysis based on the $2^{-\Delta\Delta Ct}$ method were performed using the ViiA 7 ™ Software (version 1.2.2.). Target genes were normalized against *Hprt* (mouse) or *RPL13A* (human) **(Table 5)**. Primer specificity was verified by melting curve analysis and assessing of amplification product size by gel electrophoresis.

Table 5 qRT-PCR primers.

Oligonucleotide	Specie	Forward sequence (5'-3')	Reverse sequence (5'-3')
h*RPL13A*	human	AAGTACCAGGCAGTGACAG	CCTGTTTCCGTAGCCTCATG
h*TNC*	human	TAACAGCATCACCCTGGAAT	TCCTTGTCTTCCTTCACAGC
h*LGR5*	human	CATTTGTAGGCAACCCTTCTC	GGCACCATTCAGAGTCAGTGT
h*MSI1*	human	CCAATGGGTACCACTGAAGC	CACTCGTGGTCCTCAGTCAG
h*AXIN2*	human	AGTGTGAGGTCCACGGAAAC	TGGCTGGTGCAAAGACATAG
h*HEY2*	human	AAGATGCTTCAGGCAACAGG	CGCAAGTGCTGAGATGAGAC
h*ITGB1*	human	AACTGCACCAGCCCATTTAG	ACATTCCTCCAGCCAATCAG
h*ITGB3*	human	GTGTGCCTGGTGCTCTGAT	GAGTGACCTGGGAGCTGTCT
h*NANOG*	human	CACCTATGCCTGTGATTTGTG	AAGTGGGTTGTTTGCCTTTG
h*OCT4*	human	CAAGCTCCTGAAGCAGAAGAGGAT	CTCACTCGGTTCTCGATACTGGTT
h*SOX2*	human	TGTCAAGGCAGAGAAGAGAGTG	GCCGCCGATGATTGTTATTA
h*ANXA2*	human	AGCGGGATGCTTTGAACA	TGGTAGGCGAAGGCAATATC
h*EGFR*	human	CACCACGTACCAGATGGATGT	GCCCTTCGCACTTCTTACAC
h*GPC1*	human	GGCCCTGCCCTGACTATT	GTGAGCGTGTCCCTGTTGT
h*ITGA2*	human	CTGGAGTGGCTTTCCTGAGA	GTTCCCATGTTCCTGGTGAG
h*ITGAV*	human	TGGTTTGGAGCATCTGTGAG	TACCAGGACCACCAAGAAGT
h*SDC4*	human	GAGCCCTACCAGACGATGAG	CACCAAGGGATGGACAACTT
h*TLR4*	human	ACCTGGACCTGAGCTTTAATC	CACAGCCACCAGCTTCTGTA
m*Hprt*	mouse	TCAGTCAACGGGGGACATAAA	GGGGCTGTACTGCTTAACCAG
m*Krt14*	mouse	AGCGGCAAGAGTGAGATTTCT	CCTCCAGGTTATTCTCCAGGG
m*Fzd1*	mouse	CAGCAGTACAACGGCGAAC	GTCCTCCTGATTCGTGTGGC
m*Itgb1*	mouse	ATGCCAAATCTTGCGGAGAAT	TTTGCTGCGATTGGTGACATT
m*Itgb3*	mouse	GTGGGAGGGCAGTCCTCTA	CAGGATATCAGGACCCTTGG
m*Tnc*	mouse	GCATCGGTCACTGGATACCT	TGCTGAGTAGTGGGTGGATG
m*Lgr5*	mouse	CCTACTCGAAGACTTACCCAGT	GCATTGGGGTGAATGATAGCA
m*Rspo1*	mouse	CTGCCCACCTGGATACTTCG	CTTGTGCAGGTACAAGCCCT
m*Rspo3*	mouse	ATTGCCCAGAAGGGTTGGAA	TTTCTCGGACCCGTGTTTCA
m*Msi1*	mouse	TCAGCCAAAGGAGGTGATGTC	GTTGTGGCTTGGAAACCTGG
m*Hey2*	mouse	AGATGCTTCAGGCAACAGGG	GCGCAACTTCTGTTAGGCAC

5.4 Protein work

5.4.1 Generation of whole cell protein lysates

Cells were lysed in NP-40 lysis buffer (250 mM Tris-HCl pH7.4 (Sigma), 150 mM NaCl (Sigma), 1 mM EDTA (Sigma), 1% NP-40 (Sigma), 5% glycerol (Sigma)) supplemented with 1x HALT Protease and Phosphatase Inhibitor Cocktail (Thermo). Cells were washed three times with ice-

cold PBS (Sigma) and incubated in NP-40 lysis buffer for 5 min on ice. The resulting homogenate was transferred into a pre-cooled reaction tube, vigorously mixed by vortexing and incubated on ice for further 20 min. Finally, the lysate was centrifuged at 20,000 rpm for 15 min at 4 °C and the supernatant was transferred to a fresh, pre-cooled reaction tube. Protein lysates were stored at -20 °C until use.

Concentrations of protein lysates were quantified using the Pierce™ Micro BCA Protein Assay Kit (Thermo) according to manufacturer's protocol. Absorbance at 562 nm was measured at the SpectraMax M5 (Molecular Devices) and concentration were determined using the SoftMax Pro5.4 software (Molecular Devices).

5.4.2 Co-immunoprecipitation

Co-immunoprecipitation (Co-IP) was performed using the Pierce™ Crosslink Magnetic IP/Co-IP Kit (Thermo) according to manufacturer's instructions. Cells were cultured as oncospheres. Whole cell protein lysates were generated as described above without vigourous mixing of the homogenate. 625 µg and 1250 µg whole cell protein lysates were loaded per Co-IP for MDA MB231 LM2 and SUM159 LM1, respectively, elution volume was 50 µl per Co-IP.

5.4.3 Single reaction monitoring analysis

Single reaction monitoring (SRM) analysis was performed by Dr. Sabrina Hanke. The eluates of 16 Co-IPs per sample were combined, neutralized and concentrated in a vacuum concentrator. Proteins were reduced with 5 mM tris(2-carboxyethyl)phosphine (TCEP, BioVision) at 60 °C for 30 min followed by alkylation with 15 mM iodoacetamide (IAA, Sigma-Aldrich) for 30 min at 37 °C. Subsequently, proteins were precipitated with chloroform/methanol as described previously [1]. The protein pellets were resolubilized in 0.1% RapiGest SF Surfactant (Waters) in Tryptic Digestion Buffer (50 mM Tris-HCl, 1 mM CaCl2 in water, pH 8) by sonication for 30 min and digested with Sequencing Grade Modified Trypsin (1:25, w/w, Promega) for 15 h at 37 °C and 1200 rpm. Samples were acidified to 0.5% TFA (10% TFA in water, ProteoChem) and incubated for 30 min at 37 °C at 1200 rpm. Acidified protein solutions were separated from insoluble detergent by-products by 10 min centrifugation at 20,000 × g. Samples were desalted using a 96-well, C18 Lab-in-a-plate Flow-Thru Plate (Glygen), dried in a vacuum concentrator and resuspended in 3% acetonitrile, 0.1% formic acid, 0.01% TFA in water containing the heavy peptide pool (see below).

Based on the SRM Atlas data (www.srmatlas.org, January 2016), up to five proteotypic peptides per target protein were selected for selected reaction monitoring (SRM). Peptides were restricted to a mass range of 600-2000 Da, methionine and cysteine containing peptides were excluded if possible. To determine the levels of the endogenous target peptides in the IP samples, heavy peptide standards corresponding to their natural counterparts (light) were synthesized with heavy isotopic lysine (13C615N2) or arginine (13C615N4) at the C terminus (Intavis, Germany), pooled and spiked into the digested and desalted samples to a final concentration of 0.5 pmol/µL.

SRM analysis was performed on a QTRAP 6500 mass spectrometer (SCIEX) operated with Analyst software (v1.6.2) and coupled to a nanoAcquity UPLC system (Waters) equipped with a nanocapillary, reversed-phase M-Class Peptide CSH C18 Column (130 Å pore size, 1.7 µm particle size, 300 µm x 150 mm, Waters). Column temperature was set to 55 °C. 10 µL of each sample were injected by full-loop injection and loaded on the column within 4 min (3% acetonitrile in 0.1% formic acid, 0.01% TFA in water). Samples were separated over 120 min at a flow rate of 6 µl/min using 4 to 30% (1-110 min), 30-85% (110-115 min), 85-3% (115-120 min) acetonitrile gradient in 0.1% formic acid, 0.01% TFA in water (Biosolve).

For SRM method optimization and validation, MS/MS spectra of the heavy peptide pool were acquired in the trap mode (enhanced product ion) with dynamic fill time, Q1 resolution low, scan speed of 10000 Da/s, m/z range of 100-2000. Peptides and transitions are listed in **Table 6**. Scheduled SRM were performed with Q1 operated in unit resolution, Q3 in low resolution, a target scan time of 2 s, a median (minimal) dwell time of 106 ms (37 ms) and retention time windows of ±2.75 min around the specific elution time.

SRM data were processed using the Skyline software (version 3.5.0.9319). For correct peak detection, the default peak boundary assignment based on Savitzky-Golay smoothing was manually reassigned if required. Peptides with unfavorable elution profile or interfering peaks in the light transitions were excluded from further data analysis. Information including background-reduced peak area of heavy and light peptides were exported for further analysis. For each peptide, peak areas of corresponding transitions were summed for analysis. The ratio between the background reduced peak area of the light transition and the background reduced peak area of the heavy transition was calculated to correct for ionization or spray differences between runs. To obtain a reliable quantification, peptides with an average peak area of the light peak less than two-fold up-regulated in the samples compared to the background signal of three averaged SRM measurements of heavy peptide pool in solvent were excluded from analysis. For visualization, peak areas were normalized to the maximal peak area.

Table 6 Peptides and transitions for SRM analysis.

Accession	Accession Name	Peptide Sequence	Transition	Modification	Precursor m/z	Fragment m/z	Retention Time (min)	Declustering Potential	Collision Energy
P02751	FINC_HUMAN	WC[CAM]GTTQNYDADQK	+2y11	light	793.830637	1240.544036	12.7	89	37.4
P02751	FINC_HUMAN	WC[CAM]GTTQNYDADQK	+2y9	light	793.830637	1082.474893	12.7	89	37.4
P02751	FINC_HUMAN	WC[CAM]GTTQNYDADQK	+2y7	light	793.830637	853.368637	12.7	89	37.4
P02751	FINC_HUMAN	WC[CAM]GTTQNYDADQK	+2y11	heavy	797.837736	1248.558235	12.7	89	37.4
P02751	FINC_HUMAN	WC[CAM]GTTQNYDADQK	+2y9	heavy	797.837736	1090.489092	12.7	89	37.4
P02751	FINC_HUMAN	WC[CAM]GTTQNYDADQK	+2y7	heavy	797.837736	861.382836	12.7	89	37.4
P05106	ITB3_HUMAN	WDTANNPLYK	+2y9	light	611.29857	1035.510551	31.8	75.7	30.9
P05106	ITB3_HUMAN	WDTANNPLYK	+2y8	light	611.29857	920.483607	31.8	75.7	30.9
P05106	ITB3_HUMAN	WDTANNPLYK	+2y7	light	611.29857	819.435929	31.8	75.7	30.9
P05106	ITB3_HUMAN	WDTANNPLYK	+2y9	heavy	615.305669	1043.52475	31.8	75.7	30.9
P05106	ITB3_HUMAN	WDTANNPLYK	+2y8	heavy	615.305669	928.497806	31.8	75.7	30.9
P05106	ITB3_HUMAN	WDTANNPLYK	+2y7	heavy	615.305669	827.450128	31.8	75.7	30.9
P24821	TENA_HUMAN	ITAQGQYELR	+2y8	light	589.811844	964.48467	19	74.1	30.1
P24821	TENA_HUMAN	ITAQGQYELR	+2y7	light	589.811844	893.447556	19	74.1	30.1
P24821	TENA_HUMAN	ITAQGQYELR	+2y6	light	589.811844	765.388979	19	74.1	30.1
P24821	TENA_HUMAN	ITAQGQYELR	+2y8	heavy	594.815979	974.492939	19	74.1	30.1
P24821	TENA_HUMAN	ITAQGQYELR	+2y7	heavy	594.815979	903.455825	19	74.1	30.1
P24821	TENA_HUMAN	ITAQGQYELR	+2y6	heavy	594.815979	775.397248	19	74.1	30.1

5.4.4 Western blot

Protein lysates were mixed with 4x NuPAGE LDS sample buffer (Thermo) and 10x NuPAGE reducing agent (Thermo) and heated to 95 °C for 12 min. Protein lysates were resolved on 4-12% Bis-Tris NuPAGE gels (Thermo) with 1x MOPS buffer (Thermo) for 2 h at 120 V and blotted on PVDF membrane (Biorad) for 2 h at 25 V. Membranes were blocked overnight at 4 °C in 1x TBS (10x TBS: 48.4 g Tris-Base (Sigma), 160 g NaCl (Sigma), 2 l water, pH 7.5) supplemented with 0.1% (vol/vol) Tween-20 (Sigma) and 5% (wt/vol) non-fat dry milk powder (Sigma) (blocking solution). Primary antibodies (**Table 5**) were incubated for 2 h at room temperature in blocking solution. Membranes were washed 5 times for 5 min in 1x TBS supplemented with 0.1% (vol/vol) Tween-20 (Sigma; washing buffer). HRP-conjugated secondary antibodies (1:10,000; Dako) were incubated for 1 h at room temperature in blocking solution. Membranes were washed again 5 times for 5 min in washing buffer and the formed immunocomplexes were revealed using the ECL Prime Western Blotting Detection Reagent according to manufacturer's instructions (Amersham International).

5.4.5 Fluorescence-activated cell sorting

For fluorescence-activated cell sorting (FACS), 0.2 x 10^^{6} cells were washed twice in staining solution (PBS (Sigma) supplemented with 2% (vol/vol) Fetal Bovine Serum (Thermo)) and incubated in Cytofix/Cytoperm™ buffer (BD) for 20 min at 4 °C for permeabilization. After washing in Perm/Wash™ buffer, the cells were labelled with a CK FITC-conjugated antibody (**Table 5**) for 45 min in the dark at 4 °C. The cells were washed twice with Perm/Wash™ buffer, filtered and acquisition was performed at the Cyan ADP cytometer (Beckman Coulter). The same protocol was applied for ITGAV PE-conjugated antibody (**Table 5**) labelling with omission of the fixation and permeabilization steps. Instead, the cells were washed in staining solution. Data analysis was conducted using the FlowJo Software.

Cell sorting experiments were performed with FACS Aria I or II (BD) for blue fluorescent protein (BFP) or tdTomato expression at the Imaging and Cytometry DKFZ Core Facility.

5.5 Tissue analysis

5.5.1 Immunohistochemistry

For immunohistochemical stainings, dissected lungs were fixed in formalin (Sigma) overnight at 4 °C, dehydrated with increasing concentrations of ethanol (Sigma) followed by xylene (Sigma) and subsequently embedded in paraffin. 5 µm sections were deparafinized, rehydrated and quenched by H_2O_2 (Sigma). Antigen retrieval was performed by incubating the sections in Pepsin (DAKO) at 37 °C for 14 min (TNC) or by boiling the sections in pH 6 target retrieval solution (DAKO) in a steam pot for 20 min (VIM). The sections were incubated in blocking solution (1% bovine serum albumin (Sigma), 0.1% Triton X 100 (AppliChem) in PBS). Primary antibody (**Table 7**) staining in blocking solution was performed overnight at 4 °C. On the next day, the sections were incubated for 30 min with appropriate biotinylated secondary antibody (1:200, Vector Laboratories) at room temperature. The immunocomplexes were revealed by using the Vectastain ABC HRP Kit and the DAB Substrate Kit (Vector Laboratories) according to manufacturer's instructions. Between each step the sections were washed in PBS (10 mM Na_2HPO_4 (Sigma), 2.68 mM KCl (Sigma), 140 mM NaCl (Sigma), pH 7.45) for 5 min. The sections were counterstained with hematoxylin solution according to Mayer (Sigma) and washed in tap water. Before mounting in Cytoseal XYL (Thermo), dehydration and clearing in xylenes (Sigma) was performed.

For hematoxylin and eosin (HE) staining, 5 µm sections were deparafinized, rehydrated and stained for 6 min with hematoxylin solution according to Mayer (Sigma). Differentiation was obtained by a short incubation in alcoholic acidic solution (200 ml ethanol supplemented with 0.3% concentrated hydrogen chloride) followed washing in tap water. The sections were counterstained with eosin Y alcoholic solution (Sigma), dehydrated and cleared in xylenes (Sigma) before mounting in Cytoseal XYL (Thermo).

Images were acquired at the Cell Observer.Z1 (Zeiss) microscope at the Imaging and Cytometry DKFZ Core Facility and processed with the ZEN software (Zeiss).

Table 7 Antibodies for Western Blot (WB), fluorescence-activated cell sorting (FACS) and immunohistochemistry (IHC).

Antigen	Manufacturer (catalogue number)	Specie	Technique (dilution)
TNC	Santa Cruz (sc-20932)	rabbit	WB (1:1,000)
ITGB1	Cell Signaling (4706S)	rabbit	WB (1:1,000)
ITGB3	Cell Signaling (13166)	rabbit	WB (1:1,000)
GAPDH	Abcam (ab9484)	mouse	WB (1:10,000)
CK	Miltenyi (130-080-101)	mouse	FACS (1:10)
ITGAV	Biolegend (104105)	mouse	FACS (1:10)
TNC	Sigma (T2551)	mouse	IHC (1:4,000)
VIM	Novocastra (NCL-L-VIM-572)	mouse	IHC (1:400)

5.5.2 Tissue microarray analysis

The tissue microarray (TMA) was constructed from mammary carcinoma biopsy samples at the Pathology Department of the University Hospital of Heidelberg between 2001 and 2002 under the supervision of Prof. Dr. Med. Peter Sinn. Analysis was performed using the Definiens software Tissue Studio® version 4.2. Percental score was calculated using the following formula:

Percental score = 3x [% area immunohistochemistry TNC high stain] + 2x [% area immunohistochemistry TNC medium stain] + 1x [% area immunohistochemistry TNC low stain]

5.6 *In vivo* lung colonization assay

Animal care and all procedures followed the German legal regulations and were previously approved by the governmental review board of the state of Baden-Wuertemberg, Regierungspraesidium Karlsruhe (authorization numbers G51-13).

Mice were bred and housed in individually ventilated cages in the animal facility of the DKFZ under specific pathogen-free conditions.

Lung colonization assay was performed on 6- to 8-week old NSG mice by intravenous injection of 200,000 single cells labelled with a triple modality reporter proteins and resuspended in 100 µl PBS (Sigma) [193]. Metastatic growth was monitored weekly *in vivo*. For this purpose, 200 µl D-Luciferin (15 mg/ml, Biosynth) was injected intraperitoneally 10 min prior measurement. Bioluminescence was acquired by the IVIS Spectrum In Vivo Imaging System (PerkinElmer) under inhalational anesthesia by Isoflurane (Ecuphar). The mice were sacrificed when the *in vivo* photon flux reached 10^9 photon / sec or when the mice showed any sign of distress. At

experimental end point, the mice were sacrificed and bioluminescence of the lung was acquired *ex vivo*. Data processing was performed with the Living Image® software.

5.7 Whole mount staining of the mammary fat pad

TNC-deficient mice (C57BL/6J *Tnc*^{tmRef1}) were provided by Prof. Dr. Reinhard Faessler. Age-matched TNC knockout and wildtype mice were sacrificed and the third and fourth mammary fat pads were dissected and stretched on a glass slide. Whole mount stainings were performed using VitroView™ Mammary Gland Whole Mount Stain Kit (GeneCopoeia™) following manufacturer's instructions. The slides were imaged using the Perfection V850 Pro scanner (Epson) at the Imaging and Cytometry DKFZ Core Facility. Quantification of the epithelial area was performed semiautomatically using the ImageJ software.

5.8 Survival analysis of breast cancer patients

The Kaplan-Meier Plotter compiles 26 publically available gene expression datasets (Affymetrix) from 3554 BrCa primary breast tumors [194] (www.kmplot.com/analysis/). The patients were stratified based on the 2013 St Gallen criteria (TN: *ESR1*-/*HER2*-, luminal A: *ESR1*+/*HER2*-/*MKI67* low, luminal B: *ESR1*+/*HER2*-/*MKI67* high and *ESR1*+/*HER2*+, HER2 subtype: *ESR1*-/*HER2*+). Classification of the patients according to *TNC* median expression value was performed automatically.

Normalized gene expression profiling (Illumina) of 1992 fresh frozen primary breast tumors was obtained from METABRIC (Molecular Taxonomy of Breast Cancer International Consortium) [195]. The patients were stratified according to PAM50 intrinsic breast cancer subtypes (luminal A, luminal B, HER2 or basal). Classification of the patients according to *TNC*, *ITGB1* and *ITGB3* expression values was performed manually.

5.9 Graphical output and statistical testing

Graphical illustration of analyzed data and statistical testing were performed using the GraphPad Prism software, version 6.

6 Results

6.1 TNC mediates metastasis in triple-negative breast cancer

6.1.1 Cancer cell-derived TNC is associated with poor clinical prognosis in triple-negative breast cancer

TNC is expressed in many different tumor entities and its expression is often associated with poor clinical outcome. In breast malignancies, growing evidence suggests that high expression of TNC correlates with poor metastasis-free and overall survival of the patients [94, 100, 147-150]. Interestingly, a negative correlation between ER positivity and TNC expression has been suggested by independent studies [145, 146]. We sought to investigate further the prognostic value of TNC in breast cancer and its potential association to a particular subtype. To this end, I performed a survival analysis according to TNC level on gene expression profiling of breast cancer patients. I used the Kaplan-Meier Plotter, an online tool, which integrates gene expression and clinical annotations from 3554 primary breast cancer tumors in order to assess putative biomarkers [194]. In order to include as many patients as possible in the analysis, stratification was based on gene expression of the biomarkers *ER*, *HER2* and *Ki67*. Indeed, although IHC remains the golden standard for determining receptor status, the use of microarray-derived gene expression for *ER*, *HER2* and *Ki-67* has been demonstrated to stratify patients in a reliable manner [5, 6]. The patients were separated into four groups: luminal A, luminal B, HER2-enriched and triple-negative. Upon stratification of the patients according to subtype, the patients were classified as '*TNC* high' or '*TNC* low'. *TNC* lower quartile (0 – 25%) was defined as cutoff value. Kaplan-Meier analysis of relapse-free survival was then generated for the different subtypes according to *TNC* expression. Surprisingly, the analysis of all subtypes did not show any significant difference in relapse-free survival between the '*TNC* high' and the '*TNC* low' groups. However, patient stratification revealed striking differences between the subtypes regarding *TNC* prognostic value. While in the luminal (A and B) and in the HER2-enriched subtypes expression of *TNC* did correlate with clinical prognosis, high expression of *TNC* in triple-negative primary tumors was associated with significantly shorter relapse-free survival of the patients compared to those displaying low expression of TNC **(Figure 14, A - E)**. Therefore, we concluded that the prognostic value of TNC in breast cancer is specific to the triple-negative subtype. These results were confirmed by using IHC based subtypes: In patients negative for ER, PR and HER2, high expression of *TNC* is associated with shorter relapse-free survival, while *TNC* does not predict clinical outcome in the other subtypes (data not shown).

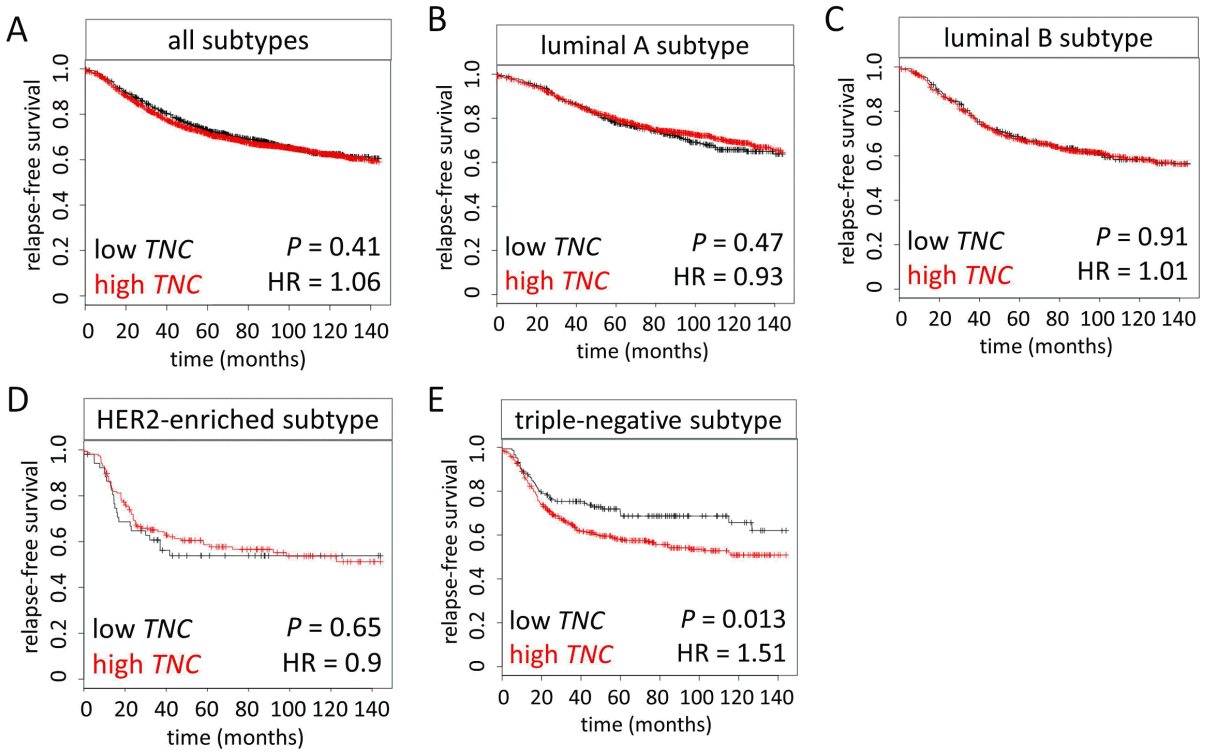

Figure 14 TNC predicts relapse-free survival in triple-negative breast cancer (Kaplan-Meier plotter).

Kaplan-Meier analysis of relapse-free survival of breast cancer patients (*n* = 3554), luminal A breast cancer patients (*n* = 2069), luminal B breast cancer patients (*n* = 1166), HER2-enriched breast cancer patients (*n* = 239) and triple-negative breast cancer patients (*n* = 580). Subjects were classified according to subtypes (luminal A: *ER1+/HER2-/Ki67* low, luminal B: *ER1+/HER2-/Ki67* high and *ER1+/HER2+*, HER2-enriched subtype: *ER1-/HER2+*, triple-negative: *ER1-/HER2-*) and TNC lower quartile value using Kaplan-Meier plotter online tool for breast cancer (probe: 201645_at). *P* value was calculated by log-rank test. HR : hazard ratio.

We next sought to validate this finding using an independent dataset. To this purpose, I performed a meta-analysis on a gene expression profiling dataset of 1992 breast cancer patients originally published by the Molecular Taxonomy of Breast cancer International Consortium (METABRIC) [195]. This dataset is clinically annotated and allows the stratification of the patients according to the PAM50 intrinsic breast cancer subtypes (luminal A, luminal B, HER2 and basal-like-like subtypes). As expected, the basal-like subtype strongly overlaps with negativity for ER, (PR) and HER2: 78% of the patients classified as basal-like are negative for ER expression and display normal expression of HER2, as determined by IHC. When considering gene expression, 76.8% of the basal-like-like patients are negative for ER, PR and HER2.

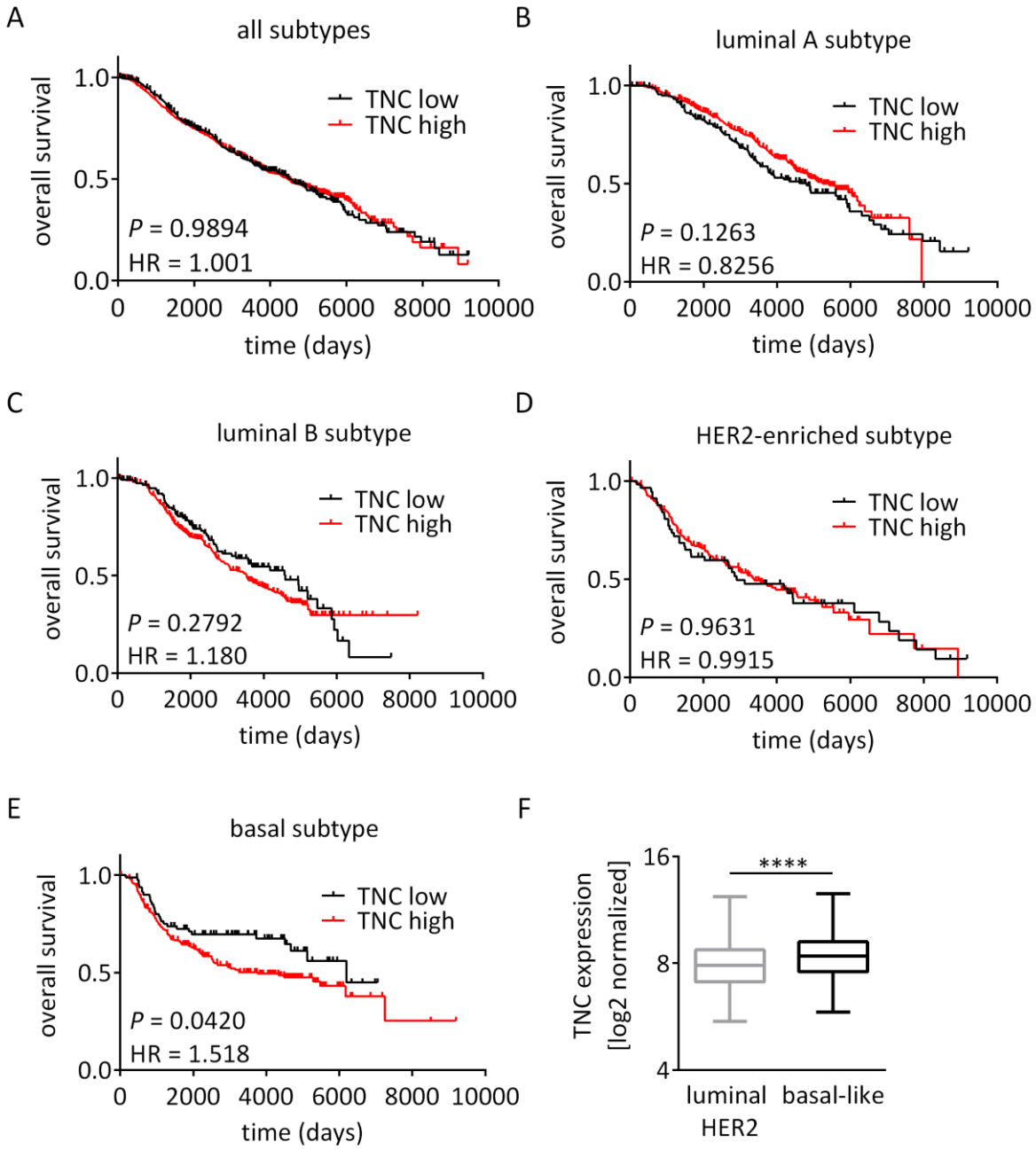

Figure 15 TNC expression is enriched and predicts poor overall survival in the basal-like subtype of breast cancer (METABRIC dataset).

(A – D) Kaplan-Meier analysis of overall survival of patients belonging to (C) all subtypes (n = 1774), (D) the luminal A subtype (n = 718), (E) the luminal B subtypes (n = 490) and (F) the HER2-enriched subtype (n = 238) were classified according to TNC lower quartile (probe: 201645_at). P values were calculated by log-rank Mantel Cox test. **(E)** Kaplan-Meier analysis of overall survival of basal-like breast cancer patients (*n* = 328) in the METABRIC datasets. Patients were stratified

according to PAM50 assay and TNC lower quartile (probe: 201645_at). P value was calculated by log-rank test. HR : hazard ratio. **(F)** TNC expression in the METABRIC datasets. Patients were stratified according to PAM50 assay (n = 1774). ****P < 0.0001; by two-tailed Mann-Whitney test.

The patients were first stratified according to PAM50 intrinsic breast cancer subtypes. In each subtype, the lower quartile (0 – 25%) of *TNC* expressing tumors was defined as '*TNC* low', whereas the '*TNC* high' group comprised the rest of the cohort. In the basal-like subtype, which comprises 328 patients, high expression of *TNC* in the primary tumor correlated with significantly shorter overall survival of the patients when compared to low expression of *TNC* (*P* = 0.0420, HR = 1.518) **(Figure 15, E)**. Remarkably, this did not apply to the other three subtypes (luminal A, luminal B, HER2) or when considering all subtypes. In these cohorts, expression level of TNC did not show any significant prognostic value in term of overall survival **(Figure 15, A – D)**. Interestingly, we observed a significant enrichment in TNC expression in the basal-like patients compared to other subtypes **(Figure 15, F)**.

These findings prompted us to further investigate the expression level and the cellular origin of TNC in breast tumor. To address this, we made use of a clinically annotated tissue microarray (TMA) composed of 205 cores, each of them corresponding to a mammary carcinoma primary tumor. Semi-automatic quantification using the Definiens Software Tissue Studio® was performed on each core to determine a percental score for TNC expression. This scoring allows weighting of tissue areas according to signal intensity, i.e. within a core, a tissue area with high TNC expression contributes three-times more to the scoring than a sized-matched area with low TNC expression. The tumors were then classified according to their receptor status as annotated by a pathologist. This analysis revealed a significantly higher TNC percental score in triple-negative tumors compared to luminal and HER2 tumors, indicating that the overall protein expression of TNC is higher in the triple-negative subtype than in other subtypes **(Figure 16, A and B)**.

The cancer-associated stroma, especially myofibroblasts, has been reported to be the major source of TNC in tumors. However, in some cases cancer cells can also express TNC in an autocrine manner [141, 142]. Accordingly, many cores showed a typical stromal TNC expression pattern and no expression by the cancer cells (CaC TNC-). Nevertheless, some tumors clearly showed autocrine TNC expression by the cancer cells (CaC TNC+, **Figure 16, D**). Stratifying the patients according to their receptor status revealed that 60% of triple-negative tumors displayed a CaC TNC+ phenotype against only 20% in the luminal and HER2 subtype (**Figure 16, C**). This finding strongly suggests that the propensity to express TNC in an autocrine manner is associated with the triple-negative subtype, while the cancer-associated stroma remains the main source of TNC in the other subtypes.

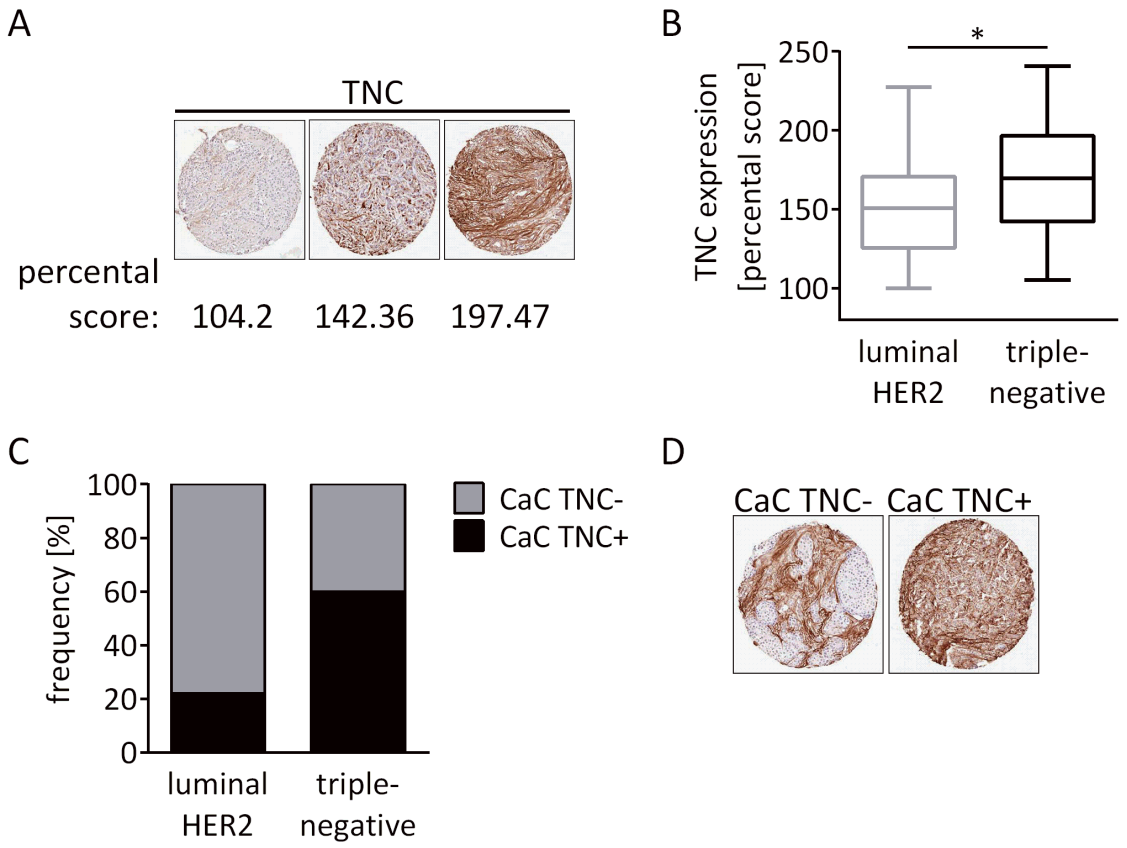

Figure 16 Cancer-cell derived TNC is enriched in triple-negative breast cancer tumors.
(A) Exemplary images showing TNC immunostaining and the corresponding percental score as determined by the Definiens Software Tissue Studio®. **(B)** TNC expression breast cancer patients primary tumors (*n* = 205). Subjects were classified according to pathological annotation of the estrogen receptor (ER), progesterone receptor (PR) and human epidermal growth factor receptor 2 (HER2) immunohistochemistry markers (luminal: ER^+/PR^+, HER2: $HER2^+$, triple-negative: $ER^-/PR^-/HER2^-$). $*P < 0.05$; by two-tailed Mann-Whitney test. **(C)** Frequency of CaC TNC- and CaC TNC+ cores in the TMA (*n* = 110). Subjects were classified according to pathological annotation of the ER, PR and HER2 immunohistochemistry markers (luminal: ER^+/PR^+, HER2: $HER2^+$, triple-negative: $ER^-/PR^-/HER2^-$). **(D)** Representative images showing exclusively cancer cell-derived negative TNC immunostaining (CaC TNC- ; left) and cancer-cell derived positive TNC immunostaining (CaC TNC+ ; right) of paraffin sections from a TMA consisting of samples from various breast cancer subtypes.

In summary, we found that the prognostic value of TNC in breast cancer is restricted to the triple-negative subtype and that this subtype expresses more TNC compared to the other subtypes. In addition, we showed that triple-negative breast cancer tumors express TNC in a cancer-cell autonomous manner.

6.1.2 TNC mediates lung colonization in a pre-clinical model

TNC has been previously shown to play a functional role in two different breast cancer metastasis mouse models [94, 164]. We used a pre-clinical xenograft model in order to validate the pro-metastatic function of TNC. Therefore, we generated two independent TNC knockdown sublines in the SUM159 LM1 cell line using shRNA interference technology **(Figure 17, A)**. The cell line was previously labelled with a triple modality reporter and expresses the oxidative enzyme luciferase, in addition to the green fluorescent protein (GFP) and thymidine kinase. The luciferase enzyme catalyzes the reaction of luciferin to oxyluciferin under the emission of light, so-called bioluminescence, which can be quantified. This technique allows *in vivo* and *ex vivo* quantification of metastatic burden upon intraperitoneal injection of luciferin [193].

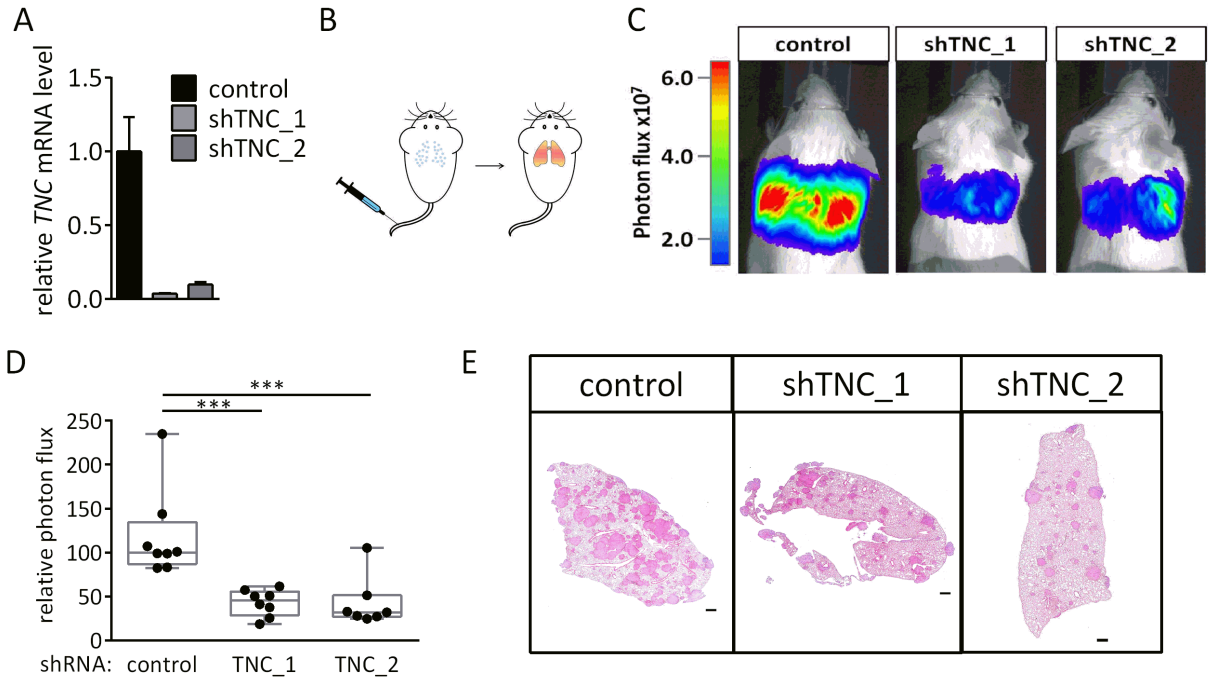

Figure 17 TNC mediates metastasis to the lungs in a triple-negative breast cancer xenograft model.
(A) Gene expression analysis by qRT-PCR of control and TNC knockdown SUM159 LM1 cells. For all genes, the expression in the knockdown line was normalized to the control line. Error bars depict means + SD of technical replicates (n = 3). **(B)** Scheme showing lung colonization assay by intravenous injection of human cancer cells into immunocompromised mouse. **(C)** Representative images showing in vivo

bioluminescence in mice injected intravenously with control and TNC knockdown SUM159 LM1 cells at experimental endpoint. **(D)** Lung colonization, as determined by *ex vivo* bioluminescence, in mice injected intravenously with control and TNC knockdown SUM159 LM1 cells (n = 7-8 per group). Whiskers represent minimum and maximum values. ***P < 0.001; by one-way ANOVA with Dunnett's multiple comparisons test. **(E)** Representative images showing HE staining of paraffin-embedded lungs of mice injected intravenously with control and TNC knockdown SUM159 LM1 cells at experimental endpoint. Scale bars, 500 µm.

Together with a non-targeting shRNA control, we injected the TNC knockdown sublines intravenously into immunocompromised NSG mice and assessed their ability to colonize the lungs by bioluminescence imaging **(Figure 17, B)**. Knocking down TNC in the cancer cells resulted in a significant 2- to 3-fold decrease in lung colonization ability of the cancer cells **(Figure 17, C and D)**. Hematoxylin and eosin (HE) staining on paraffin-embedded lungs confirmed that TNC knockdown cells formed less metastatic foci compared to control cells **(Figure 17, E)**. These results, together with previously published studies, confirmed that autocrine TNC mediates metastasis to the lung in breast cancer.

6.2 Identification of ITGB1 and ITGB3 as TNC receptors in triple-negative breast cancer metastasis to the lungs

6.2.1 Candidates and workflow

In order to understand how TNC signals to the cancer cells, we sought to identify the receptor(s) mediating this pro-metastatic signaling cascade in triple-negative breast cancer. Various cell surface receptors have been suggested to support TNC activity in different biological processes (see 3.3.1). Based on the literature, we used microarray and qRT-PCR gene expression analysis (data not shown) to establish a list of receptor candidates expressed in the triple-negative cell line MDA-231 LM2. We obtained a list of 9 receptors: ANXA2, EGFR, GPC1, ITGA2, ITGAV, ITGB1, ITGB3, SDC4 and TLR4. I then applied the following workflow: Each candidate was knocked down separately by shRNA interference technology using two independent hairpins and the expression of known TNC target genes (*LGR5*, *MSI1* and *HEY2*) was monitored upon knockdown. We selected the receptor candidates, whose knockdown caused at least 50% decrease in mRNA expression of at least one of the target genes. The scoring candidates were further analyzed for their ability to bind to TNC and to mediate lung colonization *in vivo* **(Figure 18, A and B)**.

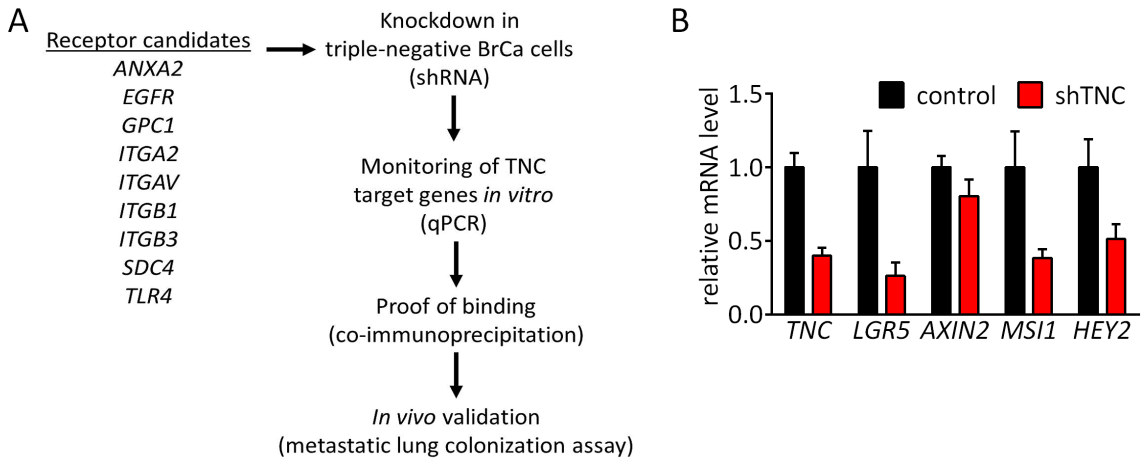

Figure 18 Workflow followed for identification of receptor(s) mediating the TNC signaling. **(A)** Scheme showing workflow for identification of TNC cell surface receptors. Shortly, receptor candidates, as suggested by literature and gene expression data, were knocked down by shRNA and gene expression analysis of the TNC target genes was performed *in vitro*. For the scoring candidates, binding to TNC was verified by endogenous co-immunoprecipiation. The final candidates were validated *in vivo* in a metastatic lung colonization assay. **(B)** Gene expression analysis by qRT-PCR of control and TNC knockdown in MDA231 LM2 cells. For all genes, the expression in the knockdown line was normalized to control. Error bars depict means + SD of biological replicates (n = 3).

6.2.2 ANXA2, EGFR, GPC1, SDC4 and TLR4 do not control the expression of the TNC target genes

The knockdown screen allowed ruling out of 5 of the receptor candidates. Indeed, upon knockdown of ANXA2, EGFR, GPC1, SDC4 and TLR4 in triple-negative metastatic breast cancer cells no major decrease of the TNC target genes *LGR5*, *MSI1* and *HEY2* could be observed **(Figure 19)**. Therefore, these receptors were not considered in further analyses.

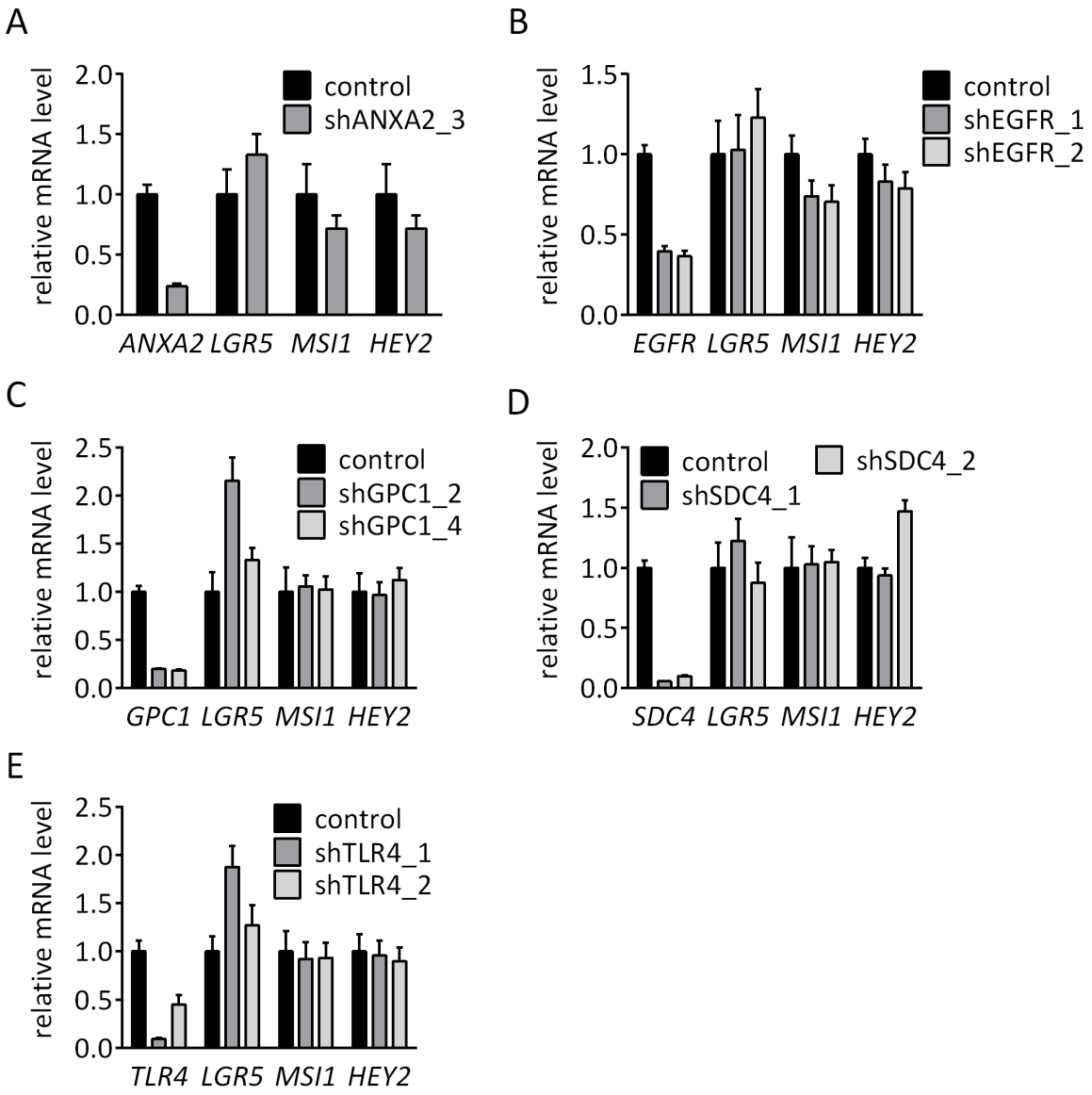

Figure 19 TNC signaling upon knockdown of ANXA2, EGFR, GPC1, ITGAV, SDC4 and TLR4.
(A) Gene expression analysis by qRT-PCR of control and ANXA2 knockdown oncospheres. For all genes, the expression in the knockdown line was normalized to the control line. Error bars depict means + SD of biological replicates (*n* = 3). **(B)** Gene expression analysis by qRT-PCR of control and EGFR knockdown oncospheres. For all genes, the expression in the knockdown lines was normalized to the control line. Error bars depict means + SD of biological replicates (*n* = 3). **(C)** Gene expression analysis by qRT-PCR of control and GPC1 knockdown oncospheres. For all genes, the expression in the knockdown lines was normalized to the control line. Error bars depict means + SD of biological replicates (*n* = 3). **(D)** Gene expression analysis by qRT-PCR of control and SDC4 knockdown oncospheres. For

all genes, the expression in the knockdown lines was normalized to the control line. Error bars depict means + SD of biological replicates (*n* = 3). **(E)** Gene expression analysis by qRT-PCR of control and TLR4 knockdown oncospheres. For all genes, the expression in the knockdown lines was normalized to the control line. Error bars depict means + SD of biological replicates (*n* = 3).

6.2.3 ITGB1 and ITGB3 control the expression of the TNC and Wnt target gene *LGR5*

ITGB1 and ITGB3 were as well knocked down using shRNA interference technology in two triple-negative metastatic breast cancer cell lines (MDA231 LM2 and SUM159 LM1). The MDA231 cell line was generated out of the pleural effusion of a 51-year old patient with disseminated disease who relapsed several years after removal of the primary tumor [196, 197]. Later on, MDA231 cells were used to generate organ-specific metastatic derivative cell lines by the mean of *in vivo* selection using immunocompromised mice [100, 198]. Briefly, the MDA231 parental cells able to form metastasis in the lung upon inoculation in the blood stream were isolated and denoted lung metastatic derivative 1 (LM1). The MDA231 LM1 line was then submitted to a second round of *in vivo* selection in order to generate the MDA231 LM2, which increased ability to colonize the lung compared to the parental MDA231 cell line. Comparison of the gene expression profiling of the metastatic line to the parental line has led to the definition of a gene expression signature predicting lung metastasis. This allowed the identification of various functional mediator of breast cancer lung metastasis [100]. Importantly, the enrichment of TNC in the metastatic derivative cells was the starting point for the investigation of this molecule in the context of breast cancer metastasis [94, 159]. Furthermore, we used an additonal triple-negative cell line called SUM159 originating from a primary anaplastic carcinoma tumor [197, 199]. In a collaborative effort, our lab generated a metastatic derivative of the parental SUM159 cell line by selecting the cells which were able to grow in the lungs. The resulting SUM159 LM1 cell line shows increased ability to colonize the lung compared to its parental counterpart (data not shown). In addition, I also used the primary metastatic breast cancer cells BPE16. These cells were isolated from a pleural effusion sample of a metastatic breast cancer patient. Previously, the BPE16 cells had been analyzed by FACS for the expression of the epithelial marker cytokeratin (CK) with a pan-cytokeratin-specific antibody. Thereby, I aimed to exclude a possible contamination by stromal fibroblast. The human prostatic stromal myofibroblast cell line WPMY-1 was used as a negative control and the breast cancer cell line MDA231 LM2 served as a positive control. As expected, WPMY-1 cells were negative for CK expression, while the MDA231 LM2 displayed a positive signal, as compared to isotype control. The BPE16 cells were exclusively positive for CK expression, therefore a contamination of the cancer cell culture by myofibroblasts was excluded. In addition, when cultured under serum-free and low-adhesion conditions, the BPE16 spheres formed oncopsheres **(Figure 20)**. Importantly, characterization and knockdown analysis of the BPE16 cells were performed on cells, which had been passaged less than 10 times.

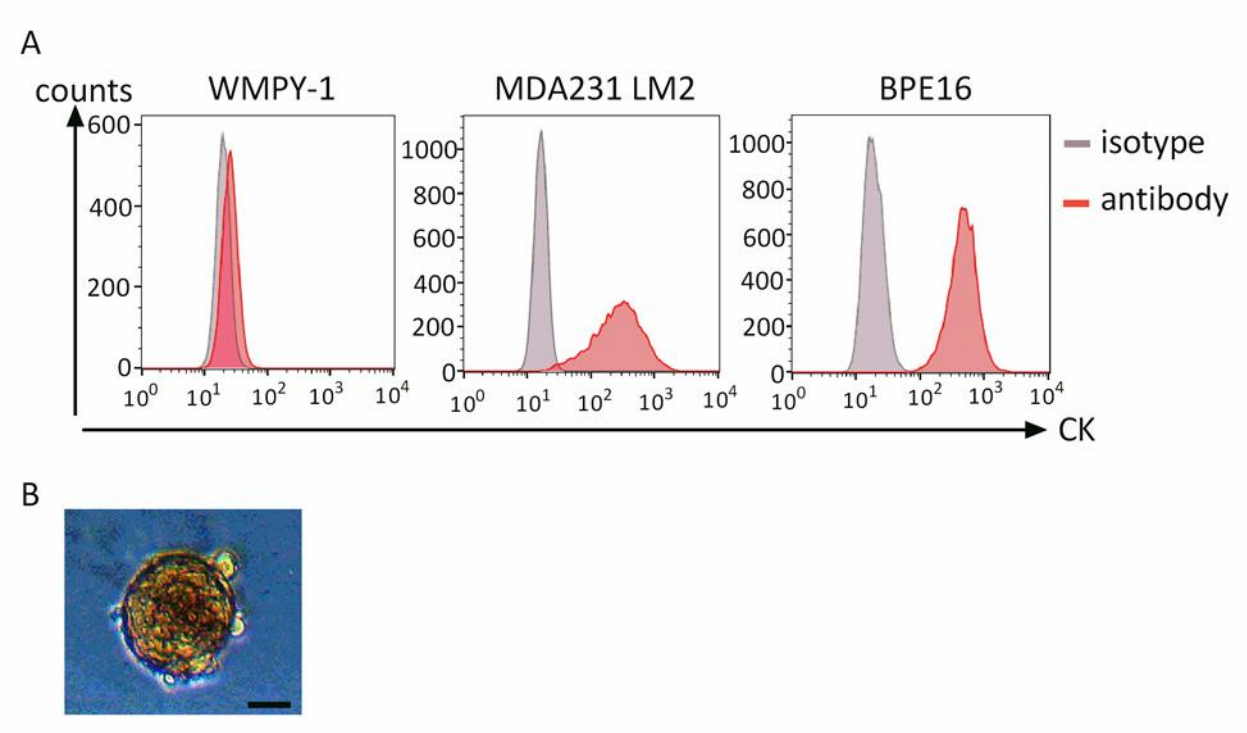

Figure 20 Characterization of BPE16 primary breast cancer pleural effusion cells.
(A) FACS analysis showing CK expression in WMPY-1 fibroblasts, MDA231 LM2 breast cancer cells and BPE16 cells. **(B)** Representative images of a tighly cohesive oncosphere formed by BPE16 cells grown in serum-free, non-adhesive conditions for 7 days. Scale bars, 50 µm.

The efficiency of the ITGB1 and ITGB3 knockdown varied from 75% to 95% in the different lines **(Figure 21, A and C)**. Upon knockdown of ITGB1 and of ITGB3, the expression of *LGR5* was decreased in the triple-negative breast cancer cell lines MDA231 LM2 and SUM159 LM1 by 50% as well as in the primary metastatic breast cancer cells BPE16 by 75% **(Figure 21, A and C)**. TNC was shown to control the expression of *LGR5* while it does not regulate the expression of the canonical Wnt target gene *AXIN2* [94]. Therefore, the expression of *AXIN2* was as well monitored upon knockdown of ITGB1 and ITGB3. In line with the TNC phenotype, ITGB1 and ITGB3 knockdown sublines expressed *AXIN2* to the same level as the control subline **(Figure 21, A and C)**. The Notch regulator *MSI1* and the Notch target gene *HEY2* of the TNC signaling were not affected by the knockdown of ITGB1 and ITGB3 **(Figure 21, B and D)**. We concluded that both ITGB1 and ITGB3 control the expression of the TNC and Wnt target gene *LGR5*.

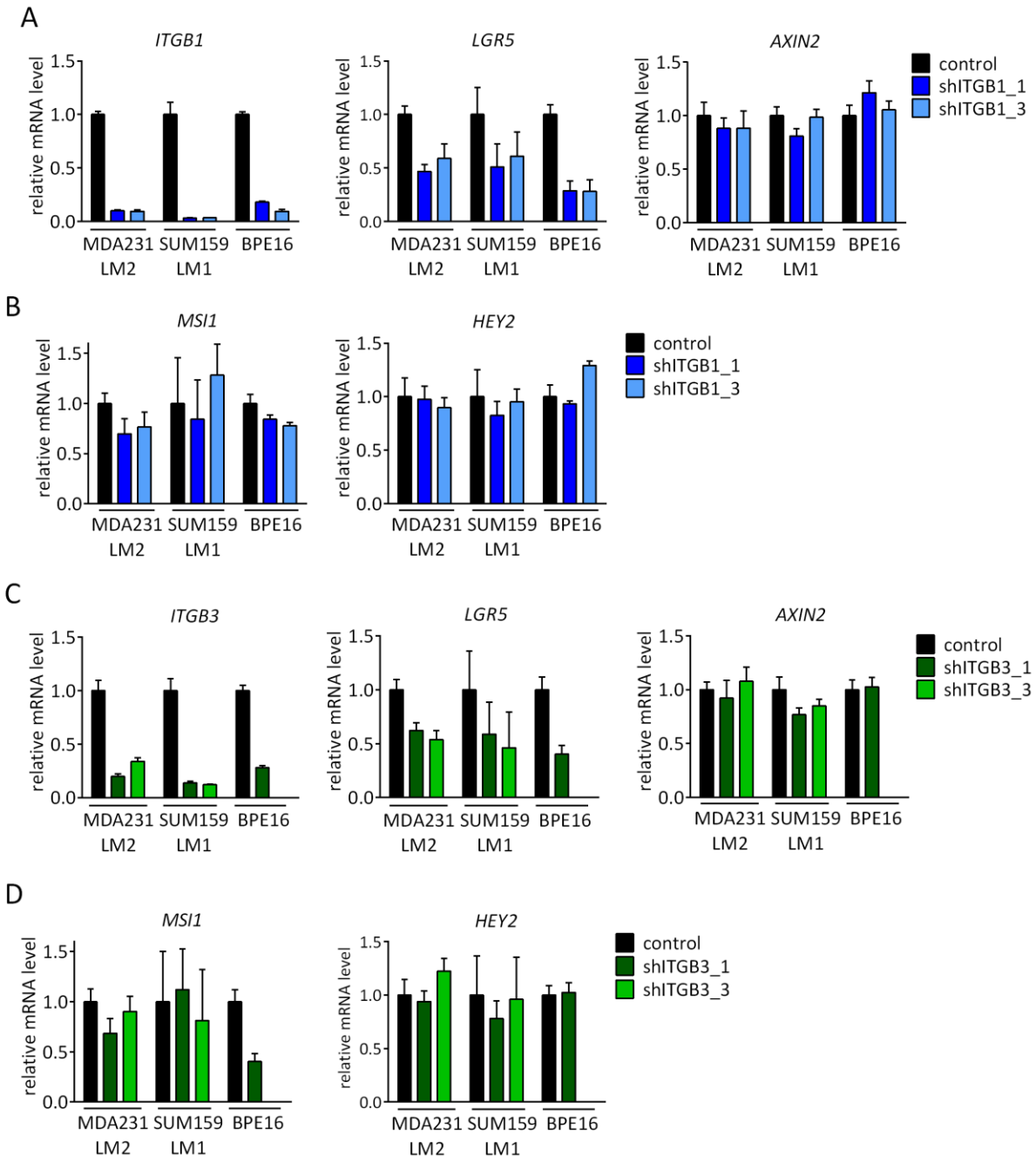

Figure 21 ITGB1 and ITGB3 control the expression of the TNC target gene *LGR5* in triple-negative breast cancer cells.

(A and B) Gene expression analysis by qRT-PCR of control and ITGB1 knockdown in MDA231 LM2, SUM159 LM1 and primary BPE16 oncospheres. For all genes, the expression in the knockdown lines was normalized to control. Error bars depict means + SD of biological replicates (*n* = 3). **(C and D)** Gene expression analysis by qRT-PCR of control and ITGB3 knockdown in MDA231 LM2, SUM159 LM1 and

primary BPE16 oncospheres. For all genes, the expression in the knockdown lines was normalized to control. Error bars depict means + SD of biological replicates (n = 3).

6.2.4 ITGB1 and ITGB3 are both required for the regulation of the TNC signaling

Prompted by the results obtained upon single knockdown of ITGB1 and ITGB3, I generated double knockdown for ITGB1 and ITGB3 in the triple-negative breast cancer cell lines MDA231 LM2 and SUM159 LM1. For this purpose, I used two lentiviral vectors encoding for the shRNA targeting ITGB1 or ITGB3 and carrying different antibiotic resistance cassette (zeocin and puromycin), transduced the target cells successively with the different lentiviral particles and selected the transduced cells with the adequate antibiotic. The knockdown of both integrins was tested by qRT-PCR at mRNA level and by western blot at protein level. For both receptors, the efficiency of the knockdown was at least 80% in the MDA231 LM2 cell line and 90% in the SUM159 LM1 cell line **(Figure 22, A and B)**. The knockdown cells were passaged every 2nd to 3rd day, together with the control cells. Gene expression analysis by qRT-PCR revealed that double knockdown of ITGB1 and ITGB3 lead to a decrease of 75% in *LGR5* expression. Interestingly, Notch-related TNC target genes *MSI1* and *HEY2* were as well affected with a decrease in expression of 55% and 50% respectively **(Figure 22, C)**. Therefore, we concluded that together ITGB1 and ITGB3 mediate the TNC signaling.

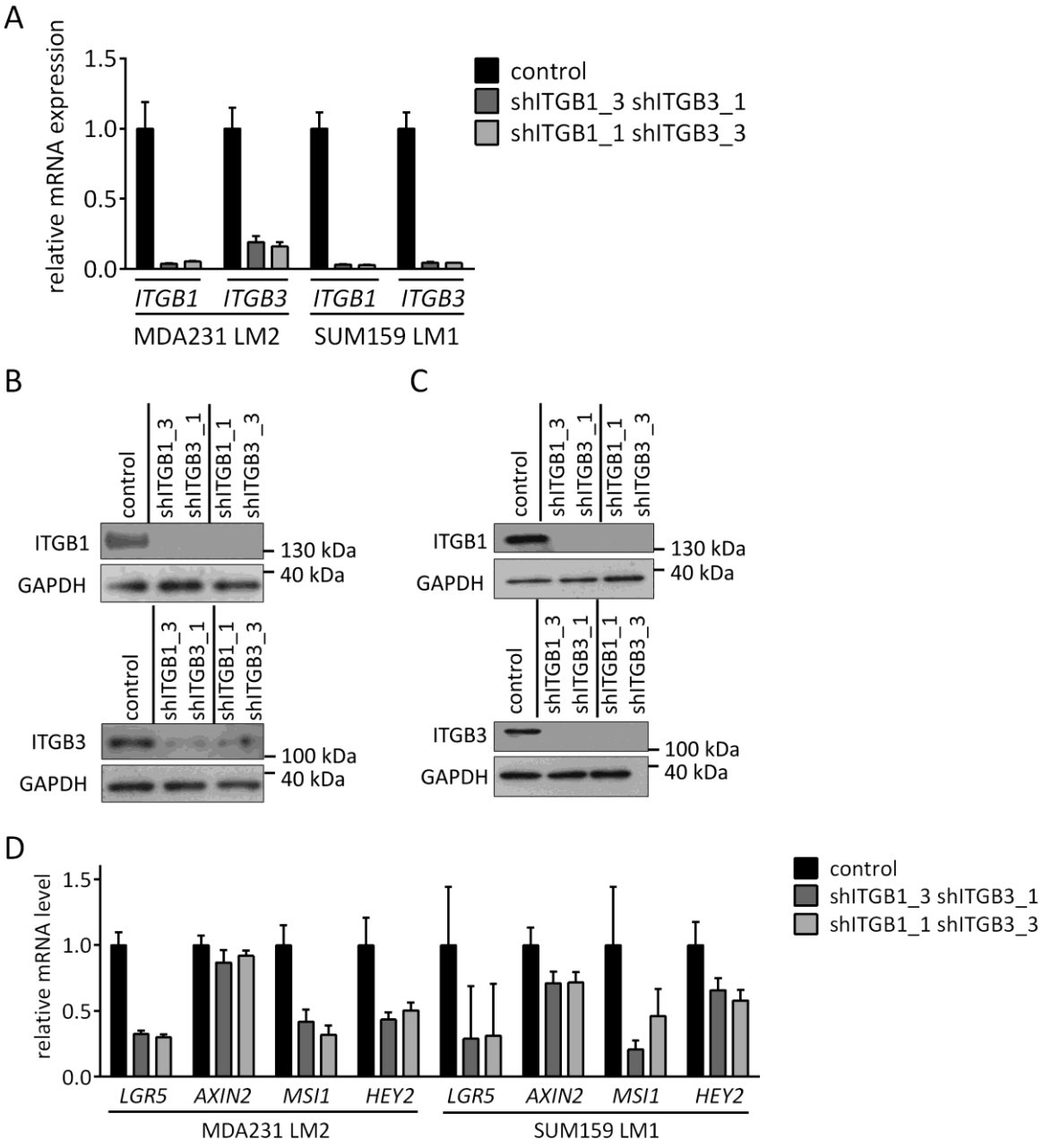

Figure 22 ITGB1 and ITGB3 mediate the TNC signaling in triple-negative breast cancer cells. **(A)** Gene expression analysis by qRT-PCR of control and ITGB1/ITGB3 knockdown MDA231 LM2 and SUM159 LM1 oncospheres. For all genes, the expression in the knockdown lines was normalized to the control line. Error bars depict means + SD of biological replicates (n = 3). **(B)** Protein expression analysis by western blot of ITGB1 (top) and ITGB3 (bottom) in control and ITGB1/ITGB3 double knockdown MDA231 LM1 oncospheres. GAPDH was used as a loading control. **(C)** Gene expression analysis by qRT-PCR of control and ITGB3 knockdown in MDA231 LM2,

SUM159 LM1 and primary BPE16 oncospheres. For all genes, the expression in the knockdown lines was normalized to control. Error bars depict means + SD of biological replicates (*n* = 3).

6.2.5 TNC binds to ITGB1 and ITGB3

Having shown that ITGB1 and ITGB3 regulate the expression of known target genes of the TNC signaling, we next sought to prove the physical binding of TNC to the identified receptors. For this purpose, endogenous TNC was immunoprecipitated out of whole cell lysate (WCL) from 3-dimensional oncosphere culture of triple-negative breast cancer cells (MDA231 LM2 and SUM159 LM1). Magnetic beads coupled to a polyclonal antibody directed against TNC were used in order to pull down TNC and its putative binding partners. The resulting elution samples were analyzed for their protein content, using immunoblotting and single reaction monitoring **(Figure 23, A)**. When using an antibody targeting TNC, immunocomplexes corresponding to the various TNC isoforms were detected in the eluate sample by western blot. WCL was used as a positive control. The pulldown reaction was very specific as attested by the lack of the TNC immunocomplexes when using an IgG antibody control instead of the anti-TNC antibody. This was observed in both cell lines used. The same samples were then tested for the presence of ITGB1. Indeed ITGB1 immunocomplexes could be detected in the TNC co-IP sample. The lack of ITGB1 in the IgG co-IP sample showed that the binding was specific to TNC and that it was not the result of unspecific binding to other components of the system **(Figure 23, B)**. Using a 3-dimensional endogenous system, we concluded that TNC and ITGB1 bind to each other in our breast cancer triple-negative models.

At the time of analysis, the lack of an antibody for ITGB3 detection by western blot analysis lead us to use an alternative approach to test for the presence of ITGB3 in the TNC co-IP lysates. In collaboration with Dr. Sabrina Hanke, we performed a targeted tandem mass spectrometry analysis named selected reaction monitoring (SRM) upon TNC immunoprecipitation. This technique detects peptide-specific fragment ions from target analytes that have been selected beforehand. SRM analysis validated the specificity of the TNC pull-down by showing a 120-fold and 3200-fold TNC enrichment in the TNC co-IP sample compared to the IgG co-IP sample in MDA231 LM2 and SUM159 LM1, respectively. As a proof of principle, we aimed to show the interaction between TNC and FN, a well characterized binding partner of TNC [116]. Indeed, a 2- to 3-fold enrichment for FN was measured in the TNC co-IP sample compared to the IgG co-IP sample in both MDA231 LM2 and SUM159 LM1. This measurement validated our technical approach. Analysis of an ITGB3-specific peptide by SRM revealed a 2- to 3-fold enrichment in the TNC co-IP sample compared to the IgG co-IP sample in MDA231 LM2 and SUM159 LM1 **(Figure 23, C)**. Meanwhile, the presence of ITGB3 in the TNC co-IP sample was also confirmed by immunoblotting in the SUM159 LM1 cell line (**Figure 23, D**).

In summary, using immunoblotting and SRM, we showed that TNC endogenously binds to ITGB1 and ITGB3 in our triple-negative breast cancer model.

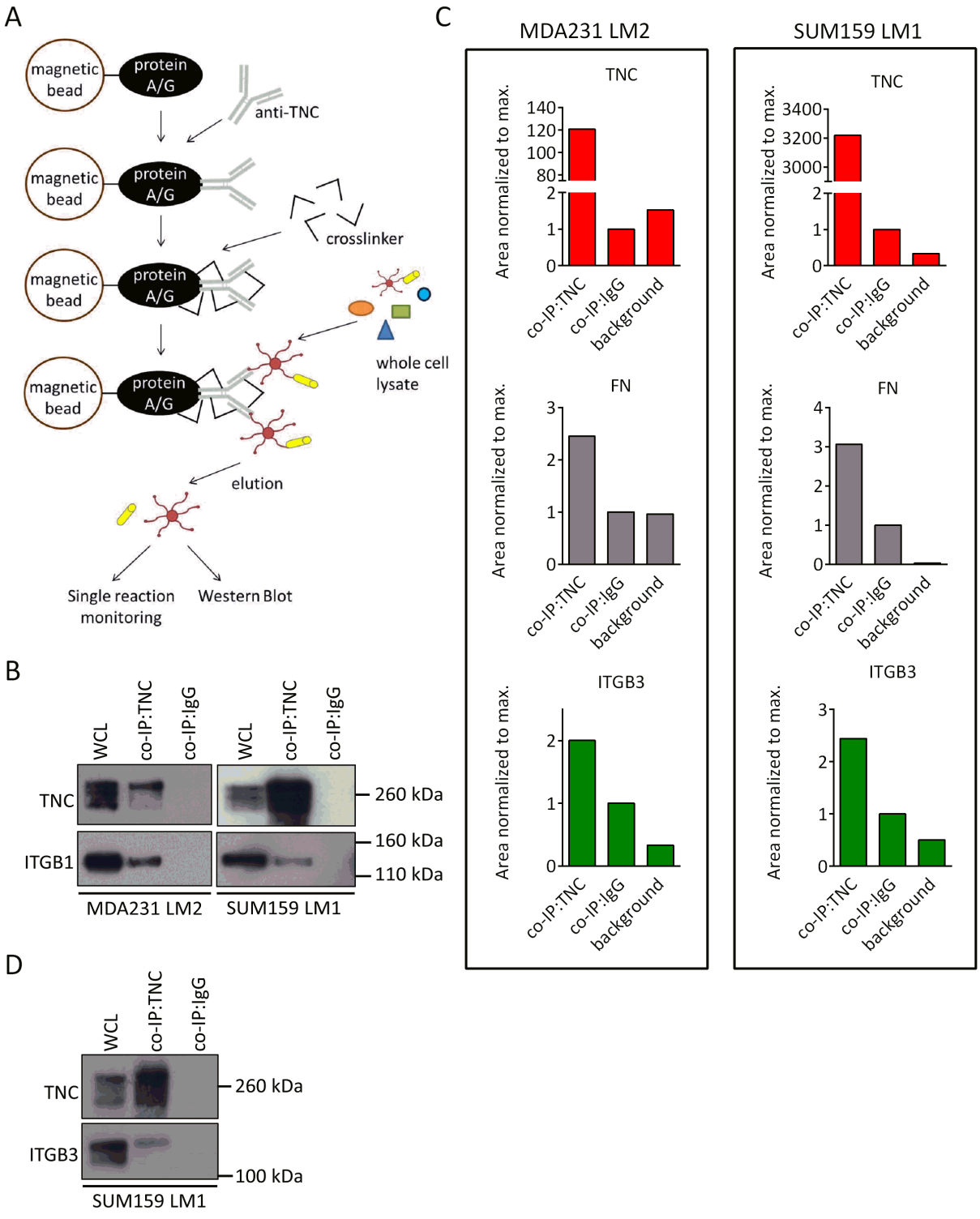

Figure 23 ITGB1 and ITGB3 bind to TNC in triple-negative breast cancer cells.
(A) Scheme showing workflow for proof of binding. Shortly, anti-TNC antibody was coupled and crosslinked to protein A/G attached to magnetic beads Whole cell lysate from breast cancer oncospheres was added to the beads complex and TNC

and its binding partners were eluted after significant washing. Single reaction monitoring (SRM) and western blot analysis was performed on the eluates samples. **(B)** Protein expression analysis by western blot of TNC and ITGB1 in whole cell lysate, TNC and IgG co-immunoprecipitation (co-IP) using MDA231 LM2 and SUM159 LM1 oncospheres. **(C)** SRM analysis of TNC and ITGB3 following TNC immunoprecipitation in MDA231 LM2 and SUM159 LM1 oncospheres. For both proteins, the abundance in the TNC immunoprecipitation eluate was normalized to the IgG immunoprecipitation. Water was used as background measurement. **(D)** Protein expression analysis by western blot of TNC and ITGB3 in whole cell lysate, TNC and IgG co-immunoprecipitation (co-IP) using SUM159 LM1 oncospheres.

6.2.6 ITGB1 and ITGB3 mediate lung colonization in pre-clinical models

As TNC is known to mediate metastasis to the lung of triple-negative breast cancer cells, we expected its receptors to promote this process as well. In order to further challenge the two receptors identified, I tested the ability of receptor knockdown cells to colonize the lung of immunocompromised mice. For this purpose, single and double ITGB1 and/or ITGB3 knockdown MDA231 LM2 cells were injected intravenously in NSG mice and the growth of the cancer cells in the lung was monitored *in vivo* by bioluminescence measurement as described previously. At experimental endpoint, the animals were sacrificed and bioluminescence was measured *ex vivo*. A 2- to 3-fold significant decrease in lung colonization was observed when comparing ITGB1 and ITGB3 single knockdown cells to the control cells. Interestingly, the double knockdown cells for ITGB1 and ITGB3 showed a 12-fold decreased potential to colonize the lungs when compared to the respective control cells **(Figure 24, A and B)**. This suggests that ITGB1 and ITGB3 act in synergy in mediating metastasis to the lung. The metastatic burden was visualized by IHC staining of human vimentin (VIM) in the lung tissues. VIM is a type III intermediate filament protein that is expressed by mesenchymal cells or cells which have undergone epithelial-to-mesenchymal transition. Therefore, VIM staining allowed specific detection of the cancer cells in the lung. While the control cells have invaded most of the lung parenchyma, ITGB1 and ITGB3 knockdown cells formed smaller metastatic nodules, leaving most of the tissue intact **(Figure 24, C)**. The pro-metastatic role of ITGB1 and ITGB3 was confirmed in the SUM159 LM1 cell line. Similarly to what we observed using the MDA231 LM2 cell line, the double knockdown cells for ITGB1 and ITGB3 showed a dramatic decrease in their ability to colonize the lungs of immunocompromised mice **(Figure 24, D)**.

This set of *in vivo* experiments showed that the two receptors identified mediate lung colonization of triple-negative breast cancer cells. Together with our previous findings, these data confirmed the identification of ITGB1 and ITGB3 as the receptors mediating the TNC pro-metastatic signaling.

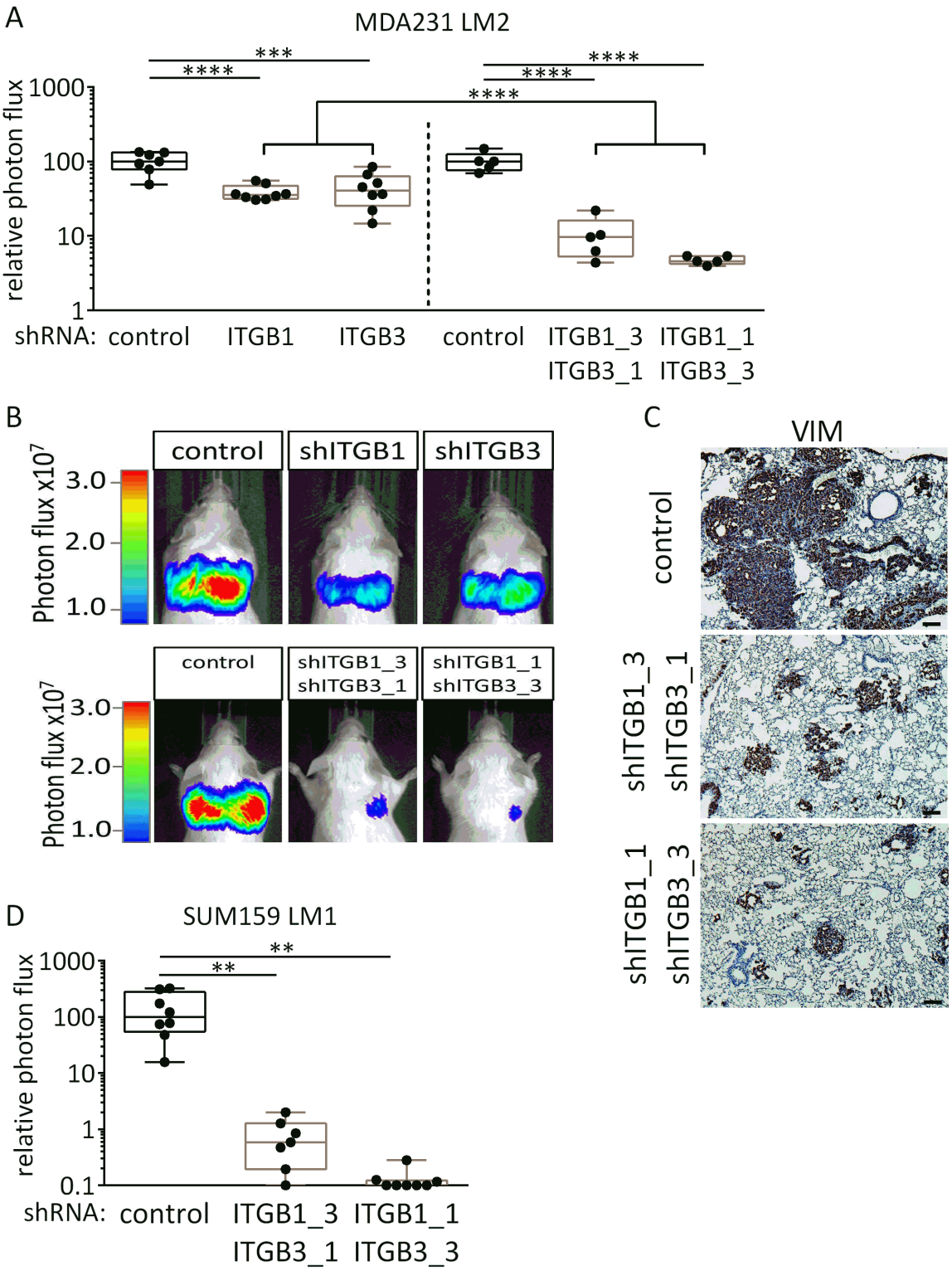

Figure 24 ITGB1 and ITGB3 mediate lung colonization in triple-negative breast cancer.

(A) Lung colonization, as determined by *ex vivo* bioluminescence, in mice injected intravenously with control, ITGB1 knockdown, ITGB3 knockdown and ITGB1/ITGB3 double knockdown MDA231 LM2 cells (n = 5 or n = 8 per group). Whiskers represent minimum and maximum values. ***P < 0.005, **** P < 0.001; by two-tailed Mann-Whitney test (single versus double knockdown) and by one-way ANOVA with Tukey's multiple comparisons test (single and double knockdown versus respective control). **(B)** Representative images showing *in vivo* bioluminescence in mice injected intravenously with control, ITGB1 knockdown, ITGB3 knockdown and ITGB1/ITGB3 double knockdown MDA231 LM2 cells at experimental endpoint. **(C)** Representative images showing brown immunostaining for human VIM in paraffin-embedded lungs of mice injected intravenously with control and ITGB1/ITGB3 double knockdown MDA231 LM2 cells at experimental endpoint. Scale bars, 50 µm. **(D)** Lung colonization, as determined by *ex vivo* bioluminescence, in mice injected intravenously with control and ITGB1/ITGB3 double knockdown SUM159 LM1 cells (n = 8 per group). Whiskers represent minimum and maximum values. **P < 0.01; by one-way ANOVA with Dunnett's multiple comparisons test.

6.2.7 ITGA2 is a putative alpha subunit pairing with ITGB1 in the mediation of the TNC signaling

Integrins are heterodimeric cell surface receptors acting as the main receptors for ECM molecules. In human, the integrin family comprises 18 alpha subunits and 8 beta subunits pairing in order to form at least 24 different functional heterodimeric receptors [189]. Having identified two integrin beta subunits as receptors mediating the TNC pro-metastatic signaling, the next step consisted in investigating which alpha subunits could pair with ITGB1 and ITGB3.

ITGB1 can bind to virtually all known alpha subunits [189]. Nevertheless, in the context of its interaction with TNC, ITGB1 has been suggested to pair with ITGA2, ITGA7, ITGA8 and ITGA9 [127]. Out of the four candidates, only ITGA2 was expressed in our triple-negative breast cancer model based on microarray data. In addition, the Human Protein Atlas database indicates strong expression of ITGA2 in breast cancer tissues and absence or very low expression of ITGA7, ITGA8 and ITGA9 (www.proteinatlas.org, data not shown). Therefore, I generated a stable knockdown of ITGA2 in triple-negative metastatic breast cancer cells. A knockdown efficiency of 75% was achieved as determined by qRT-PCR after antibiotic selection. The gene expression analysis of the TNC target genes (*LGR5*, *MSI1* and *HEY2*) upon ITGA2 knockdown revealed a 70% decrease in LGR5 expression while the Notch-related target genes remained unaffected. In accordance to the ITGB1 and TNC phenotype, ITGA2 knockdown did not impact the expression of *AXIN2* **(Figure 25, A)**. From this analysis, we concluded that ITGA2 is a putative partner of ITGB1 in the mediation of the TNC signaling.

Unlike ITGB1, there are only two integrin alpha subunits which are known to be able to bind to ITGB3, ITGAV and ITGA2b [189]. In cancer, the ITGB3-ITGAV complex has been shown to promote cancer progression [200]. In addition, TNC can bind ITGB3-ITGAV and mediate the attachment of endothelial cells [119]. Therefore, I generated a stable knockdown of ITGAV in triple-negative metastatic breast cancer cells using two independent shRNAs. A knockdown efficiency of minimum 85% was achieved at mRNA level and the knockdown was verified by FACS at protein level. Surprisingly, the TNC target genes remained unaffected upon ITGAV knockdown **(Figure 25, B and C)**. The ITGB3-ITGA2b complex is expressed by platelets and supports platelet activation and aggregation by binding to von Willebrand factor (vWF) and fibrinogen. Until now, expression of ITGA2b at protein level on cancer cells has not been shown in cancer cells.

Our data suggest that ITGA2 is a strong candidate as the partner of ITGB1 binding to TNC. Though, identifying the alpha subunits pairing with ITGB1 and ITGB3 in the mediation of the TNC pro-metastatic signaling will require further investigation.

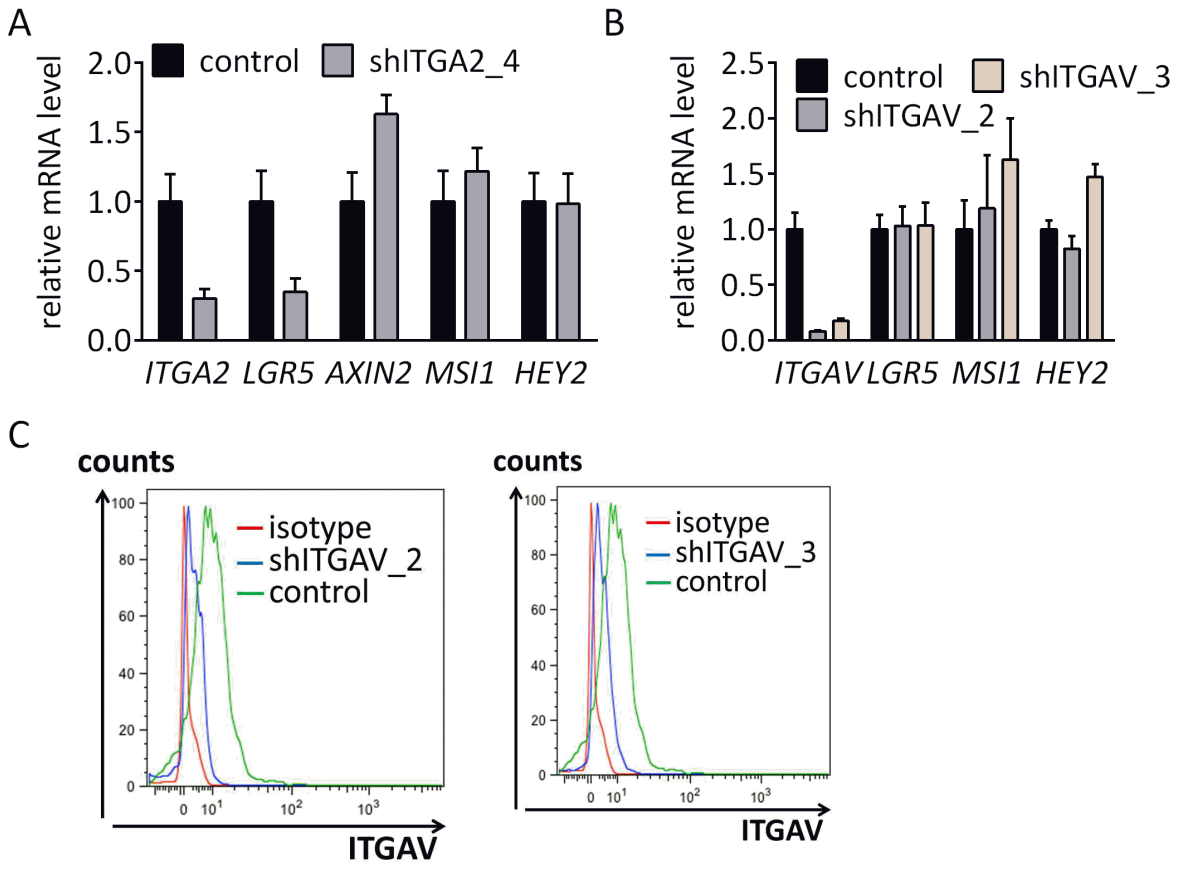

Figure 25 TNC signaling upon knockdown of ITGA2 and ITGAV.
(A) Gene expression analysis by qRT-PCR of control and ITGA2 oncospheres. For all genes, the expression in the knockdown line was normalized to the control line.

Error bars depict means + SD of biological replicates (n = 3). **(B)** Gene expression analysis by qRT-PCR of control and ITGAV knockdown CN34 LM1 oncospheres. For all genes, the expression in the knockdown lines was normalized to the control line. Error bars depict means + SD of biological replicates (n = 3). **(C)** Flow cytometry analysis showing ITGAV expression in control cells, ITGAV_2 (left) and ITGAV_3 (right) knockdown cells.

6.2.8 TNC and its receptors are enriched in triple-negative breast cancer cells

We demonstrated that ITGB1 and ITGB3 mediate the TNC pro-metastatic signaling in triple-negative breast cancer **(Figure 21 and 22)**. In addition, we showed that the prognostic value of TNC was restricted to the triple-negative subtype of breast cancer and that triple-negative tumors expressed more TNC than others **(Figure 14 - 16)**. We next raised the question if the identified receptors might be differentially expressed between the different subtypes. Therefore, I monitored the expression of TNC and its receptors in a panel of breast cancer cell lines belonging to different subtypes, as defined by IHC. While the MCF7 and T47D cell lines were classified as luminal as they express both ER and PR, the BT474 and SKBR3 cell lines were shown to overexpress the HER2 receptor. MDA468, HCC1937, MDA157, MDA436, MDA231 LM2 and SUM159 LM1 do not express ER, PR and HER2 and therefore they were classified as TN [201]. Gene expression analysis by qRT-PCR analysis showed that triple-negative breast cancer cells express significantly more TNC than luminal and HER2 breast cancer cells **(Figure 26, A)**. Interestingly, triple-negative breast cancer cells are also enriched for ITGB1 and ITGB3 expression compared to the two other subtypes **(Figure 26, B and C)**. Taken together, our data indicates that triple-negative breast cancer cells are enriched for expression of TNC and its receptors ITGB1 and ITGB3.

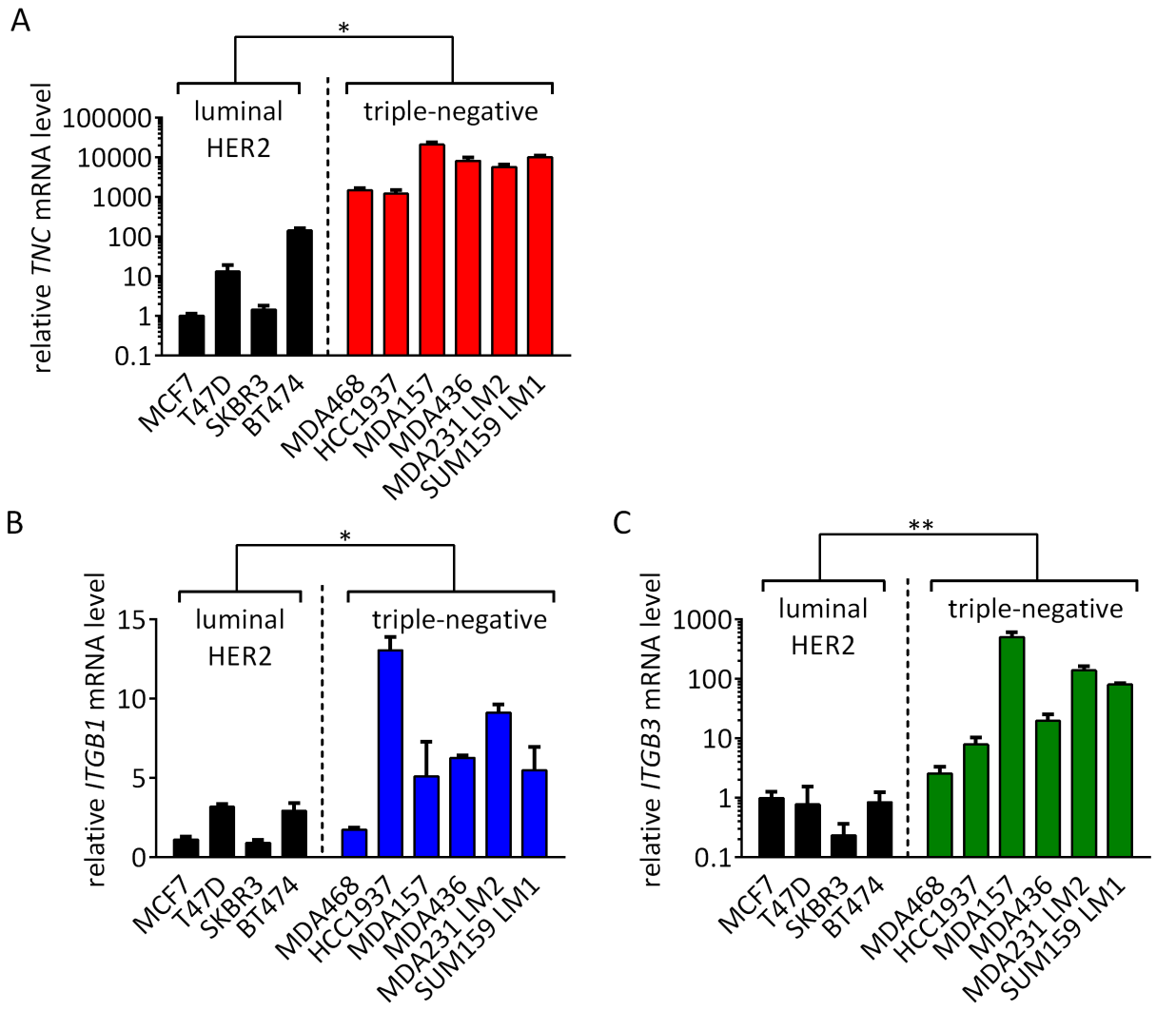

Figure 26 Triple-negative breast cancer cells are enriched for TNC, ITGB1 and ITGB3 expression.

(A) Gene expression analysis by qRT-PCR of a panel of Breast cancer cells lines. The cell lines were grouped according to their receptor status. Luminal / HER2: MCF7, T47D, SKBR3, BT474. Triple-negative: MDA468, HCC1937, MDA157, MDA436, MDA231 LM2, SUM159 LM1. The expression of *TNC* in all cell lines was normalized to the MCF7 cell line. Error bars depict means + SD of technical replicates (n = 3). **P* < 0.05; by one-way ANOVA with Dunnett's multiple comparisons test. **(B)** Gene expression analysis by qRT-PCR of a panel of Breast cancer cells lines. The cell lines were grouped according to their receptor status. Luminal / HER2: MCF7, T47D, SKBR3, BT474. Triple-negative: MDA468, HCC1937, MDA157, MDA436, MDA231 LM2, SUM159 LM1. The expression of *ITGB1* in all cell lines was normalized to the MCF7 cell line. Error bars depict means + SD of technical replicates (n = 3). *P < 0.05; by one-way ANOVA with Dunnett's multiple comparisons test. **(C)** Gene

expression analysis by qRT-PCR of a panel of Breast cancer cells lines. The cell lines were grouped according to their receptor status. Luminal / HER2: MCF7, T47D, SKBR3, BT474. Triple-negative: MDA468, HCC1937, MDA157, MDA436, MDA231 LM2, SUM159 LM1. The expression of *ITGB3* in all cell lines was normalized to the MCF7 cell line. Error bars depict means + SD of technical replicates (n = 3). *P < 0.05; by one-way ANOVA with Dunnett's multiple comparisons test.

6.3 Clinical relevance of the TNC-integrin axis in breast cancer

In vitro and *in vivo* experiments demonstrated that the ITGB1 and ITGB3 receptors mediate the pro-metastatic function of TNC in triple-negative breast cancer. We then aimed to assess the clinical relevance of our findings by asking whether the expression of TNC and its receptors correlate in breast cancer patients and whether the identified TNC-ITGB axis is associated with clinical prognosis. To address this, I performed a meta-analysis on a gene expression profiling dataset of 1992 breast cancer patients originally published by the METABRIC.

6.3.1 TNC expression correlates with ITGB1 and ITGB3 expression in breast cancer patients

In order to assess a putative correlation between TNC expression and the expression of the identified receptors ITGB1 and ITGB3, the patients were first stratified according to the PAM50 intrinsic subtype. In the basal-like subtype, within which 78% of the patients were triple-negative according to pathological annotations, the expression of TNC was plotted against ITGB1 or ITGB3 expression. Both combinations revealed a significant positive correlation with correlation coefficient of 0.3056 and 0.2666, respectively. The correlation was even stronger (r = 0.3376) when comparing TNC expression to the mean expression of ITGB1 and ITGB3 **(Figure 27, A – C)**. We concluded that basal-like patients expression of TNC correlates with expression of ITGB1 and ITGB3. Interestingly, expression of ITGB1 and ITGB3 also positively and significantly correlate with each other **(Figure 27, D)**.

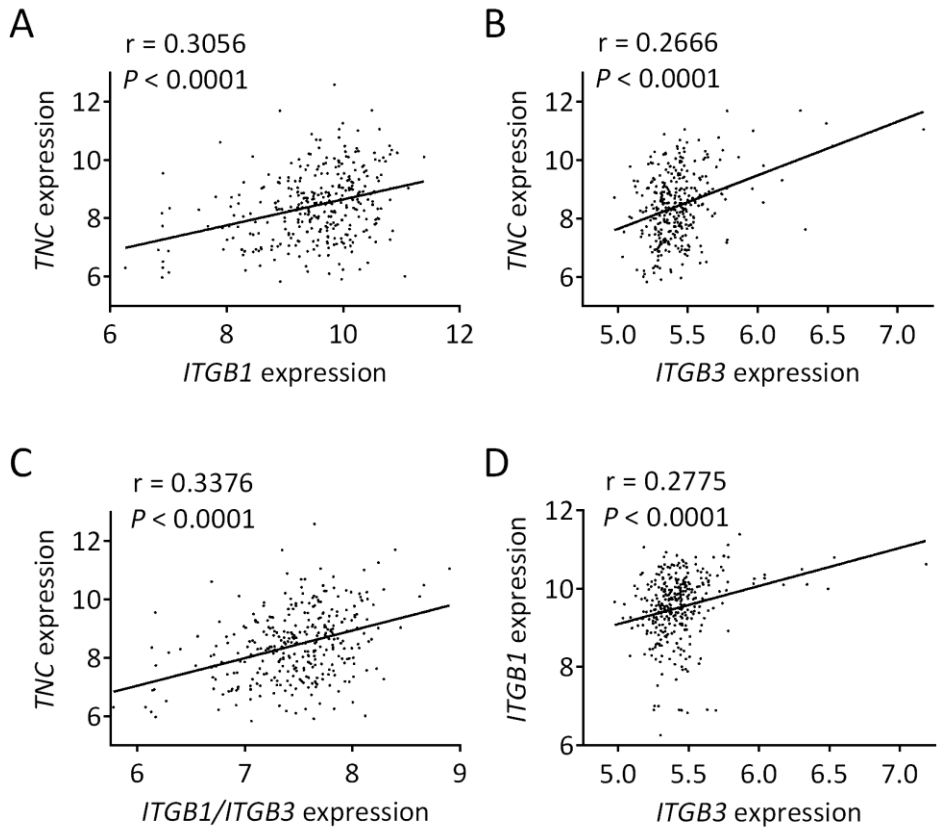

Figure 27 TNC expression positively correlates with ITGB1 and ITGB3 expression in basal-like breast cancer patients.
(A) *TNC* and *ITGB1* expression in basal-like-like breast cancer patients. **(B)** *TNC* and *ITGB3* expression in basal-like-like breast cancer patients. **(C)** *TNC* expression and mean expression of *ITGB1* and *ITGB3* in basal-like-like breast cancer patients. (D) *ITGB1* and *ITGB3* expression in basal-like-like breast cancer patients. Each dot represents one patient (n = 328). r, nonparametric Spearman correlation coefficient. P, two-tailed.

6.3.2 The TNC-integrin axis is associated with poor overall survival in basal-like breast cancer

We then investigated the clinical prognosis of patients showing high expression of *TNC* and of the identified receptors, *ITGB1* and *ITGB3*, in the METABRIC dataset.

To this purpose, the basal-like patients were selected according to PAM50 intrinsic breast cancer subtypes and stratified according to *TNC* expression, as previously described (see 6.1.1, **Figure 15**). In each subtype, the lower quartile (0 – 25%) of *TNC* expressing tumors was defined

as '*TNC* low', whereas the '*TNC* high' group comprised the rest of the cohort. Next, the patients within the 'TNC high' group were classified according to the expression level of *ITGB1*. The '*ITGB1* high' group was defined as the upper quartile (75 – 100%) of the *ITGB1* expressing patients, while the remaining patients were classified as '*ITGB1* low'. High expression of both *TNC* and *ITGB1* correlated with significantly shorter overall survival when compared to the *'TNC* low' group (*P* = 0.0411, HR = 1.678) **(Figure 28, A)**. Remarkably, the 'TNC high' patients with high expression of ITGB1 lived shorter than patients with low expression of ITGB1 with median survival time of 8.3 and 12.3 years, respectively **(Figure 28, C and D)**. When applying the same workflow, we observed that high expression of both TNC and ITGB3 also correlated with significantly shorter overall survival when compared to the 'TNC low' group (P = 0.0208, HR = 1.797) **(Figure 28, B)**. The median survival of 'TNC high' patients with high expression of *ITGB3* was 8.1 years, against 11.9 years for patients with low expression of *ITGB3* **(Figure 28, C and D)**.

We next investigated the clinical prognosis of patients expressing *TNC* and both receptors, *ITGB1* and *ITGB3*, was investigated. Therefore, the previously described cutoff values were used to refine further the *TNC* classification by defining a '*TNC / ITGB1 / ITGB3* high' group, which was compared to the 'TNC low' group. The analysis revealed a median survival of only 5.8 years for patients expressing high level of TNC and of the two identified receptors. This represents a strong drop compared to patients expressing only high level of *TNC* or high level of *TNC* and of one of its receptor **(Figure 28, C and D)**. The median survival of patients expressing high level of *TNC* and low level of both *ITGB1* and *ITGB3* is 14.5 years. Remarkably, this value was higher than all other groups decribed above, enhancing the fact that the prognostic value of *TNC* depends on the expression of the identified receptors **(Figue 28, C and D)**.

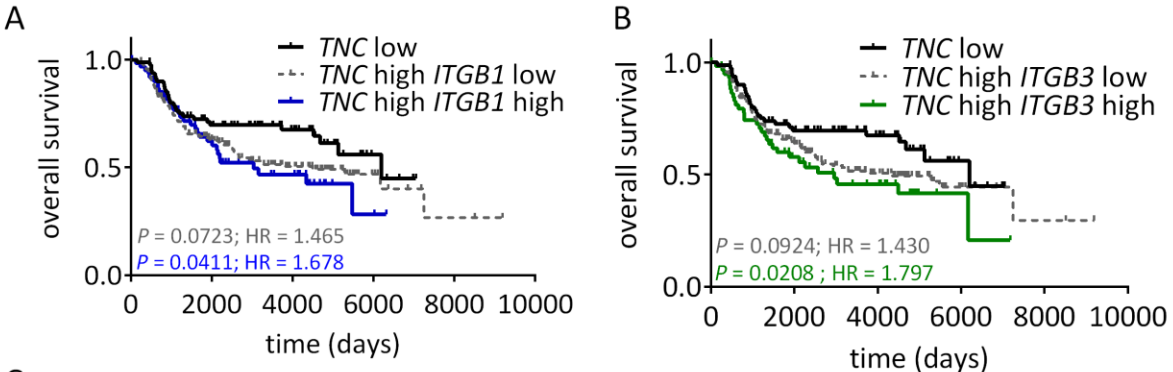

C

	n	median survival (years)
***TNC* low**	247	17
***TNC* high**	81	9.8
***TNC* high *ITGB1* low**	186	12.3
***TNC* high *ITGB1* high**	61	8.3
***TNC* high *ITGB3* low**	187	11.9
***TNC* high *ITGB3* high**	60	8.1
***TNC* high *ITGB1/ITGB3* low**	146	14.5
***TNC* high *ITGB1/ITGB3* high**	20	5.8

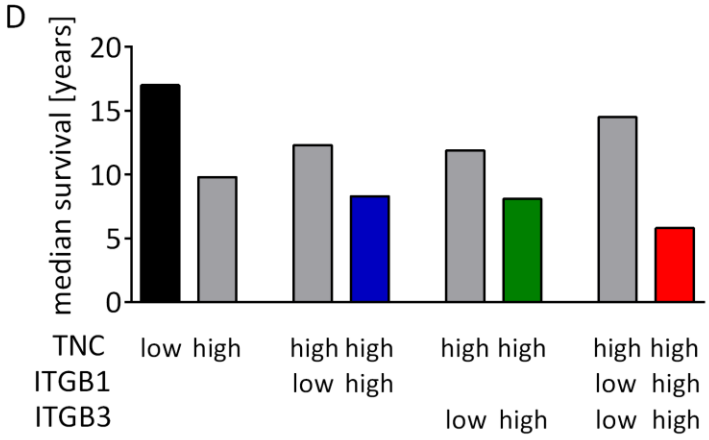

Figure 28 The TNC-integrin axis predicts poor patient outcome in basal-like breast cancer patients.

(A) Kaplan-Meier analysis of overall survival of basal-like breast cancer patients (n = 328). Subjects were classified according to TNC lower quartile and ITGB1 upper quartile. **(B)** Kaplan-Meier analysis of overall survival of basal-like breast cancer patients (n = 328). Subjects were classified according to TNC lower quartile and ITGB3 upper quartile. **(C)** Patient numbers and median survival in years of the groups depicted in (A - C) and in Figure 2, E. *P* values were calculated by log-rank Mantel Cox test. **(D)** Graphical representation of the values listed in (C).

6.4 ITGB1 and ITGB3 promote the formation of oncospheres

TNC expression pattern in stem cell niches and the fact that it controls the expression of adult stem cell markers (LGR5 and MSI1) links this molecule to stemness properties [92]. This prompted us to investigate the role played by ITGB1 and ITGB3 in breast cancer stemness. For this purpose, we used a 3-dimensional spheroid assay. When cultured in serum-free medium under low-adhesion conditions, triple-negative breast cancer cells (MDA157, MDA231 LM2 and SUM159 LM1) formed cohesive structures, more or less tight, called oncospheres **(Figure 29, A)**. These culture conditions enriches for stemness properties, as attested by an enrichment in typical stemness markers (*NANOG*, *OCT4*, *SOX2*) as well as an increase in *TNC* expression when compared to monolayer culture **(Figure 29, B)**. In order to investigate a putative link between stemness and ITGB1 / ITGB3 expression, a time course experiment was performed. SUM159 LM1 cells were cultivated as monolayer and oncospheres and harvested for protein analysis after 3, 7 and 14 days of spheroid culture. Immunoblotting confirmed the enrichment in TNC at protein level in oncosphere culture compared to monolayer. Interestingly, TNC expression level continuously increased until day 14. A similar expression pattern was observed for ITGB3: immunoblotting showed enrichment in oncosphere culture compared to monolayer culture and an increase in ITGB3 expression with time. Unlike TNC and ITGB3, ITGB1 was enriched upon oncosphere culture but its expression remained constant after 7 and 14 days **(Figure 29, C)**. I then aimed to confirm the enrichment for ITGB1 and ITGB3 in oncosphere culture in a further triple-negative cell line (MDA157) using FACS. Oncospheres showed an increase in ITGB1 and ITGB3 expression. To note is that the entire cell population shifted towards an $ITGB1^{high}$ $ITGB3^{high}$ phenotype, indicated that the same cells upregulate both molecules **(Figure 29, D)**. Next, I tested whether ITGB1 and ITGB3 played a functional role in the formation of oncospheres. Therefore, single ITGB1 or ITGB3 knockdown SUM159 LM1 cells were seeded for oncosphere assay and after 7 days the area of randomly selected oncospheres was quantified. No significant difference in size was observed when comparing the single ITGB1 or ITGB3 knockdown sublines to the control **(Figure 29, E)**. However, knocking down both ITGB1 and ITGB3 resulted in a strong decrease in size of the oncospheres formed **(Figure 29, F)**. We concluded that ITGB1 and ITGB3 promote sphere formation.

In summary, our data showed that the TNC receptors identified are associated with stemness properties in triple-negative breast cancer and promotes the formation of oncospheres.

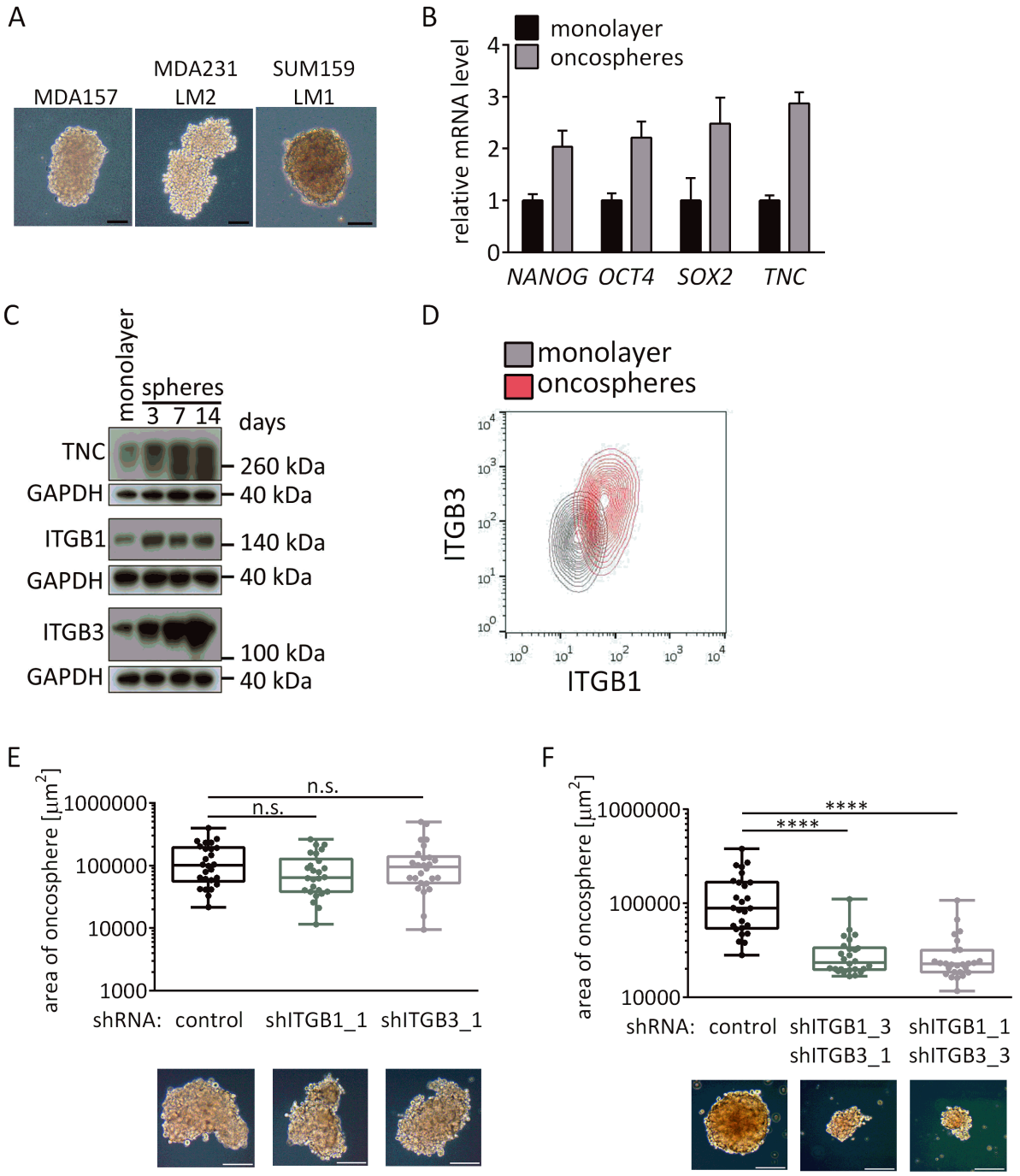

Figure 29 ITGB1 and ITGB3 are associated with stemness properties in triple-negative breast cancer cells.

(A) Representative images of oncospheres formed by MDA157, MDA231 LM2 and SUM159 LM1 breast cancer cells grown in serum-free, non-adhesive conditions for 7 days. Scale bars, 50 µm. (B) Gene expression analysis by qRT-PCR of SUM159 LM1 cells grown as monolayer and oncospheres. For all genes, the expression of the oncosphere samples was normalized to monolayer samples. Error bars depict

means + SD of technical replicates (n = 3). (C) Protein expression analysis by western blot of TNC, ITGB1 and ITGB3 in SUM159 LM1 cells grown as monolayer and oncospheres for 3, 7 and 14 days. GAPDH was used as a loading control. (D) Protein expression analysis of ITGB1 and ITGB3 by FACS of MDA157 cells grown as monolayer and oncospheres. (E) Quantitative analysis of oncosphere formation showing area of oncosphere (top) and representative images of corresponding oncospheres in control, ITGB1 and ITGB3 knockdown SUM159 LM1 cells grown in serum-free, non-adhesive conditions for 7 days (bottom). Scale bars, 50 µm. Whiskers represent minimum and maximum values. n.s., not significant; by one-way ANOVA with Dunnett's multiple comparisons test. (F) Quantitative analysis of oncosphere formation showing area of oncosphere (top) and representative images of corresponding oncospheres in control and ITGB1/ITGB3 double knockdown SUM159 LM1 cells grown in serum-free, non-adhesive conditions for 7 days (bottom). Scale bars, 50 µm. ****P < 0.0001 ; by one-way ANOVA with Dunnett's multiple comparisons test.

6.5 TNC supports stem cell properties in the mammary epithelium and promotes pregnancy-associated alveogenesis

The link between TNC, its receptors and stemness properties in triple-negative breast cancer prompted us to investigate a putative role of the TNC signaling in the context of normal mammary gland and mammary stem cells.

To address this, we tested the ability of mammary epithelial cells lacking TNC to form mammospheres. This assay has been used as a surrogate reporter of stem cell activity in the mammary gland as it is assumed that only undifferentiated cells will survive and self-renew in suspension culture [201]. The mammary epithelial cells from 5 adult $TNC^{+/-}$ and $TNC^{-/-}$ mice were isolated and cultivated in serum-free low-adhesion conditions and mammosphere formation capability was assessed by measuring the size of the resulting organoids. We observed a significant decrease in mammospheres size isolated from $TNC^{-/-}$ adult mice compared to control mice, suggesting a functional role of TNC self-renewal and stemness properties of the mammary epithelial cells **(Figure 30, A and B)**.

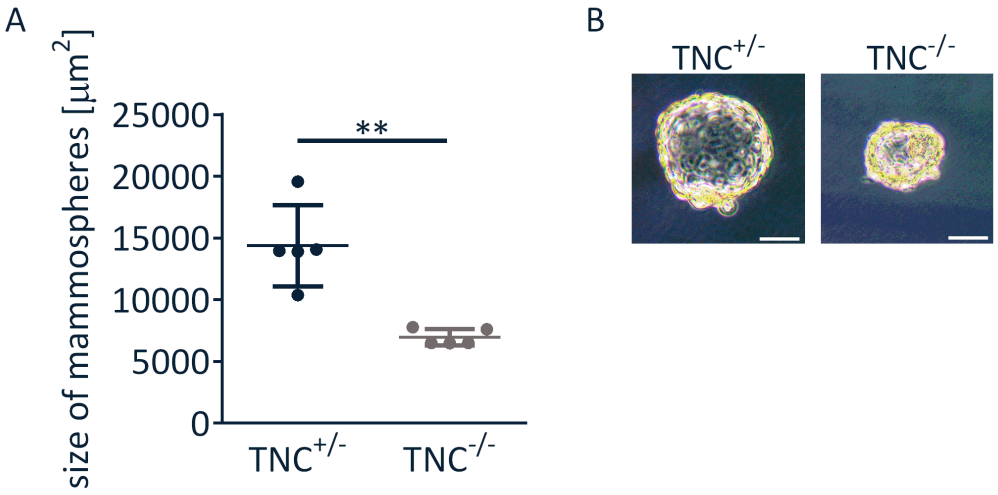

Figure 30 Mammosphere formation ability of mammary epithelial cells from TNC$^{+/-}$ and TNC$^{-/-}$ **(A)** Quantitative analysis of mammosphere size generated from mammary epithelial cells isolated from Tnc$^{+/-}$ and Tnc$^{-/-}$ mice. Each dot represents one mouse (n = 5). **P < 0.001; by two-tailed Mann-Whitney test. **(B)** Representative images of corresponding mammospheres. Scale bars, 50 µm.

In order to further investigate the role of TNC in mammary stem cells, we took advantage of the unique developmental pattern of the mammary gland. In contrast to other organs, which arise during embryogenesis, the development of the mammary gland occurs mainly after birth. Indeed, mammary gland is a highly plastic tissue, which undergoes tremendous structural changes during the life of a mammal. In the mouse, a rudimentary ductal structure invading the fat pad can be visualized at the age of 3 weeks. The first expansion of the mammary gland can be characterized as ductal elongation and takes place during puberty. Between 3 and 9 weeks, the ductal growth takes place led by proliferative regions called terminal end buds (TEB) and the ductal tree invades further the underlying fat pad until it is completely filled with ducts in the virgin adult animal. The next major structural and functional change begins at the onset of pregnancy. In order to prepare for lactation, the epithelium proliferates and differentiates in order to form grape-like milk-secretory structures called alveoli. When lactation is not required anymore, the mammary gland involutes and returns to a stage resembling the virgin gland [185, 202, 203]. The development of mouse mammary glands can be visualised using whole mount analysis, which were performed on NSG 4th mammary glands at key stages of development: pre-puberty (3 weeks), puberty (5 weeks), virgin adult (9 weeks) and mid-pregnancy (12.5 days post coitum (dpc)) **(Figure 31, A)**. Both developmental stages highlighted, puberty and mid-pregnancy, are driven by the coordinated division and differentiation of mammary stem cells.

In order to investigate a putative role of the TNC signaling in the mammary gland development, the expression of the TNC signaling members was monitored by qRT-PCR in the mammary gland of pre-puberty, puberty, adult virgin and pregnant NSG mice. In puberty mice, the expression of

Tnc and its receptor *Itgb3* were significantly increased compared to pre-puberty mice, while *Itgb1* remained unchanged. The downstream target genes of TNC, *Lgr5*, *Msi1* and *Hey2* were as well significantly enriched in the pubertal mammary fat pads. Interestingly, two known ligands of the LGR5 receptors, *Rspo1* and *Rspo3* were upregulated in the pubertal mammary fat pads **(Figure 31, C)**. The same analysis was performed on mammary fat pads of age-matched pregnant mice (12.5 dpc) versus virgin mice. An upregulation of both TNC receptors, *Tnc* itself, its downstream targets (*Lgr5*, *Msi1* and *Hey2*) as well as the LGR5 ligand *Rspo1* was observed **(Figure 31, E)**. In addition, the expression of markers of the basal epithelial lineages enriched in mammary stem cells (*Krt14*, *Krt15*, *Cdh5*) was also monitored [204]. These markers were significantly upregulated during puberty and pregnancy, suggesting an expansion of the mammary stem cell compartment **(Figure 31, B and D)**.

The induction of the TNC signaling in two independent stages of mammary development lead to the hypothesis, that TNC might play a functional role in these processes. I performed a morphological analysis of the mammary gland of TNC knockout ($TNC^{-/-}$) C57BL/6 compared to wildtype animals. Both 4^{th} mammary fat pads of 3 mice per group were stained with carmine alum as a whole mount. Compared to the wildtype organs, mammary fat pads from $TNC^{-/-}$ showed fewer alveolar structures. Interestingly, the alveoli in the $TNC^{-/-}$ animals were concentrated at the tip of the ducts while in the wildtype setting, the branches were covered by alveoli **(Figure 31, F)**. The observed difference was quantified by assessing the epithelial area within the layer of fat of 6 mammary fat pad per group in total. This revealed that the epithelium was reduced by approximately 33% in the $TNC^{-/-}$ mice compared to the wildtype situation **(Figure 31, G)**.

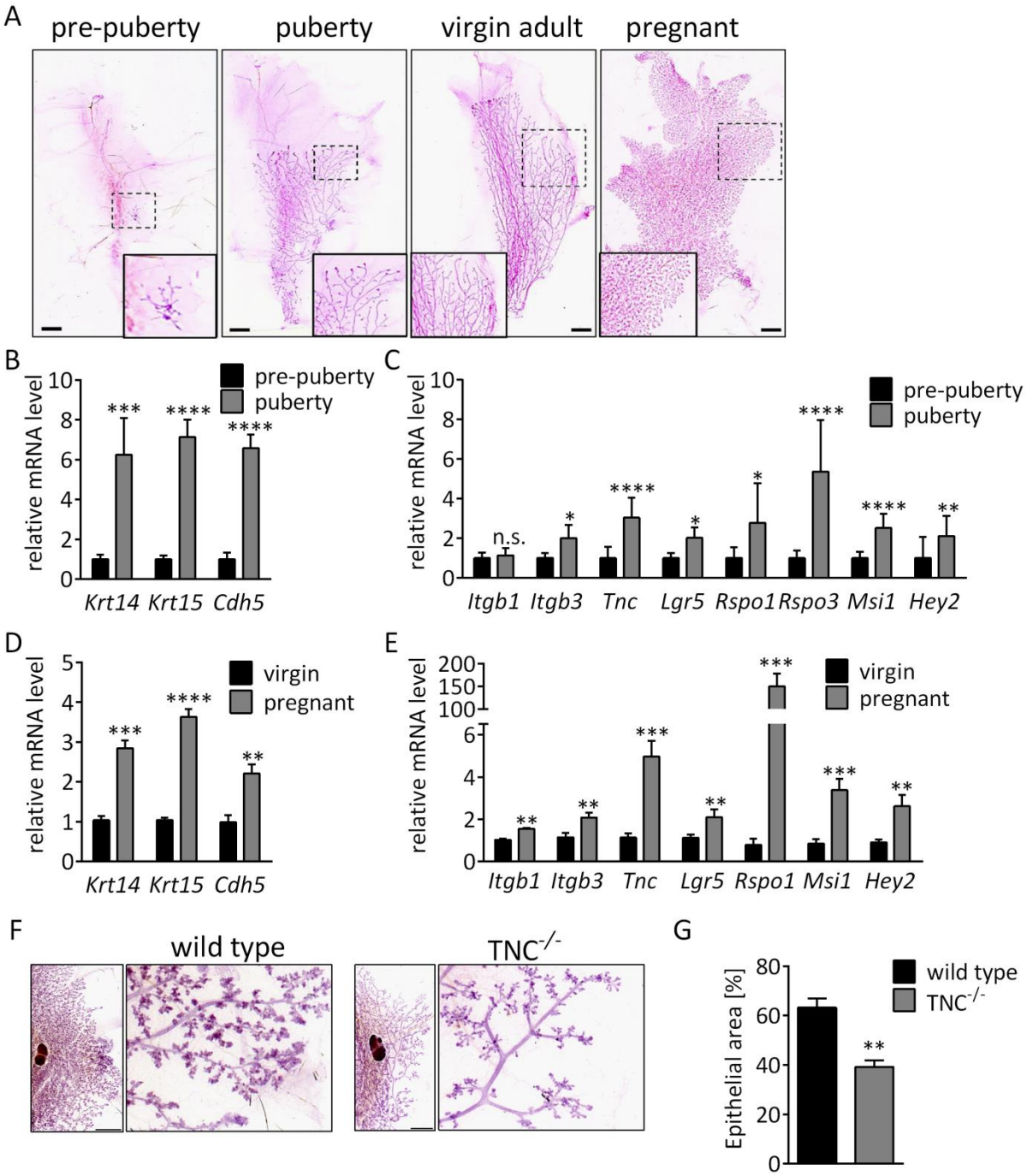

Figure 31 The TNC signaling supports the development of the mammary gland.
(A) Representative images of carmine alum stained 4th mouse mammary gland at different stages of development (from left to right: pre-puberty, 3 weeks; puberty, 5 weeks; virgin adult; 9 weeks; pregnant). **(B - C)** Gene expression analysis of basal markers and TNC signaling members by qRT-PCR in mammary glands of pre-puberty and puberty mice. For all genes, the expression in the puberty samples was normalized to pre-puberty samples. Error bars depict means + SD of biological

replicates (n = 5). *P < 0.05, **P < 0.01, ****P < 0.0001; by two-tailed Mann-Whitney test. **(D - E)** Gene expression analysis of basal markers and TNC signaling members by qRT-PCR in mammary glands of virgin and pregnant mice. For all genes, the expression in the pregnant samples was normalized to virgin samples. Error bars depict means + SD of biological replicates (n = 3). **P < 0.01, ***P < 0.001; by two-tailed Mann-Whitney test. **(F)** Representative images of Carmine Alum stained 4th mouse mammary gland of wild type and TNC$^{-/-}$ mice. Scale bars, 0.5cm. **(G)** Quantitative analysis of epithelial area in Carmine Alum stained 4th mammary gland in wild type and TNC$^{-/-}$ mice (*n* = 3 per group; 2 mammary gland per mouse). **P < 0.01; by two-tailed Mann-Whitney test.

As our data suggest a defect in alveogenesis in the TNC$^{-/-}$ mice, I wondered if this lead to a defect in lactation. TNC$^{-/-}$ mice are known to breed as well as their wildtype counterpart [17]. I hypothesized that a defect in lactation might lead to the death of pups after birth due to insufficient milk intake. As a preliminary attempt to address this question, we assessed the number of weaned pups of 3 wildtype matings and 3 TNC$^{-/-}$ matings (2 – 4 liters per mating). This analysis did not reveal any difference in litter viability between the groups **(Figure 32, A and B)**. This result suggests that the observed defect in alveogenesis might be temporary and that other mechanisms might compensate for it at later stages of pregnancy and during lactation. Further investigations are required to clarify this point.

A

mating / litter	number of pups weaned	genotype
1 / 1	8	WT
1 / 2	8	WT
1 / 3	6	WT
2 / 1	8	WT
2 / 2	7	WT
2 / 3	6	WT
3 / 1	7	WT
3 / 2	7	WT
3 / 3	8	WT
4 / 1	8	$TNC^{-/-}$
4 / 2	7	$TNC^{-/-}$
5 / 1	9	$TNC^{-/-}$
5 / 2	5	$TNC^{-/-}$
5 / 3	6	$TNC^{-/-}$
6 / 1	5	$TNC^{-/-}$
6 / 4	8	$TNC^{-/-}$
6 / 2	8	$TNC^{-/-}$
6 / 3	8	$TNC^{-/-}$

B

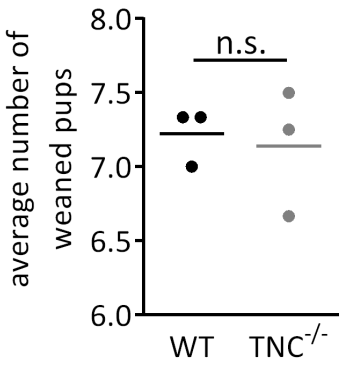

Figure 32 Weaned litter size in wildtype and $TNC^{-/-}$ mice.
(A) Detailled number of weaned wild type and $TNC^{-/-}$ pups for 3 matings and 2-4 litters per mating. **(B)** Average weaned wild type and $TNC^{-/-}$ pups. Line shows mean value (n = 3 matings, 2-4 litters / mating). n.s., not significant; by two-tailed Mann-Whitney test

7 Discussion

In this study, we investigated the role of TNC in breast cancer metastasis to the lungs focusing on two specific aspects. First, we aimed to identify the cellular receptors of TNC in metastatic breast cancer cells mediating the published pro-metastatic signaling [94]. Second, we sought to investigate the link between the pro-metastatic function of TNC and the different subtypes of breast cancer. We were able to shed significant light on both aspects of the TNC biology in metastatic breast cancer. Furthermore, our findings guided further investigation regarding a putative functional role of TNC in the normal mammary stem cell biology.

7.1 ITGB1 and ITGB3 mediate the TNC signaling *in vitro* and promote metastasis *in vivo*

The role of TNC in promoting metastasis has been established by independent comprehensive studies [94, 164]. However, the cellular receptors mediating the pro-metastatic signaling of TNC remained unclear. Since its original discovery 30 years ago, TNC and its cellular functions have been extensively studied and reviewed. Remarkably, several cell surface receptors have been suggested to mediate the cellular function of TNC [92, 107, 108, 129, 136]. In order to identify the cellular receptors of TNC in the particular context of breast cancer metastasis to the lung, we filtered the list of suggested receptors based on whole transcriptome datasets and gene expression analysis of our metastatic breast cancer models (MDA231, MDA231 LM2, SUM159 LM1). This approach allowed us to establish a list of nine putative TNC receptors, which could be readily tested *in vitro*.

The TNC signaling in breast cancer metastatic cells have been investigated by Oskarsson *et al.*, who showed that TNC control the expression of the Notch signaling positive regulator and adult stem cell marker *MSI1* and of the Wnt target gene and adult stem cell marker *LGR5*, while the canonical Wnt target gene *AXIN2* remained unaffected [94]. We reasoned that the receptor(s) of TNC in this particular context should control these target genes in a similar way. Therefore, I generated knockdown for the nine receptor candidates and monitored the expression of *LGR5*, *AXIN2*, *MSI1* and the Notch target gene *HEY2*. Two integrin beta subunits, ITGB1 and ITGB3, showed an interesting gene expression pattern upon knockdown. Indeed, knocking down these genes in two different cell lines separately resulted in a decrease in *LGR5* expression while *AXIN2* was not affected. Importantly, we validated this finding in primary metastatic breast cancer cells, emphasizing the potential clinical relevance of our finding **(Figure 21)**. We

hypothesized that targeting of both receptors might recapitulate the full TNC signaling and generated double knockdown cells for both ITGB1 and ITGB3. Indeed, knockdown of both integrin beta subunit receptors lead to further reduction of *LGR5* level as compared to the single knockdown and a decrease in expression in both *MSI1* and *HEY2* **(Figure 22)**. These findings imply that the TNC signaling is mediated by ITGB1 and ITGB3. A recent study using a syngeneic mouse breast cancer model showed that depletion of ITGB1 elicited a compensatory mechanism leading to increased expression of ITGB3 [205]. As such as phenomenon might explain the difference observed between the single and double knockdown, I tested this hypothesis in our system. However, I did not observe any effect on ITGB3 expression upon knockdown of ITGB1 or vice-versa (data not shown). Compensatory mechanisms between ITGB1 and ITGB3 might as well happen at a non-transcriptional level. One can easily imagine that upon knockdown of ITGB1 (or ITGB3) more TNC-ITGB3 (or TNC-ITGB1) complex might form as a consequence of the greater availability of TNC. However this mechanism does not provide the cells with a full compensation as attested by the effect on *LGR5* upon knock down of the single receptors.

In order to prove the binding of TNC to the identified receptors, we decided to immunoprecipitate TNC and to test for the presence of ITGB1 and ITGB3 in the pull-down sample. This type of biochemical proof-of-binding analysis is typically performed on overexpressed, tagged proteins of interest. We aimed to established an endogenous assay. As attested by western blot technique, we managed to pull down endogenous TNC in a specific and efficient manner. Together with TNC, we could also detect ITGB1, proving that both molecules formed a complex and that indeed TNC binds to ITGB1. In addition, we used mass spectrometry to perform targeted SRM analysis for ITGB3 in a collaborative effort with Dr. Sabrina Hanke. We validated our technical approach by showing enrichment in FN, a well-characterized binding partner of TNC, upon TNC immunoprecipitation [116]. Targeted SRM analysis revealed that ITGB3 was also enriched in the TNC endogenous pull-down sample. We were later able to validate this finding using western blot technique **(Figure 23**). Together, this set of experiments demonstrates that TNC can bind both ITGB1 and ITGB3.

TNC has been shown to functionally promote survival and outgrowth of breast cancer cells at the pulmonary site [94]. In order to assess the functional role of ITGB1 and ITGB3 on the late stages of breast cancer metastasis to the lungs, I performed a set of *in vivo* experiments using immunocompromised NSG mice. Due to the lack of functional B-, T- and NK-cells, these mice offer the best engraftment rates for human cells allowing to study human disease in an *in vivo* setting [206]. In order to assess the growth of the cancer cells at the distant site *in vivo*, we previously labelled the cancer cells with a triple-modality reporter gene encoding for thymidine kinase, GFP and luciferase allowing whole body bioluminescence imaging upon intraperitoneal

injection of luciferin [193]. *In vivo*, this technique is particularly useful for assessing the overall metastatic spread. For quantification purpose, we assessed the bioluminescence signal upon dissection of the lungs, *ex vivo.* Quantification of the metastatic burden revealed that deficiency in ITGB1 or ITGB3 caused a 2- to 3-fold significant decrease in metastatic ability in the MDA231 LM2 metastatic derivative, which was confirmed by IHC **(Figure 24)**. This strongly suggests that both ITGB1 and ITGB3 promote the growth of breast cancer cells at the distant site. There have been contradictory studies on the role of ITGB1 in metastatic progression, one study showing that ITGB1 plays a critical pro-metastatic role in breast cancer, while another one states that ITGA2-ITGB1 is a metastasis suppressor [207, 208]. Importantly, both studies used HER2 driven transgenic mouse models for *in vivo* analysis. In contrast, our work was performed in the context of human triple-negative breast cancer, where ITGB1 clearly promoted metastatic outgrowth. The pro-metastatic function of ITGB3 was suggested in a syngeneic mouse model where overexpression of ITGB3 in a mammary carcinoma cell line promoted spontaneous metastasis to the bone [209]. Remarkably, TNC was shown to promote metastasis to the lung in our xenograft model [94]. Therefore it would be of interest to address the role of ITGB3 in bone metastasis in our model.

Assessing the metastatic ability of breast cancer cells deficient for both ITGB1 and ITGB3 revealed a 12-fold decrease compared to control cells, compared to 2- to 3-fold for the single knockdowns **(Figure 24)**. Importantly, the strong decrease in metastatic ability upon double knockdown of ITGB1 and ITGB3 was confirmed in a second cell line. This shows that ITGB1 and ITGB3 have more than an additive effect in promoting the growth of metastatic cancer cells at the distant site. We validated the previously demonstrated pro-metastatic role of TNC *in vivo* [94]. In this setting, TNC knockdown breast cancer cells showed only a 3-fold decreased metastatic ability **(Figure 16)**. The divergence between the TNC-knockdown and the ITGB1/3-knockdown metastatic phenotype indicates that the functions of ITGB1 and ITGB3 are not only the result of a TNC binding but rather that additional roles are likely to exist.

The identification of two TNC binding integrin receptors prompted us to investigate which alpha subunits are pairing with ITGB1 and ITGB3. Among the four candidates which have been associated with ITGB1 as TNC receptors (ITGA2/7/8/9) only *ITGA2* was expressed at mRNA level in the MDA231 and its metastatic derivative cell lines. In order to assess the expression of those proteins in breast cancer, we made use of the Human Protein Atlas database. The Human Protein Atlas portal is a publicly available database of immunohistochemistry analysis showing the distribution of proteins in normal and malignant human tissues. Out of the four candidates, ITGA2 was the only one showing strong and broad expression in breast cancer tissues. This prompted us to investigate further a potential role for ITGA2 in regulating the TNC signaling. The generation of an ITGA2 knockdown down revealed that ITGA2 controls the expression of

LGR5, to a similar extend as ITGB1, making of ITGA2 a strong candidate as a partner of ITGB1 **(Figure 25)**. This finding should be validated in further cell lines though. ITGAV has been suggested to pair with ITGB3 as a TNC receptor. In addition, ITGAV-ITGB3 has been shown to promote metastasis to the lungs in a syngeneic mouse model for mammary tumors [209]. Hence, we did not observe any effect on the TNC signaling upon knockdown of ITGAV in metastatic breast cancer cells. To note is that the knockdown efficiency was of 85% at mRNA level and that it was verified at protein level **(Figure 25)**. However, it might be necessary to eliminate the protein completely using a knockout technology such as the CRISPR/Cas system to be able to impair the TNC signaling [210]. A further binding partner of ITGB3 is ITGA2b. However, expression of ITGA2b is known to be restricted to the hematopoietic system, where it supports platelet activation and aggregation during blood coagulation. Therefore to date, identification of the alpha partner of ITGB3 requires further investigations.

7.2 The TNC-integrin axis in breast cancer metastasis is associated with the triple-negative subtype

The tight regulation of TNC expression throughout life is well studied and it is widely recognized for many cancer entities that high expression of TNC in a tumor is associated with poor clinical outcome for patients [107]. To date, breast cancer is not considered a single disease, but rather a collection of subtypes with different phenotypes which have been classified in a collective effort of the breast cancer research community. In a clinical setting, expression of the biomarkers ER, PR and HER2 remains the golden standard for patient stratification. Interestingly, histological studies on breast cancer patients' specimen have suggested a negative correlation between TNC and ER expression [145, 151]. This prompted us to investigate a putative link between the prognostic value of TNC and the different breast cancer subtypes. Using multiple gene expression datasets compiled in the Kaplan-Meier online tool for breast cancer, we found that the prognostic value of TNC was exclusively restricted to the triple-negative subtype, while it does not apply to other specific subtypes or all subtypes **(Figure 14)** [194]. This finding was validated in the METABRIC dataset, which comprises gene expression profiling data of almost 2000 breast cancer patients **(Figure 15)** [195]. Correlation between high TNC expression in breast cancer and disease recurrence has already been suggested by various studies [94, 149, 150]. However the strict association to one of the breast cancer subtype, the triple-negative subtype, had not been recognized previously and represents a novel finding with putative therapeutic consequences.

Having established the link between the triple-negative subtype and TNC prognostic value and as ER negative tumors were suggested to express more TNC compared to ER positive tumors,

we aimed to correlate the expression level of TNC with the different breast cancer subtypes. To this purpose, we quantitatively analyzed a TMA comprising 205 patients for TNC expression. In this patient cohort, 13% of the patients were classified as triple-negative according to pathological annotations. In the clinic, about 10-20% of breast cancer tumors test negative for all three biomarkers. Therefore we can assume that our patient cohort is not over- or underrepresenting the triple-negative subtype. Our analysis using automated quantification revealed that TNC expression is higher in the triple-negative tumors compared to the other subtypes **(Figure 16)**. This finding was confirmed in the METABRIC gene expression dataset **(Figure 15)**. Interestingly, we observed differential expression pattern of TNC among the different cores of the TMAs. In a large number of cores, TNC expression was associated with the stromal compartment. However, some cores also showed clear tumor-cell derived expression of TNC and these cores mainly belonged to the triple-negative subtype. This strongly suggests that triple-negative breast cancer cells express TNC on their own and do not rely on the stromal compartment as a source of TNC. As our and previous data showed that autocrine TNC represents an advantage in term of survival at the distant site, we suggest that the prognostic value of TNC in the triple-negative breast cancer subtype might not only be due to absolute amount of TNC but also to its cellular source. Indeed, we observed that 60% of the triple-negative patients express cancer-cell derived TNC against only 20% in the other subtypes **(Figure 15)**. Accordingly, triple-negative breast cancer cell lines expressed significantly more TNC than cell lines belonging to another subtype **(Figure 26)**. This finding was confirmed and extended using the GOBO (Gene expression-based Outcome for Breast cancer Online) gene expression dataset, which comprises 51 breast cancer cell lines (data not shown) [211]. Interestingly, we showed that triple-negative breast cancer cells also express more ITGB1 and ITGB3 as cancer cells belonging to the other subtypes **(Figure 26)**. Hence, we postulate that triple-negative breast cancer cells express high level of autocrine TNC as well as its receptors ITGB1 and ITGB3. As a consequence, triple-negative breast cancer cells do not rely on the stroma for TNC production and the TNC pro-metastatic signaling can be readily activated due to high expression of the mediating receptors. Clinically, this phenomenon is illustrated by the strict association of the TNC prognostic value to the triple-negative, which is due to higher expression of autocrine TNC level and greater availability of its receptors.

7.3 Clinical relevance and putative therapeutic targeting of the TNC-integrin axis in triple-negative breast cancer

Having identified a functional pro-metastatic axis for triple-negative breast cancer to the lungs, we next aimed to evaluate its clinical relevance using the METABRIC gene expression profiling dataset of basal-like patients, out of which 80% are triple-negative. Therefore we can assume that characteristics of basal-like patients in this dataset are very likely to apply the the triple-negative subtype. We observed that the expression of *TNC* positively and significantly correlates with the expression of *ITGB1* (r = 0.3056). Similarly, *TNC* expression significantly correlates with *ITGB3* expression, although the correlation coefficient is lower (r = 0.2666). This might be a consequence of the low spread of the *ITGB3* values. Indeed, the dispersion of the *ITGB3* expression values was much less pronounced that the one of *ITGB1* with standard deviations values of 0.1884 and 0.7924, respectively. Interestingly, when the *TNC* expression values were correlated to the mean of the *ITGB1* and *ITGB3* expression values, the positive correlation became even stronger (r = 0.3376). This is due to the fact that expression of *ITGB1* and *ITGB3* also positively and significantly correlates with each other (r = 0.2775) **(Figure 27)**. In summary, we observed a positive correlation in expression between the two TNC receptors and between TNC and its receptors in basal-like breast cancer patients, which encouraged us to further investigate the clinical relevance of the TNC-integrin axis.

We decided to investigate the putative clinical relevance of the identified TNC-integrin axis in the context of triple-negative breast cancer. To address this, we stratified the patients expressing high level of *TNC* according to *ITGB1/3* expression. Within the '*TNC* high' group, we observed a separation according to *ITGB1* expression: the '*ITGB1* high' group performed worse in term of overall survival compared to the '*ITGB1* low' group. This observation held true when we performed the same analysis with *ITGB3*. Patients with high expression of both TNC and ITGB1 or ITGB3 lived significantly shorter than patients with low expression of TNC. In contrast, even if patients with high expression of *TNC* but low expression of *ITGB1* or *ITGB3* live shorter than patients with only low expression of *TNC,* this difference did not reach statistical significance. These findings strongly support the idea of a functional link between TNC and ITGB1 and ITGB3 in a clinical setting **(Figure 28)**.

The overall survival of patients further declined when TNC high tumors expressed high level of both ITGB1 and ITGB3. Interestingly, 'TNC high' patients with low expression level of ITGB1/3 lived nearly as long as patients with low expression of TNC **(Figure 28)**. This observation further emphasizes the fact that TNC promotes cancer progression through the identified receptors, ITGB1 and ITGB3.

All in all, we demonstrated in a representative cohort of basal-like breast cancer patients that the prognostic value of TNC depends on the expression of the identified receptors and that patients displaying high level of both TNC and its receptors perform significantly worse than patients expressing only high amount of TNC. These results imply that our findings might be of clinical relevance and raise the question of a therapeutic targeting of the identified TNC-ITGB axis in triple-negative breast cancer.

Due to its tumor-specific expression pattern, TNC appears to be an appealing candidate for cancer treatment. Indeed, TNC-targeted therapy strategies for cancer have been developed in the last years. It is important to mention that to date TNC is used as a biomarker to direct the delivery of cytotoxic molecules to the cancer site. Targeting the molecular functions of TNC in cancer progression has only been performed in very preliminary settings [212, 213]. The most promising approach to date is the TNC-targeting antibody F16, which has reached phase III in clinical trial for several cancer entities [214]. Of particular interest for us it the use of F16 antibody in the treatment of metastatic breast cancer [215]. In a phase II clinical study published in 2015, the F16 antibody was coupled to IL2 in order to attract immune cells into the tumor and to facilitate the engagement of the immune system against the tumor. When combined to a chemotherapy regimen (doxorubicin), anti-cancer activity was observed in 9/10 patients and the treatment showed a very good safety profile. These results are very encouraging and the F16 antibody for treatment of metastatic breast cancer will hopefully be challenged in a larger patient cohort rapidly. In regards of our results, it might be important to consider patient stratification upon therapy. Indeed, we showed that autocrine TNC expression is greater in triple-negative breast cancer patients and that it mediates metastasis in this particular subtype. Therefore any therapy targeting TNC would have better chances to show anti-cancer activities in this particular subtype. Unfortunately, information on patient subtype was not stated by Catania *et al.* in their study using the F16 antibody in metastatic breast cancer [215]. Targeting of integrin signaling through integrin inhibitors have reached phase III clinical studies or clinical approvment [216]. Particularly interesting in the context of this study, the peptide Cilengitide targets ITGAV-ITGB3 and has reached phase II clinical trial in patient with recurrent glioblastoma [217]. If ITGB3 would work with ITGAV in the promotion of breast cancer metastasis, it would make sense to test the effect of this drug in our model system. To our knowledge, there is no specific inhibitor of ITGA2-ITGB1 under clinical investigations. However, the ITGB1 blocking antibody AIIB2 has been used safely used in mice where it was showed to inhibit the seeding of osteosarcoma cells in the lung [218] In addition, this antibody has been shown to induced apoptosis and decrease growth of breast cancer cells *in vitro* and *in vivo*. We have preliminary data showing that in our model, *in vitro* treatment with AIIB2 leads to a decrease in *LGR5* expression (data not shown). All in all, this suggests that blocking of ITGB1 with AIIB2 might be a clinically relevant strategy to tackle breast cancer metastasis.

According to our data, combination of TNC targeting and integrin inhibition should be considered in the future. In order to avoid possible negative side effects due to the broad range of action of ITGB1, it would be particularly appealing to use the tumor-specific expression pattern of TNC to direct compounds targeting integrins. The multimodal nanoparticle-based SMART (Simultaneously Multiple Aptamers and RGD Targeting) probe targets TNC, ITGAV-ITGB3 and nucleolin at the same time. This probe has shown a strong specificity and binding affinity to multiple human cancer cells *in vitro,* while its efficiency *in vivo* remains to be addressed [219]. It would be interesting to investigate whether the SMART probe might disrupt the binding between TNC and ITGB3. This raises a crucial point, which is the identification of the precise binding sites of TNC to the ITGB1 and ITGB3 receptors. While ITGB3 has been suggested to bind to the third FNIII-like domain and to the C-terminal FG domain, the binding site for ITGA2-ITGB1 remains unknown [123]. Co-immunoprecipitation of mutant TNC lacking specific domains and ITGB3 or ITGB1 could be used to address this question. Knowledge about the exact binding site of integrins within the TNC molecule would facilitate the design of specific targeting molecules.

7.4 The TNC-integrin axis promotes stem cell properties in triple-negative breast cancer

Pluripotent epithelial mammary cells and breast cancer cells have been shown to form spheroid structures called respectively mammospheres and oncospheres when grown on non-adhesive plates in serum-free conditions. Interestingly, TNC expression is enriched upon spheroid culture of mammary epithelial and breast cancer cells [94, 201]. This prompted us to investigate the expression of the identified TNC receptors upon spheroid formation, as well as a putative functional role for ITGB1 and ITGB3 in sphere formation. We confirmed the induction of TNC expression at protein level by western blot upon sphere formation and observed a gradual enrichment of TNC protein with time. Interestingly, ITGB3 protein expression followed the same pattern of induction and gradual enrichment, while ITGB1 was induced upon sphere formation without being further enriched **(Figure 29)**. It is important to note that spheroid culture represents a stressful environment for the cancer cells due to partial lack of nutrients (serum-free conditions) and adhesion. These conditions have been shown to enrich for aggressive breast cancer cells with stemness and early progenitor properties [220]. Accordingly, the expression of the stemness markers *NANOG*, *OCT4* and *SOX2* was induced upon sphere formation **(Figure 29)**. Interestingly, TNC has been previously linked to the formation of oncospheres [94]. Together with the similarity in expression pattern of TNC and its receptors upon spheroid formation, this prompted us to investigate the functional role of ITGB1 and ITGB3 in sphere formation. The lack of one or the other receptor did not impact sphere formation, indicating that ITGB1 and ITGB3 alone are sufficient to support sphere formation.

However, upon double knockdown of both ITGB1 and ITGB3, we observed a dramatic reduction in sphere formation capacity, as attested by significantly smaller spheres. Interestingly, both the Notch and the Wnt pathways have been linked to the formation of mammo- and oncospheres. More in detail, activation of the Notch signaling pathway was shown to increase the formation of mammospheres and genetic and pharmacologic deletion of the Notch receptors 1 and 4 reduced the formation of oncospheres [221, 222]. On the other hand, the PTEN/Akt pathway was shown to regulate the formation of mammospheres and oncospheres via the Wnt singaling pathway and a further independent study demonstrated that both canonical and non-canonical Wnt signaling promote stem cell growth in mammospheres [223, 224]. We have shown that ITGB1 and ITGB3 control the expression of the Wnt target gene LGR5 and at least part of the Notch signaling. Therefore, it is reasonable to assume that in our model ITGB1 and ITGB3 promote spheroid formation via the Wnt and the Notch pathways. As TNC was previously shown to be necessary for sphere formation and we have shown that both ITGB1 and ITGB3 are necessary to mediate the TNC signaling, this assay strongly suggests that ITGB1 and ITGB3 promote sphere formation via TNC. It also implies that the cells expressing TNC, ITGB1 and ITGB3 are cancer cells with stemness properties capable of surviving and proliferating under stress conditions. Importantly, we showed by FACS that the same cells are able to upregulate both ITGB1 and ITGB3 under spheroid conditions. Accumulating evidences suggest that within a tumor, a relatively small number of cells are capable of self-renewal, initiation of tumorigenesis and generation of heterogeneous cancer cell populations. These cells are termed tumor initiating cells (TIC) or cancer stem cells (CSC) [225]. Recently, several integrins have been described as markers of TIC. In two independent mouse models, ITGB3, in collaboration with the TGF-beta signaling pathway, was shown to be necessary and sufficient for the TIC phenotype in breast cancer [200, 226]. Additionally, ITGB3 was described as a TIC marker in a further mouse model for mammary tumorigenesis [227]. The ITGA6 and ITGB1 integrins are also required for breast cancer initiation, as shown in two independent mouse models for human breast cancer [228, 229]. Our findings on the role of ITGB1 and ITGB3 for in oncosphere formation are in line with the idea of ITGB1 and ITGB3 being markers of tumor-initiating cells.

7.5 The TNC-integrin axis promotes stem cell properties in the mammary gland

As previously mentioned, TNC expression has been detected in the mammary gland during embryonic development as well as upon mammary gland engraftment upon transplantation [134, 135].In this study, we showed that TNC and its receptors, ITGB1 and ITGB3, are associated with stemness properties in triple-negative breast cancer cells. This prompted us to investigate a putative role for TNC signaling in the normal mammary stem cells. Mammary stem cells are multipotent adult stem cells, which are thought to reside in the basal position in the mammary

ducts and which can give rise to all mammary epithelial lineages [202]. In order to assess the putative role of TNC in mammary stem cells we used mammosphere formation as a surrogate assay for stemness activity. Indeed, mammosphere cultures have been shown to enrich for mammary stem and progenitor cells [201]. We observed a significant decrease in mammosphere formation capacity in the TNC knockout mammary epithelial cells, indicating an impairment in stemness properties **(Figure 30)**. As already mentioned, both the Wnt and the Notch signaling were shown to promote stem cell growth in mammospheres. More experiments are required to determine if these signaling pathways are responsible for the phenotype observed in the TNC knockout mammospheres.

In order to analyze the functional role of TNC in mammary stem cells, we assessed the expression of the TNC signaling members in the murine mammary fat pad at developmental and maturation stages which strongly rely on functional stem cells and are characterized by an expansion of the stem cell compartment. These are mainly ductal elongation during puberty and alveogenesis during pregnancy. We observed an induction of *Itgb1* and *Itgb3* during pregnancy-associated alveogenesis. In 2006, two independent reports showed that integrins (ITGB1 and ITGA6) can be used as cell surface markers of the mammary stem cell population, from which a single cell is able to reconstitute a functional mammary gland *in vivo* upon transplantation [230, 231]. A year later, expression of ITGB3 was shown to distinguish between luminal progenitor cells (ITGB3 positive) and differentiated luminal cells (ITGB3 negative) [232]. Therefore upregulation of these receptors during alveogenesis strongly suggests expansion of the stem and early progenitor compartment at this stage of pregnancy. Accordingly, the mammary stem cell markers and basal-markers *Krt14*, *Krt15* and *Cdh5* were also significantly upregulated [185, 204]. Remarkably, we observed an induction of *Tnc*, *Lgr5*, *Msi1* and *Hey2* during pregnancy-associated alveogenesis compared to virgin mice, indicating that the TNC signaling is associated with expansion of the mammary stem cell compartment. Interestingly, one of the ligands of *LGR5, RSPO1,* was also induced, possibly indicating a collaboration of these two molecules in enhancement of the Wnt pathway. Indeed, Wnt signaling was shown to promote the expansion of mammary stem cells [233]. Similarly, we also observed an upregulation of stem and early progenitor markers as well as of the TNC signaling members upon ductal expansion at puberty. **(Figure 31)**. All in all, the correlation between TNC signaling members and stem cell markers upregulation during crucial developmental phase of the mammary gland prompted us to address further the role of TNC in mammary gland stem cells.

For this purpose, we performed morphological analysis of the mammary gland in TNC knockout mice and compared it to wildtype mice. We specifically chose mid-pregnancy, corresponding to 12.5 dpc, as we observed an enrichment of the TNC signaling members at this stage. In addition, upregulation of ITGB3 at 12.5dpc followed by a decrease in expression at later stage

of the pregnancy was shown in a previous study [234]. In the TNC knockout mice, we consistently observed a defect in the mammary gland tree. Indeed compared to the wildtype mice, the alveolar structures at mid-pregnancy in the TNC knockout mice were less numerous and concentrated only at the tip of the ducts **(Figure 31)**. This indicates an impairment in pregnancy-associated alveogenesis possibly due to decreased stemness properties. Interestingly, an independent study has described a similar phenotype at this stage of pregnancy in ITGB3 knockout mice, as well as in mice lacking ITGB1 expression in the mammary basal compartment. Indeed ITGB3 knockout mice showed impaired alveogenesis at 12.5 dpc and ITGB3 was shown to be required for mammary stem cell expansion during puberty with no effect on luminal progenitor cells [234]. This study shed a new light on the role of ITGB3 in the mammary epithelial lineages showing that ITGB3 is not only a marker of early luminal progenitor but it is required for mammary stem cells upon pregnancy-associated activation. In mice lacking ITGB1 in the basal mammary compartment, impairment of alveogenesis at mid-pregnancy accompanied by decreased stem cell number was observed [235]. In a transcription profiling analysis of the different epithelial compartment of the mammary gland, *TNC* and *LGR5* expression was shown to be enriched in the mammary stem cell compartment [204]. Furthermore, it has been repeatedly shown that *LGR5* expression is heterogeneous in the mammary gland epithelium and one study suggested that cells expressing high level of *LGR5* display enriched repopulating capacity [184]. Therefore, we propose that the TNC signaling initially identified in the context of triple-negative breast cancer plays a functional role in the normal mammary stem cell biology at mid-pregnancy. Interestingly, comparative studies of gene expression signatures of the different intrinsic breast cancer subtypes with those of the mammary epithelial lineages revealed striking similarities in gene expression profiles. In detail, the claudin-low and the basal-like subtypes showed significant similarities with mammary stem cells and early luminal progenitor cells, respectively, while the HER2-enriched and the luminal subtypes resemble more differentiated cells [185]. In recent years, several triple-negative breast cancer cells lines have been defined as claudin-low. This is the case for the *in vitro* models used for investigating the TNC signaling in this study, strengthening the idea that our model for triple-negative metastatic breast cancer is likely to share some similarities with mammary stem cells [17].

In an attempt to address a possible defect in lactation in TNC knockout mice, we assessed the number of pups surviving the early life phase until weaning. We did not observe any significant decrease in viability of the TNC knockout animals, which would suggest impaired lactation **(Figure 32)**. This indicates that the defect in alveogenesis might be transient and compensated at later phases of pregnancy. Interestingly, the ITGB3 knockout animals also did not display reduced ability to feed their pups while lactation was strongly impaired in the mice lacking

ITGB1 in the mammary basal compartment. This suggests that ITGB1 might have a broader TNC-independent function in the mammary gland stem cells [234, 235].

As TNC and its associated signaling members are increased at mid-pregnancy in the mouse mammary gland, one might ask whether pregnancy increases the risk for breast cancer. It is important to note that the link between pregnancy and breast cancer is not well characterized. Nevertheless, studies have suggested that pregnancy results in an increased risk for breast cancer within 10 years following birth [236]. This is probably the consequence of massive cellular proliferation during alveogenesis and age-related accumulation of genetic mutations or epigenetic modifications in the breast epithelium, which can result in tumorigenic growth of premalignant epithelial cells. In this context, enrichment in TNC expression could indeed support the development of a pre-malignant lesion to a breast tumor. However, this hypothesis needs to be investigated experimentally. Furthermore, previous studies have shown that TNC is strongly expressed upon lactation during the involution of the mammary gland and we have confirmed it in our mouse model (data not shown) [134, 135]. One can easily imagine that enhanced expression of TNC in the context of post-lactational tissue remodeling might support pregnancy-associated carcinogenesis.

8 Conclusion and model

In this study, we showed that the prognostic value of TNC in breast cancer is restricted to the triple-negative subtype. Using different approaches, we could show that triple-negative tumors are enriched for TNC expression in breast cancer patients. Interestingly, despite the fact that the stromal compartment represents a significant source of TNC in breast tumors in general, we found that triple-negative breast cancer cells preferably produce TNC in an autocrine manner. Accordingly, TNC expression is increased in triple-negative breast cancer cell lines *in vitro* compared to cell lines belonging to other subtypes. In a triple-negative model, we identified two integrin beta subunit receptors mediating the TNC signaling *in vitro*. Following the pattern observed for TNC, ITGB1 and ITGB3 expression was enriched in triple-negative breast cancer cells. We showed that ITGB1 and ITGB3 promote breast cancer metastasis to the lungs in an *in vivo* model for human breast cancer. Interestingly, we observed that the TNC-ITGB axis supports stem cell properties in triple-negative breast cancer cells. We investigated the role of the TNC signaling in the mammary stem cell biology and found that it is associated with crucial developmental and maturation stages of the mammary gland. More importantly, our data indicate that TNC supports stem cell properties in the mammary epithelium and that it promotes pregnancy-associated alveogenesis.

This study suggests interesting parallels between the role of TNC in triple-negative breast cancer and in the mammary stem cells. We propose that the pro-metastatic TNC-integrin axis identified in triple-negative, claudin-low breast cancer cells plays an important role in the mammary stem cell. While in the mammary stem cell TNC promotes stem cell properties and alveogenesis during pregnancy, triple-negative disseminated tumor cells take advantage of high expression of TNC and its receptors to promote their growth at the distant site. **(Figure 33)**.

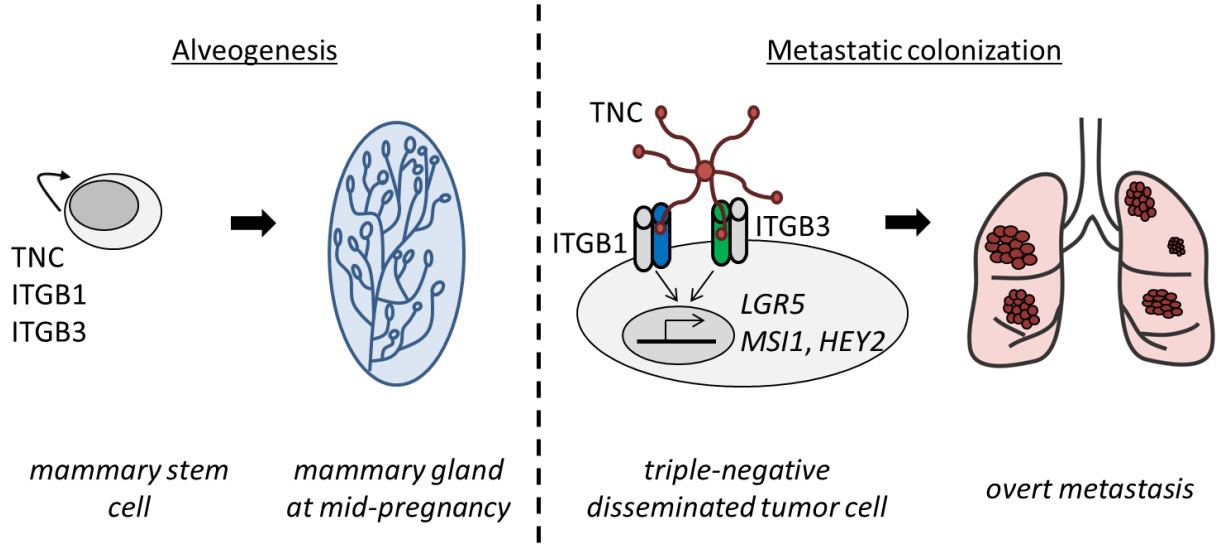

Figure 33 Model.

During pregnancy, mammary stem cells express high level of ITGB1, ITGB3 and TNC, which play a functional role in alveogenesis [204, 234, 235]. In disseminated triple-negative breast cancer cell, which are enriched for TNC, ITGB1 and ITGB3 expression, TNC binds to ITGB1 and ITGB3 and promotes stem cell properties and the expression of *LGR5*, *MSI1* and *HEY2*. This signaling axis supports metastatic growth in the lungs.

9 Outlook and perspectives

We have identified a TNC-integrin axis mediating lung metastasis in triple-negative breast cancer. In order to target this pro-metastatic axis, further investigations are required to determine the exact binding site of ITGB1 and ITGB3 to TNC. Our signaling data suggest that the two receptors can partially compensate for each other. However, in the context of stemness maintenance and metastatic colonization, ITGB1 and ITGB3 are likely to collaborate. Therefore, it would be of interest to study the binding affinity of TNC for each receptor. In addition, further investigations are required to clarify which alpha subunits are binding to ITGB1 and ITGB3. This knowledge would be beneficial for the testing of compounds blocking integrin function and would be highly relevant to the development of therapeutic strategies against the TNC-integrin axis.

TNC has been suggesteded to collaborate with another matricellular protein called POSTN in the regulation of the Wnt pathway. We have evidence that TNC can bind to POSTN in triple-negative breast cancer cells. In addition, we observed that TNC and POSTN promote breast cancer metastasis to the lung (data not shown). More work is required to determine the exact role of POSTN in the TNC-integrin beta axis. In addition, a possible functional collaboration of TNC and POSTN in the development of the mammary gland is currently under investigation.

10 Appendix

10.1 Abbreviations

AD	assembly domain
AJCC	American Joint Committee on Cancer
ANXA2	annexin 2
BCS	breast-conserving surgery
BFP	blue fluorescent protein
BPE	breast pleural effusion
CDK	cyclin dependent kinase
CK	cytokeratin
CNTN1	contactin 1
Co-IP	co-immunoprecipitation
CSC	cancer stem cell
DCIS	ductal carcinoma *in situ*
DKK1	dickkopf-related protein 1
DMSO	dimethyl sulfoxide
DTX1	deltex 1
ECM	extracellular matrix
EGF	epidermal growth factor
EGFR	epidermal growth factor receptor
EMT	epithelial-to-mesenchymal transition
ER	estrogen receptor
FACS	fluorescence-activated cell sorting
FBS	fetal bovine serum
FDA	food and drug administration
FG	fibrinogen globe
FN	fibronectin
GFP	green fluoresent protein
GOBO	Gene expression-based Outcome for Breast cancer Online
GPC1	glypican 1
HE	hematoxilin and eosin
HER2	human epidermal growth factor receptor 2
HEY2	hairy/Enhancer-Of-Split Related With YRPW Motif 2
HR	hormone receptor
IFN	interferon
IHC	immunohistochemistry
ITGA	integrin alpha
ITGB	integrin beta

ITGB	integrin beta
JAG1	Jagged-1
JAK / STAT	janus kinase / signal transduced and activator of transcription
LEF1	lymphoid enhancer-binding factor 1
LGR5	leucine-rich repeat-containing G protein-coupled receptor
LM	lung metastatic
LOX	lysyl oxidase
METABRIC	Molecular Taxonomy of Breast Cancer International Consortium
MMP	matrix metalloproteinase
MSI1	musashi homolog 1
NaN	sodium channel Xia
NSCLC	non-small cell lung carcinoma
NSG	NOD/SCID interleukin-2 receptor gamma chain null
PCR	polymerase chain reaction
PBS	phosphate buffered saline
POSTN	periostin
PR	progesterone receptor
PTPRZ1	phosphacan
PyMT	polyoma middle T
qRT-PCR	quantitative real time polymerase chain reaction
RSPO	R-spondin
SDC4	syndecan 4
SEER	surveillance, epidemiology and end results
shRNA	short hairpin RNA
SMA	smooth muscle actin
SMART	Simultaneously Multiple Aptamers and RGD Targeting
SPARC	secreted protein acidic and rich in cysteine
SPP1	secreted phosphoprotein 1
SRM	single reaction monitoring
TEB	terminal end buds
TGF	transforming growth factor
THBS1	thrombospondin-1
TIC	tumor initiating cell
TLR4	toll-like receptor 4
TMA	tissue microarray
TNC	tenascin C
US	United States
VEGF	vascular endothelial growth factor
VEGFR	vascular endothelial growth factor receptor
VIM	vimentin
vWF	von Willebrand factor
WCL	whole cell lysate
αSMA	alpha smooth muscle actin

10.2 List of figures

10.3 List of tables

11 Bibliography

1. Society., A.C., *Cancer Facts & Figures 2016.* 2016.
2. Society., A.C., *Breast Cancer Facts & Figures 2015-2016.* 2015.
3. Edge, S., et al., *AJCC Cancer Staging Manual.* 2010.
4. Howlader N, N.A., Krapcho M, Miller D, Bishop K, Altekruse SF, Kosary CL, Yu M, Ruhl J, Tatalovich Z, Mariotto A, Lewis DR, Chen HS, Feuer EJ, Cronin KA, *SEER Cancer Statistics Review, 1975-2013, National Cancer Institute.* 2016.
5. Roepman, P., et al., *Microarray-based determination of estrogen receptor, progesterone receptor, and HER2 receptor status in breast cancer.* Clin Cancer Res, 2009. **15**(22): p. 7003-11.
6. Gong, Y., et al., *Determination of oestrogen-receptor status and ERBB2 status of breast carcinoma: a gene-expression profiling study.* Lancet Oncol, 2007. **8**(3): p. 203-11.
7. Scholzen, T. and J. Gerdes, *The Ki-67 protein: from the known and the unknown.* J Cell Physiol, 2000. **182**(3): p. 311-22.
8. Goldhirsch, A., et al., *Personalizing the treatment of women with early breast cancer: highlights of the St Gallen International Expert Consensus on the Primary Therapy of Early Breast Cancer 2013.* Ann Oncol, 2013. **24**(9): p. 2206-23.
9. Perou, C.M., et al., *Molecular portraits of human breast tumours.* Nature, 2000. **406**(6797): p. 747-52.
10. Sorlie, T., et al., *Gene expression patterns of breast carcinomas distinguish tumor subclasses with clinical implications.* Proc Natl Acad Sci U S A, 2001. **98**(19): p. 10869-74.
11. Sorlie, T., et al., *Repeated observation of breast tumor subtypes in independent gene expression data sets.* Proc Natl Acad Sci U S A, 2003. **100**(14): p. 8418-23.
12. Network, C.G.A., *Comprehensive molecular portraits of human breast tumours.* Nature, 2012. **490**(7418): p. 61-70.
13. Sinn, P., et al., *Multigene Assays for Classification, Prognosis, and Prediction in Breast Cancer: a Critical Review on the Background and Clinical Utility.* Geburtshilfe Frauenheilkd, 2013. **73**(9): p. 932-940.
14. Lehmann, B.D., et al., *Identification of human triple-negative breast cancer subtypes and preclinical models for selection of targeted therapies.* J Clin Invest, 2011. **121**(7): p. 2750-67.
15. Herschkowitz, J.I., et al., *Identification of conserved gene expression features between murine mammary carcinoma models and human breast tumors.* Genome Biol, 2007. **8**(5): p. R76.
16. Hennessy, B.T., et al., *Characterization of a naturally occurring breast cancer subset enriched in epithelial-to-mesenchymal transition and stem cell characteristics.* Cancer Res, 2009. **69**(10): p. 4116-24.
17. Prat, A., et al., *Phenotypic and molecular characterization of the claudin-low intrinsic subtype of breast cancer.* Breast Cancer Res, 2010. **12**(5): p. R68.

18. Taube, J.H., et al., *Core epithelial-to-mesenchymal transition interactome gene-expression signature is associated with claudin-low and metaplastic breast cancer subtypes.* Proc Natl Acad Sci U S A, 2010. **107**(35): p. 15449-54.
19. Creighton, C.J., et al., *Residual breast cancers after conventional therapy display mesenchymal as well as tumor-initiating features.* Proc Natl Acad Sci U S A, 2009. **106**(33): p. 13820-5.
20. Millikan, R.C., et al., *Epidemiology of basal-like breast cancer.* Breast Cancer Res Treat, 2008. **109**(1): p. 123-39.
21. Carey, L.A., et al., *Race, breast cancer subtypes, and survival in the Carolina Breast Cancer Study.* JAMA, 2006. **295**(21): p. 2492-502.
22. Hu, Z., et al., *The molecular portraits of breast tumors are conserved across microarray platforms.* BMC Genomics, 2006. **7**: p. 96.
23. Cheang, M.C., et al., *Ki67 index, HER2 status, and prognosis of patients with luminal B breast cancer.* J Natl Cancer Inst, 2009. **101**(10): p. 736-50.
24. Nielsen, T.O., et al., *Immunohistochemical and clinical characterization of the basal-like subtype of invasive breast carcinoma.* Clin Cancer Res, 2004. **10**(16): p. 5367-74.
25. Parker, J.S., et al., *Supervised risk predictor of breast cancer based on intrinsic subtypes.* J Clin Oncol, 2009. **27**(8): p. 1160-7.
26. Carey, L.A., et al., *The triple negative paradox: primary tumor chemosensitivity of breast cancer subtypes.* Clin Cancer Res, 2007. **13**(8): p. 2329-34.
27. Rouzier, R., et al., *Breast cancer molecular subtypes respond differently to preoperative chemotherapy.* Clin Cancer Res, 2005. **11**(16): p. 5678-85.
28. Prat, A. and C.M. Perou, *Deconstructing the molecular portraits of breast cancer.* Mol Oncol, 2011. **5**(1): p. 5-23.
29. Badve, S., et al., *Basal-like and triple-negative breast cancers: a critical review with an emphasis on the implications for pathologists and oncologists.* Mod Pathol, 2011. **24**(2): p. 157-67.
30. Prat, A., et al., *Molecular characterization of basal-like and non-basal-like triple-negative breast cancer.* Oncologist, 2013. **18**(2): p. 123-33.
31. Reis, P.P., et al., *mRNA transcript quantification in archival samples using multiplexed, color-coded probes.* BMC Biotechnol, 2011. **11**: p. 46.
32. Perou, C.M., et al., *Clinical implementation of the intrinsic subtypes of breast cancer.* Lancet Oncol, 2010. **11**(8): p. 718-9; author reply 720-1.
33. Geiss, G.K., et al., *Direct multiplexed measurement of gene expression with color-coded probe pairs.* Nat Biotechnol, 2008. **26**(3): p. 317-25.
34. DeSantis, C.E., et al., *Cancer treatment and survivorship statistics, 2014.* CA Cancer J Clin, 2014. **64**(4): p. 252-71.
35. Darby, S., et al., *Effect of radiotherapy after breast-conserving surgery on 10-year recurrence and 15-year breast cancer death: meta-analysis of individual patient data for 10,801 women in 17 randomised trials.* Lancet, 2011. **378**(9804): p. 1707-16.
36. von Minckwitz, G., et al., *Neoadjuvant chemotherapy and bevacizumab for HER2-negative breast cancer.* N Engl J Med, 2012. **366**(4): p. 299-309.
37. Coates, A.S., M. Colleoni, and A. Goldhirsch, *Is adjuvant chemotherapy useful for women with luminal a breast cancer?* J Clin Oncol, 2012. **30**(12): p. 1260-3.

38. Anampa, J., D. Makower, and J.A. Sparano, *Progress in adjuvant chemotherapy for breast cancer: an overview.* BMC Med, 2015. **13**: p. 195.
39. Thompson, A.M. and S.L. Moulder-Thompson, *Neoadjuvant treatment of breast cancer.* Ann Oncol, 2012. **23 Suppl 10**: p. x231-6.
40. Cardoso, F., et al., *Second and subsequent lines of chemotherapy for metastatic breast cancer: what did we learn in the last two decades?* Ann Oncol, 2002. **13**(2): p. 197-207.
41. Davies, C., et al., *Relevance of breast cancer hormone receptors and other factors to the efficacy of adjuvant tamoxifen: patient-level meta-analysis of randomised trials.* Lancet, 2011. **378**(9793): p. 771-84.
42. Davies, C., et al., *Long-term effects of continuing adjuvant tamoxifen to 10 years versus stopping at 5 years after diagnosis of oestrogen receptor-positive breast cancer: ATLAS, a randomised trial.* Lancet, 2013. **381**(9869): p. 805-16.
43. Dowsett, M., et al., *Meta-analysis of breast cancer outcomes in adjuvant trials of aromatase inhibitors versus tamoxifen.* J Clin Oncol, 2010. **28**(3): p. 509-18.
44. Knauer, M., et al., *The predictive value of the 70-gene signature for adjuvant chemotherapy in early breast cancer.* Breast Cancer Res Treat, 2010. **120**(3): p. 655-61.
45. Markopoulos, C., *Overview of the use of Oncotype DX((R)) as an additional treatment decision tool in early breast cancer.* Expert Rev Anticancer Ther, 2013. **13**(2): p. 179-94.
46. Eiermann, W., et al., *The 21-gene recurrence score assay impacts adjuvant therapy recommendations for ER-positive, node-negative and node-positive early breast cancer resulting in a risk-adapted change in chemotherapy use.* Ann Oncol, 2013. **24**(3): p. 618-24.
47. Chia, S.K., et al., *A 50-gene intrinsic subtype classifier for prognosis and prediction of benefit from adjuvant tamoxifen.* Clin Cancer Res, 2012. **18**(16): p. 4465-72.
48. Tian, S., et al., *Biological functions of the genes in the mammaprint breast cancer profile reflect the hallmarks of cancer.* Biomark Insights, 2010. **5**: p. 129-38.
49. Romond, E.H., et al., *Trastuzumab plus adjuvant chemotherapy for operable HER2-positive breast cancer.* N Engl J Med, 2005. **353**(16): p. 1673-84.
50. Capelan, M., et al., *Pertuzumab: new hope for patients with HER2-positive breast cancer.* Ann Oncol, 2013. **24**(2): p. 273-82.
51. Swain, S.M., et al., *Pertuzumab, trastuzumab, and docetaxel in HER2-positive metastatic breast cancer.* N Engl J Med, 2015. **372**(8): p. 724-34.
52. Verma, S., et al., *Trastuzumab emtansine for HER2-positive advanced breast cancer.* N Engl J Med, 2012. **367**(19): p. 1783-91.
53. Cameron, D., et al., *Lapatinib plus capecitabine in women with HER-2-positive advanced breast cancer: final survival analysis of a phase III randomized trial.* Oncologist, 2010. **15**(9): p. 924-34.
54. Finn, R.S., et al., *The cyclin-dependent kinase 4/6 inhibitor palbociclib in combination with letrozole versus letrozole alone as first-line treatment of oestrogen receptor-positive, HER2-negative, advanced breast cancer (PALOMA-1/TRIO-18): a randomised phase 2 study.* Lancet Oncol, 2015. **16**(1): p. 25-35.
55. Turner, N.C., et al., *Palbociclib in Hormone-Receptor-Positive Advanced Breast Cancer.* N Engl J Med, 2015. **373**(3): p. 209-19.

56. Bachelot, T., et al., *Randomized phase II trial of everolimus in combination with tamoxifen in patients with hormone receptor-positive, human epidermal growth factor receptor 2-negative metastatic breast cancer with prior exposure to aromatase inhibitors: a GINECO study.* J Clin Oncol, 2012. **30**(22): p. 2718-24.
57. Baselga, J., et al., *Phase II randomized study of neoadjuvant everolimus plus letrozole compared with placebo plus letrozole in patients with estrogen receptor-positive breast cancer.* J Clin Oncol, 2009. **27**(16): p. 2630-7.
58. Holohan, C., et al., *Cancer drug resistance: an evolving paradigm.* Nat Rev Cancer, 2013. **13**(10): p. 714-26.
59. Balduzzi, S., et al., *Trastuzumab-containing regimens for metastatic breast cancer.* Cochrane Database Syst Rev, 2014(6): p. CD006242.
60. O'Reilly, E.A., et al., *The fate of chemoresistance in triple negative breast cancer (TNBC).* BBA Clin, 2015. **3**: p. 257-75.
61. O'Shaughnessy, J., *Extending survival with chemotherapy in metastatic breast cancer.* Oncologist, 2005. **10 Suppl 3**: p. 20-9.
62. Valastyan, S. and R.A. Weinberg, *Tumor metastasis: molecular insights and evolving paradigms.* Cell, 2011. **147**(2): p. 275-92.
63. Thiery, J.P., et al., *Epithelial-mesenchymal transitions in development and disease.* Cell, 2009. **139**(5): p. 871-90.
64. Luzzi, K.J., et al., *Multistep nature of metastatic inefficiency: dormancy of solitary cells after successful extravasation and limited survival of early micrometastases.* Am J Pathol, 1998. **153**(3): p. 865-73.
65. Cameron, M.D., et al., *Temporal progression of metastasis in lung: cell survival, dormancy, and location dependence of metastatic inefficiency.* Cancer Res, 2000. **60**(9): p. 2541-6.
66. Fidler, I.J., *The pathogenesis of cancer metastasis: the 'seed and soil' hypothesis revisited.* Nat Rev Cancer, 2003. **3**(6): p. 453-8.
67. Pattabiraman, D.R. and R.A. Weinberg, *Tackling the cancer stem cells - what challenges do they pose?* Nat Rev Drug Discov, 2014. **13**(7): p. 497-512.
68. Shiozawa, Y., et al., *Human prostate cancer metastases target the hematopoietic stem cell niche to establish footholds in mouse bone marrow.* J Clin Invest, 2011. **121**(4): p. 1298-312.
69. Dreesen, O. and A.H. Brivanlou, *Signaling pathways in cancer and embryonic stem cells.* Stem Cell Rev, 2007. **3**(1): p. 7-17.
70. Takebe, N., R.Q. Warren, and S.P. Ivy, *Breast cancer growth and metastasis: interplay between cancer stem cells, embryonic signaling pathways and epithelial-to-mesenchymal transition.* Breast Cancer Res, 2011. **13**(3): p. 211.
71. Carbonell, W.S., et al., *The vascular basement membrane as "soil" in brain metastasis.* PLoS One, 2009. **4**(6): p. e5857.
72. Valiente, M., et al., *Serpins promote cancer cell survival and vascular co-option in brain metastasis.* Cell, 2014. **156**(5): p. 1002-16.
73. Butler, J.M., H. Kobayashi, and S. Rafii, *Instructive role of the vascular niche in promoting tumour growth and tissue repair by angiocrine factors.* Nat Rev Cancer, 2010. **10**(2): p. 138-46.

74. Ghajar, C.M., et al., *The perivascular niche regulates breast tumour dormancy.* Nat Cell Biol, 2013. **15**(7): p. 807-17.
75. Quail, D.F. and J.A. Joyce, *Microenvironmental regulation of tumor progression and metastasis.* Nat Med, 2013. **19**(11): p. 1423-37.
76. Kalluri, R., *The biology and function of fibroblasts in cancer.* Nat Rev Cancer, 2016. **16**(9): p. 582-98.
77. Kalluri, R. and M. Zeisberg, *Fibroblasts in cancer.* Nat Rev Cancer, 2006. **6**(5): p. 392-401.
78. Ozbek, S., et al., *The evolution of extracellular matrix.* Mol Biol Cell, 2010. **21**(24): p. 4300-5.
79. Lu, P., V.M. Weaver, and Z. Werb, *The extracellular matrix: a dynamic niche in cancer progression.* J Cell Biol, 2012. **196**(4): p. 395-406.
80. Gilkes, D.M., G.L. Semenza, and D. Wirtz, *Hypoxia and the extracellular matrix: drivers of tumour metastasis.* Nat Rev Cancer, 2014. **14**(6): p. 430-9.
81. Oskarsson, T., *Extracellular matrix components in breast cancer progression and metastasis.* Breast, 2013. **22 Suppl 2**: p. S66-72.
82. Perryman, L. and J.T. Erler, *Lysyl oxidase in cancer research.* Future Oncol, 2014. **10**(9): p. 1709-17.
83. Condeelis, J. and J.E. Segall, *Intravital imaging of cell movement in tumours.* Nat Rev Cancer, 2003. **3**(12): p. 921-30.
84. Provenzano, P.P., et al., *Collagen reorganization at the tumor-stromal interface facilitates local invasion.* BMC Med, 2006. **4**(1): p. 38.
85. Radisky, E.S. and D.C. Radisky, *Matrix metalloproteinase-induced epithelial-mesenchymal transition in breast cancer.* J Mammary Gland Biol Neoplasia, 2010. **15**(2): p. 201-12.
86. Kaplan, R.N., et al., *VEGFR1-positive haematopoietic bone marrow progenitors initiate the pre-metastatic niche.* Nature, 2005. **438**(7069): p. 820-7.
87. Erler, J.T., et al., *Hypoxia-induced lysyl oxidase is a critical mediator of bone marrow cell recruitment to form the premetastatic niche.* Cancer Cell, 2009. **15**(1): p. 35-44.
88. Todaro, M., et al., *CD44v6 is a marker of constitutive and reprogrammed cancer stem cells driving colon cancer metastasis.* Cell Stem Cell, 2014. **14**(3): p. 342-56.
89. Yu, Q., B.P. Toole, and I. Stamenkovic, *Induction of apoptosis of metastatic mammary carcinoma cells in vivo by disruption of tumor cell surface CD44 function.* J Exp Med, 1997. **186**(12): p. 1985-96.
90. Chong, H.C., et al., *Matricellular proteins: a sticky affair with cancers.* J Oncol, 2012. **2012**: p. 351089.
91. Malanchi, I., et al., *Interactions between cancer stem cells and their niche govern metastatic colonization.* Nature, 2012. **481**(7379): p. 85-9.
92. Chiquet-Ehrismann, R., et al., *Tenascins in stem cell niches.* Matrix Biol, 2014.
93. Oskarsson, T. and J. Massague, *Extracellular matrix players in metastatic niches.* EMBO J, 2012. **31**(2): p. 254-6.
94. Oskarsson, T., et al., *Breast cancer cells produce tenascin C as a metastatic niche component to colonize the lungs.* Nat Med, 2011. **17**(7): p. 867-74.
95. Wang, Z. and G. Ouyang, *Periostin: a bridge between cancer stem cells and their metastatic niche.* Cell Stem Cell, 2012. **10**(2): p. 111-2.

96. Kii, I., et al., *Incorporation of tenascin-C into the extracellular matrix by periostin underlies an extracellular meshwork architecture.* J Biol Chem, 2010. **285**(3): p. 2028-39.
97. Oates, A.J., R. Barraclough, and P.S. Rudland, *The identification of metastasis-related gene products in a rodent mammary tumour model.* Biochem Soc Trans, 1996. **24**(3): p. 353S.
98. Pietras, A., et al., *Osteopontin-CD44 signaling in the glioma perivascular niche enhances cancer stem cell phenotypes and promotes aggressive tumor growth.* Cell Stem Cell, 2014. **14**(3): p. 357-69.
99. Tuck, A.B., et al., *Osteopontin induces increased invasiveness and plasminogen activator expression of human mammary epithelial cells.* Oncogene, 1999. **18**(29): p. 4237-46.
100. Minn, A.J., et al., *Genes that mediate breast cancer metastasis to lung.* Nature, 2005. **436**(7050): p. 518-24.
101. Yee, K.O., et al., *The effect of thrombospondin-1 on breast cancer metastasis.* Breast Cancer Res Treat, 2009. **114**(1): p. 85-96.
102. Chiquet, M. and D.M. Fambrough, *Chick myotendinous antigen. I. A monoclonal antibody as a marker for tendon and muscle morphogenesis.* J Cell Biol, 1984. **98**(6): p. 1926-36.
103. Chiquet, M. and D.M. Fambrough, *Chick myotendinous antigen. II. A novel extracellular glycoprotein complex consisting of large disulfide-linked subunits.* J Cell Biol, 1984. **98**(6): p. 1937-46.
104. Chiquet-Ehrismann, R., et al., *Tenascin interferes with fibronectin action.* Cell, 1988. **53**(3): p. 383-90.
105. Chiquet-Ehrismann, R., *Anti-adhesive molecules of the extracellular matrix.* Curr Opin Cell Biol, 1991. **3**(5): p. 800-4.
106. Erickson, H.P. and J.L. Inglesias, *A six-armed oligomer isolated from cell surface fibronectin preparations.* Nature, 1984. **311**(5983): p. 267-9.
107. Lowy, C.M. and T. Oskarsson, *Tenascin C in metastasis: A view from the invasive front.* Cell Adh Migr, 2015. **9**(1-2): p. 112-24.
108. Orend, G. and R. Chiquet-Ehrismann, *Tenascin-C induced signaling in cancer.* Cancer Lett, 2006. **244**(2): p. 143-63.
109. Spring, J., K. Beck, and R. Chiquet-Ehrismann, *Two contrary functions of tenascin: dissection of the active sites by recombinant tenascin fragments.* Cell, 1989. **59**(2): p. 325-34.
110. Chung, C.Y., J.E. Murphy-Ullrich, and H.P. Erickson, *Mitogenesis, cell migration, and loss of focal adhesions induced by tenascin-C interacting with its cell surface receptor, annexin II.* Mol Biol Cell, 1996. **7**(6): p. 883-92.
111. Swindle, C.S., et al., *Epidermal growth factor (EGF)-like repeats of human tenascin-C as ligands for EGF receptor.* J Cell Biol, 2001. **154**(2): p. 459-68.
112. Vaughan, L., et al., *Tenascin-contactin/F11 interactions: a clue for a developmental role?* Perspect Dev Neurobiol, 1994. **2**(1): p. 43-52.
113. Milev, P., et al., *The fibrinogen-like globe of tenascin-C mediates its interactions with neurocan and phosphacan/protein-tyrosine phosphatase-zeta/beta.* J Biol Chem, 1997. **272**(24): p. 15501-9.

114. Srinivasan, J., M. Schachner, and W.A. Catterall, *Interaction of voltage-gated sodium channels with the extracellular matrix molecules tenascin-C and tenascin-R.* Proc Natl Acad Sci U S A, 1998. **95**(26): p. 15753-7.
115. Saito, Y., et al., *A peptide derived from tenascin-C induces beta1 integrin activation through syndecan-4.* J Biol Chem, 2007. **282**(48): p. 34929-37.
116. Huang, W., et al., *Interference of tenascin-C with syndecan-4 binding to fibronectin blocks cell adhesion and stimulates tumor cell proliferation.* Cancer Res, 2001. **61**(23): p. 8586-94.
117. Orend, G., et al., *Tenascin-C blocks cell-cycle progression of anchorage-dependent fibroblasts on fibronectin through inhibition of syndecan-4.* Oncogene, 2003. **22**(25): p. 3917-26.
118. Midwood, K., et al., *Tenascin-C is an endogenous activator of Toll-like receptor 4 that is essential for maintaining inflammation in arthritic joint disease.* Nat Med, 2009. **15**(7): p. 774-80.
119. Sriramarao, P., M. Mendler, and M.A. Bourdon, *Endothelial cell attachment and spreading on human tenascin is mediated by alpha 2 beta 1 and alpha v beta 3 integrins.* J Cell Sci, 1993. **105 (Pt 4)**: p. 1001-12.
120. Mercado, M.L., et al., *Neurite outgrowth by the alternatively spliced region of human tenascin-C is mediated by neuronal alpha7beta1 integrin.* J Neurosci, 2004. **24**(1): p. 238-47.
121. Denda, S., et al., *Utilization of a soluble integrin-alkaline phosphatase chimera to characterize integrin alpha 8 beta 1 receptor interactions with tenascin: murine alpha 8 beta 1 binds to the RGD site in tenascin-C fragments, but not to native tenascin-C.* Biochemistry, 1998. **37**(16): p. 5464-74.
122. Yokosaki, Y., et al., *The integrin alpha 9 beta 1 mediates cell attachment to a non-RGD site in the third fibronectin type III repeat of tenascin.* J Biol Chem, 1994. **269**(43): p. 26691-6.
123. Yokoyama, K., et al., *Identification of amino acid sequences in fibrinogen gamma -chain and tenascin C C-terminal domains critical for binding to integrin alpha vbeta 3.* J Biol Chem, 2000. **275**(22): p. 16891-8.
124. Ramos, D.M., et al., *Stromal fibroblasts influence oral squamous-cell carcinoma cell interactions with tenascin-C.* Int J Cancer, 1997. **72**(2): p. 369-76.
125. Zisch, A.H., et al., *Neuronal cell adhesion molecule contactin/F11 binds to tenascin via its immunoglobulin-like domains.* J Cell Biol, 1992. **119**(1): p. 203-13.
126. Humphries, J.D., A. Byron, and M.J. Humphries, *Integrin ligands at a glance.* J Cell Sci, 2006. **119**(Pt 19): p. 3901-3.
127. Yoshida, T., T. Akatsuka, and K. Imanaka-Yoshida, *Tenascin-C and integrins in cancer.* Cell Adh Migr, 2015. **9**(1-2): p. 96-104.
128. Chung, C.Y., L. Zardi, and H.P. Erickson, *Binding of tenascin-C to soluble fibronectin and matrix fibrils.* J Biol Chem, 1995. **270**(48): p. 29012-7.
129. Midwood, K.S., et al., *Advances in tenascin-C biology.* Cell Mol Life Sci, 2011. **68**(19): p. 3175-99.
130. Crossin, K.L., et al., *Site-restricted expression of cytotactin during development of the chicken embryo.* J Cell Biol, 1986. **102**(5): p. 1917-30.

131. Tan, S.S., et al., *Asymmetric expression in somites of cytotactin and its proteoglycan ligand is correlated with neural crest cell distribution.* Proc Natl Acad Sci U S A, 1987. **84**(22): p. 7977-81.
132. Yuasa, S., *Bergmann glial development in the mouse cerebellum as revealed by tenascin expression.* Anat Embryol (Berl), 1996. **194**(3): p. 223-34.
133. Tucker, R.P. and R. Chiquet-Ehrismann, *The regulation of tenascin expression by tissue microenvironments.* Biochim Biophys Acta, 2009. **1793**(5): p. 888-92.
134. Inaguma, Y., et al., *Epithelial induction of stromal tenascin in the mouse mammary gland: from embryogenesis to carcinogenesis.* Dev Biol, 1988. **128**(2): p. 245-55.
135. Kalembey, I., et al., *Analysis of tenascin mRNA expression in the murine mammary gland from embryogenesis to carcinogenesis: an in situ hybridization study.* Int J Dev Biol, 1997. **41**(4): p. 569-73.
136. Midwood, K.S. and G. Orend, *The role of tenascin-C in tissue injury and tumorigenesis.* J Cell Commun Signal, 2009. **3**(3-4): p. 287-310.
137. Saga, Y., et al., *Mice develop normally without tenascin.* Genes Dev, 1992. **6**(10): p. 1821-31.
138. Forsberg, E., et al., *Skin wounds and severed nerves heal normally in mice lacking tenascin-C.* Proc Natl Acad Sci U S A, 1996. **93**(13): p. 6594-9.
139. Mackie, E.J. and R.P. Tucker, *The tenascin-C knockout revisited.* J Cell Sci, 1999. **112 (Pt 22)**: p. 3847-53.
140. Chiquet-Ehrismann, R. and M. Chiquet, *Tenascins: regulation and putative functions during pathological stress.* J Pathol, 2003. **200**(4): p. 488-99.
141. Hanamura, N., et al., *Expression of fibronectin and tenascin-C mRNA by myofibroblasts, vascular cells and epithelial cells in human colon adenomas and carcinomas.* Int J Cancer, 1997. **73**(1): p. 10-5.
142. Yoshida, T., et al., *Co-expression of tenascin and fibronectin in epithelial and stromal cells of benign lesions and ductal carcinomas in the human breast.* J Pathol, 1997. **182**(4): p. 421-8.
143. Kawakatsu, H., et al., *Human carcinoma cells synthesize and secrete tenascin in vitro.* Jpn J Cancer Res, 1992. **83**(10): p. 1073-80.
144. Hancox, R.A., et al., *Tumour-associated tenascin-C isoforms promote breast cancer cell invasion and growth by matrix metalloproteinase-dependent and independent mechanisms.* Breast Cancer Res, 2009. **11**(2): p. R24.
145. Dandachi, N., et al., *Co-expression of tenascin-C and vimentin in human breast cancer cells indicates phenotypic transdifferentiation during tumour progression: correlation with histopathological parameters, hormone receptors, and oncoproteins.* J Pathol, 2001. **193**(2): p. 181-9.
146. Herlyn, M., et al., *Characterization of tenascin secreted by human melanoma cells.* Cancer Res, 1991. **51**(18): p. 4853-8.
147. Goepel, C., et al., *Tenascin-A marker for the malignant potential of preinvasive breast cancers.* Gynecol Oncol, 2000. **79**(3): p. 372-8.
148. Jahkola, T., et al., *Expression of tenascin-C in intraductal carcinoma of human breast: relationship to invasion.* Eur J Cancer, 1998. **34**(11): p. 1687-92.

149. Ishihara, A., et al., *Tenascin expression in cancer cells and stroma of human breast cancer and its prognostic significance.* Clin Cancer Res, 1995. **1**(9): p. 1035-41.
150. Suwiwat, S., et al., *Expression of extracellular matrix components versican, chondroitin sulfate, tenascin, and hyaluronan, and their association with disease outcome in node-negative breast cancer.* Clin Cancer Res, 2004. **10**(7): p. 2491-8.
151. Ioachim, E., et al., *Immunohistochemical expression of extracellular matrix components tenascin, fibronectin, collagen type IV and laminin in breast cancer: their prognostic value and role in tumour invasion and progression.* Eur J Cancer, 2002. **38**(18): p. 2362-70.
152. Parekh, K., et al., *Tenascin-C, over expressed in lung cancer down regulates effector functions of tumor infiltrating lymphocytes.* Lung Cancer, 2005. **47**(1): p. 17-29.
153. Wang, Z., et al., *Expression of angiopoietin-like 4 and tenascin C but not cathepsin C mRNA predicts prognosis of oral tongue squamous cell carcinoma.* Biomarkers, 2010. **15**(1): p. 39-46.
154. Juhasz, A., et al., *Characteristic distribution patterns of tenascin in laryngeal and hypopharyngeal cancers.* Laryngoscope, 2000. **110**(1): p. 84-92.
155. Natali, P.G., et al., *Expression and production of tenascin in benign and malignant lesions of melanocyte lineage.* Int J Cancer, 1990. **46**(4): p. 586-90.
156. Tuominen, H. and M. Kallioinen, *Increased tenascin expression in melanocytic tumors.* J Cutan Pathol, 1994. **21**(5): p. 424-9.
157. Sis, B., et al., *Prognostic significance of matrix metalloproteinase-2, cathepsin D, and tenascin-C expression in colorectal carcinoma.* Pathol Res Pract, 2004. **200**(5): p. 379-87.
158. Grahovac, J., D. Becker, and A. Wells, *Melanoma cell invasiveness is promoted at least in part by the epidermal growth factor-like repeats of tenascin-C.* J Invest Dermatol, 2013. **133**(1): p. 210-20.
159. Tavazoie, S.F., et al., *Endogenous human microRNAs that suppress breast cancer metastasis.* Nature, 2008. **451**(7175): p. 147-52.
160. Van Obberghen-Schilling, E., et al., *Fibronectin and tenascin-C: accomplices in vascular morphogenesis during development and tumor growth.* Int J Dev Biol, 2011. **55**(4-5): p. 511-25.
161. Tanaka, K., et al., *Tenascin-C regulates angiogenesis in tumor through the regulation of vascular endothelial growth factor expression.* Int J Cancer, 2004. **108**(1): p. 31-40.
162. Saupe, F., et al., *Tenascin-C Downregulates Wnt Inhibitor Dickkopf-1, Promoting Tumorigenesis in a Neuroendocrine Tumor Model.* Cell Rep, 2013.
163. Talts, J.F., et al., *Tenascin-C modulates tumor stroma and monocyte/macrophage recruitment but not tumor growth or metastasis in a mouse strain with spontaneous mammary cancer.* J Cell Sci, 1999. **112 (Pt 12)**: p. 1855-64.
164. O'Connell, J.T., et al., *VEGF-A and Tenascin-C produced by S100A4+ stromal cells are important for metastatic colonization.* Proc Natl Acad Sci U S A, 2011. **108**(38): p. 16002-7.
165. McGill, M.A. and C.J. McGlade, *Mammalian numb proteins promote Notch1 receptor ubiquitination and degradation of the Notch1 intracellular domain.* J Biol Chem, 2003. **278**(25): p. 23196-203.

166. Okano, H., T. Imai, and M. Okabe, *Musashi: a translational regulator of cell fate.* J Cell Sci, 2002. **115**(Pt 7): p. 1355-9.
167. Nakamura, M., et al., *Musashi, a neural RNA-binding protein required for Drosophila adult external sensory organ development.* Neuron, 1994. **13**(1): p. 67-81.
168. Potten, C.S., et al., *Identification of a putative intestinal stem cell and early lineage marker; musashi-1.* Differentiation, 2003. **71**(1): p. 28-41.
169. Clarke, R.B., et al., *A putative human breast stem cell population is enriched for steroid receptor-positive cells.* Dev Biol, 2005. **277**(2): p. 443-56.
170. Fox, R.G., et al., *Image-based detection and targeting of therapy resistance in pancreatic adenocarcinoma.* Nature, 2016. **534**(7607): p. 407-11.
171. Gao, C., et al., *Downregulation of Msi1 suppresses the growth of human colon cancer by targeting p21cip1.* Int J Oncol, 2015. **46**(2): p. 732-40.
172. Liu, X., W.T. Yang, and P.S. Zheng, *Msi1 promotes tumor growth and cell proliferation by targeting cell cycle checkpoint proteins p21, p27 and p53 in cervical carcinomas.* Oncotarget, 2014. **5**(21): p. 10870-85.
173. Imai, T., et al., *The neural RNA-binding protein Musashi1 translationally regulates mammalian numb gene expression by interacting with its mRNA.* Mol Cell Biol, 2001. **21**(12): p. 3888-900.
174. Abo, A. and H. Clevers, *Modulating WNT receptor turnover for tissue repair.* Nat Biotechnol, 2012. **30**(9): p. 835-6.
175. Barker, N., et al., *Identification of stem cells in small intestine and colon by marker gene Lgr5.* Nature, 2007. **449**(7165): p. 1003-7.
176. Korinek, V., et al., *Depletion of epithelial stem-cell compartments in the small intestine of mice lacking Tcf-4.* Nat Genet, 1998. **19**(4): p. 379-83.
177. de Lau, W.B., B. Snel, and H.C. Clevers, *The R-spondin protein family.* Genome Biol, 2012. **13**(3): p. 242.
178. de Lau, W., et al., *Lgr5 homologues associate with Wnt receptors and mediate R-spondin signalling.* Nature, 2011. **476**(7360): p. 293-7.
179. de Lau, W., et al., *The R-spondin/Lgr5/Rnf43 module: regulator of Wnt signal strength.* Genes Dev, 2014. **28**(4): p. 305-16.
180. Barker, N., et al., *Very long-term self-renewal of small intestine, colon, and hair follicles from cycling Lgr5+ve stem cells.* Cold Spring Harb Symp Quant Biol, 2008. **73**: p. 351-6.
181. Barker, N., et al., *Lgr5(+ve) stem cells drive self-renewal in the stomach and build long-lived gastric units in vitro.* Cell Stem Cell, 2010. **6**(1): p. 25-36.
182. Jaks, V., et al., *Lgr5 marks cycling, yet long-lived, hair follicle stem cells.* Nat Genet, 2008. **40**(11): p. 1291-9.
183. Barker, N., S. Tan, and H. Clevers, *Lgr proteins in epithelial stem cell biology.* Development, 2013. **140**(12): p. 2484-94.
184. Plaks, V., et al., *Lgr5-expressing cells are sufficient and necessary for postnatal mammary gland organogenesis.* Cell Rep, 2013. **3**(1): p. 70-8.
185. Visvader, J.E. and J. Stingl, *Mammary stem cells and the differentiation hierarchy: current status and perspectives.* Genes Dev, 2014. **28**(11): p. 1143-58.
186. Hirsch, D., et al., *LGR5 positivity defines stem-like cells in colorectal cancer.* Carcinogenesis, 2014. **35**(4): p. 849-58.

187. Baker, A.M., et al., *Characterization of LGR5 stem cells in colorectal adenomas and carcinomas.* Sci Rep, 2015. **5**: p. 8654.
188. Yang, L., et al., *LGR5 Promotes Breast Cancer Progression and Maintains Stem-Like Cells Through Activation of Wnt/beta-Catenin Signaling.* Stem Cells, 2015. **33**(10): p. 2913-24.
189. Hynes, R.O., *Integrins: bidirectional, allosteric signaling machines.* Cell, 2002. **110**(6): p. 673-87.
190. Harburger, D.S. and D.A. Calderwood, *Integrin signalling at a glance.* J Cell Sci, 2009. **122**(Pt 2): p. 159-63.
191. Giancotti, F.G. and G. Tarone, *Positional control of cell fate through joint integrin/receptor protein kinase signaling.* Annu Rev Cell Dev Biol, 2003. **19**: p. 173-206.
192. Ginsberg, M.H., X. Du, and E.F. Plow, *Inside-out integrin signalling.* Curr Opin Cell Biol, 1992. **4**(5): p. 766-71.
193. Ponomarev, V., et al., *A novel triple-modality reporter gene for whole-body fluorescent, bioluminescent, and nuclear noninvasive imaging.* Eur J Nucl Med Mol Imaging, 2004. **31**(5): p. 740-51.
194. Gyorffy, B., et al., *An online survival analysis tool to rapidly assess the effect of 22,277 genes on breast cancer prognosis using microarray data of 1,809 patients.* Breast Cancer Res Treat, 2010. **123**(3): p. 725-31.
195. Curtis, C., et al., *The genomic and transcriptomic architecture of 2,000 breast tumours reveals novel subgroups.* Nature, 2012. **486**(7403): p. 346-52.
196. Cailleau, R., et al., *Breast tumor cell lines from pleural effusions.* J Natl Cancer Inst, 1974. **53**(3): p. 661-74.
197. Chavez, K.J., S.V. Garimella, and S. Lipkowitz, *Triple negative breast cancer cell lines: one tool in the search for better treatment of triple negative breast cancer.* Breast Dis, 2010. **32**(1-2): p. 35-48.
198. Kang, Y., et al., *A multigenic program mediating breast cancer metastasis to bone.* Cancer Cell, 2003. **3**(6): p. 537-49.
199. Ignatoski, K.M. and S.P. Ethier, *Constitutive activation of pp125fak in newly isolated human breast cancer cell lines.* Breast Cancer Res Treat, 1999. **54**(2): p. 173-82.
200. Desgrosellier, J.S., et al., *An integrin alpha(v)beta(3)-c-Src oncogenic unit promotes anchorage-independence and tumor progression.* Nat Med, 2009. **15**(10): p. 1163-9.
201. Dontu, G., et al., *In vitro propagation and transcriptional profiling of human mammary stem/progenitor cells.* Genes Dev, 2003. **17**(10): p. 1253-70.
202. Tiede, B. and Y. Kang, *From milk to malignancy: the role of mammary stem cells in development, pregnancy and breast cancer.* Cell Res, 2011. **21**(2): p. 245-57.
203. Vaillant, F., et al., *The emerging picture of the mouse mammary stem cell.* Stem Cell Rev, 2007. **3**(2): p. 114-23.
204. Soady, K.J., et al., *Mouse mammary stem cells express prognostic markers for triple-negative breast cancer.* Breast Cancer Res, 2015. **17**: p. 31.
205. Parvani, J.G., et al., *Targeted inactivation of beta1 integrin induces beta3 integrin switching, which drives breast cancer metastasis by TGF-beta.* Mol Biol Cell, 2013. **24**(21): p. 3449-59.
206. Ito, M., et al., *NOD/SCID/gamma(c)(null) mouse: an excellent recipient mouse model for engraftment of human cells.* Blood, 2002. **100**(9): p. 3175-82.

207. Huck, L., et al., *beta1-integrin is dispensable for the induction of ErbB2 mammary tumors but plays a critical role in the metastatic phase of tumor progression.* Proc Natl Acad Sci U S A, 2010. **107**(35): p. 15559-64.
208. Ramirez, N.E., et al., *The alpha(2)beta(1) integrin is a metastasis suppressor in mouse models and human cancer.* J Clin Invest, 2011. **121**(1): p. 226-37.
209. Sloan, E.K., et al., *Tumor-specific expression of alphavbeta3 integrin promotes spontaneous metastasis of breast cancer to bone.* Breast Cancer Res, 2006. **8**(2): p. R20.
210. Mali, P., et al., *RNA-guided human genome engineering via Cas9.* Science, 2013. **339**(6121): p. 823-6.
211. Ringner, M., et al., *GOBO: gene expression-based outcome for breast cancer online.* PLoS One, 2011. **6**(3): p. e17911.
212. Rolle, K., et al., *Promising human brain tumors therapy with interference RNA intervention (iRNAi).* Cancer Biol Ther, 2010. **9**(5): p. 396-406.
213. Sawada, Y., et al., *Tenascin-C synthesized in both donor grafts and recipients accelerates artery graft stenosis.* Cardiovasc Res, 2007. **74**(3): p. 366-76.
214. Spenle, C., et al., *Tenascin-C: Exploitation and collateral damage in cancer management.* Cell Adh Migr, 2015. **9**(1-2): p. 141-53.
215. Catania, C., et al., *The tumor-targeting immunocytokine F16-IL2 in combination with doxorubicin: dose escalation in patients with advanced solid tumors and expansion into patients with metastatic breast cancer.* Cell Adh Migr, 2015. **9**(1-2): p. 14-21.
216. Goodman, S.L. and M. Picard, *Integrins as therapeutic targets.* Trends Pharmacol Sci, 2012. **33**(7): p. 405-12.
217. Gilbert, M.R., et al., *Cilengitide in patients with recurrent glioblastoma: the results of NABTC 03-02, a phase II trial with measures of treatment delivery.* J Neurooncol, 2012. **106**(1): p. 147-53.
218. Kimura, H., et al., *Imaging the inhibition by anti-beta1 integrin antibody of lung seeding of single osteosarcoma cells in live mice.* Int J Cancer, 2012. **131**(9): p. 2027-33.
219. Ko, H.Y., et al., *A multimodal nanoparticle-based cancer imaging probe simultaneously targeting nucleolin, integrin alphavbeta3 and tenascin-C proteins.* Biomaterials, 2011. **32**(4): p. 1130-8.
220. Ponti, D., et al., *Isolation and in vitro propagation of tumorigenic breast cancer cells with stem/progenitor cell properties.* Cancer Res, 2005. **65**(13): p. 5506-11.
221. Dontu, G., et al., *Role of Notch signaling in cell-fate determination of human mammary stem/progenitor cells.* Breast Cancer Res, 2004. **6**(6): p. R605-15.
222. Harrison, H., et al., *Regulation of breast cancer stem cell activity by signaling through the Notch4 receptor.* Cancer Res, 2010. **70**(2): p. 709-18.
223. Korkaya, H., et al., *Regulation of mammary stem/progenitor cells by PTEN/Akt/beta-catenin signaling.* PLoS Biol, 2009. **7**(6): p. e1000121.
224. Many, A.M. and A.M. Brown, *Both canonical and non-canonical Wnt signaling independently promote stem cell growth in mammospheres.* PLoS One, 2014. **9**(7): p. e101800.
225. Kreso, A. and J.E. Dick, *Evolution of the cancer stem cell model.* Cell Stem Cell, 2014. **14**(3): p. 275-91.

226. Lo, P.K., et al., *CD49f and CD61 identify Her2/neu-induced mammary tumor-initiating cells that are potentially derived from luminal progenitors and maintained by the integrin-TGFbeta signaling.* Oncogene, 2012. **31**(21): p. 2614-26.
227. Vaillant, F., et al., *The mammary progenitor marker CD61/beta3 integrin identifies cancer stem cells in mouse models of mammary tumorigenesis.* Cancer Res, 2008. **68**(19): p. 7711-7.
228. Goel, H.L., et al., *GLI1 regulates a novel neuropilin-2/alpha6beta1 integrin based autocrine pathway that contributes to breast cancer initiation.* EMBO Mol Med, 2013. **5**(4): p. 488-508.
229. White, D.E., et al., *Targeted disruption of beta1-integrin in a transgenic mouse model of human breast cancer reveals an essential role in mammary tumor induction.* Cancer Cell, 2004. **6**(2): p. 159-70.
230. Shackleton, M., et al., *Generation of a functional mammary gland from a single stem cell.* Nature, 2006. **439**(7072): p. 84-8.
231. Stingl, J., et al., *Purification and unique properties of mammary epithelial stem cells.* Nature, 2006. **439**(7079): p. 993-7.
232. Asselin-Labat, M.L., et al., *Gata-3 is an essential regulator of mammary-gland morphogenesis and luminal-cell differentiation.* Nat Cell Biol, 2007. **9**(2): p. 201-9.
233. Zeng, Y.A. and R. Nusse, *Wnt proteins are self-renewal factors for mammary stem cells and promote their long-term expansion in culture.* Cell Stem Cell, 2010. **6**(6): p. 568-77.
234. Desgrosellier, J.S., et al., *Integrin alphavbeta3 drives slug activation and stemness in the pregnant and neoplastic mammary gland.* Dev Cell, 2014. **30**(3): p. 295-308.
235. Taddei, I., et al., *Beta1 integrin deletion from the basal compartment of the mammary epithelium affects stem cells.* Nat Cell Biol, 2008. **10**(6): p. 716-22.
236. Lambe, M., et al., *Transient increase in the risk of breast cancer after giving birth.* N Engl J Med, 1994. **331**(1): p. 5-9.

Contributions

This work would not have been possible without the contribution of several persons:

The TMA was provided by **Prof. Dr. Med. Peter Sinn** from the Pathology Department of the University Hospital of Heidelberg.

The pleural effusion sample was provided by **Prof. Dr. Med. Marc Sütterlin** and **Dr. Med. Saskia Speck** from the University Hospital of Mannheim.

Dr. Arnaud Descot generated the mire backbone vectors and the TNC knockdown sublines.

Dr. Sabrina Hanke performed SRM analysis.

Jasmin Meier assisted in several *in vivo* and *in vitro* experiments.

Miriam Butler assisted in several *in vitro* experiments

The FACS sorts were performed by **Tobias Rubner** and **Claudia Felbinger** at the DKFZ Flow Cytometry core facility.

Thordur Oskarsson, **Arnaud Descot**, **Kristin Decker**, **Tsunaki Hongu** and **Elisa Noll** critically proofread this manuscript.

Acknowledgements

During the last years, I have had the chance to be trained in an excellent scientific environment. As a PhD student, I strongly appreciated the seminars and courses opportunities at the DKFZ. Within this cosmos, **Andreas Trumpp** created a very special microenvironment at HI-STEM, allowing young, international scientists to pursue their research interests in a modern infrastructure and with state-of-the-art techniques. Dear Andreas, I would like to thank you for creating such a scientific environment and for promoting social contacts within HI-STEM. I am very grateful for your scientific input during our department meetings and my TAC meetings.

I would like to thank **Thordur Oskarsson** for hiring me as his first PhD student and trusting me from the very first day. Dear Thordur, thank for keeping your door always open, for your opened mind and for our endless discussions. The last 4 ½ years taught me a lot about cancer, metastasis, matricellular proteins… but I also learned a great deal about myself! Thank you for your scientific training and for supporting me in all situations.

I would like to express my gratitude to **Jonathan Sleeman** for his excellent scientific input during my TAC meetings and for being my second referee. Schedules are often very tight - thank you for making it work though!

I would like to thank **Karin Müller-Decker** and **Jochen Wittbrodt** for being part of my PhD defense committee.

There are rumors saying that as a scientist one may spend more time with his/her colleagues than with his/her family. This was sometimes true and therefore this work wouldn't have been possible without the rest of the *Oskarssons*! Thank you for all your input, your help and your humor: **Arnaud, Etienne, Jacob, Jasmin, Kristin, Lena, Maren, Miriam, Sabrina and Tsunaki**.
I would like to thank **Tsunaki** for his positive mind set and for reviewing parts of this work. Thank you **Maren** for our collaboration effort on a very big dataset! I really appreciated to work with you. I would like to especially thank **Jacob** for great moments in the lab. A very big 'thank you' goes to **Miriam**, who actively contributed to this work and supported me as a master student in a very special period of my life. As a short-time guest in our lab, I would like to thank **Sabrina** for being the best collaboration partner I could have imagined, for supporting me the best she could and for helping me to get more familiar with the magical world of mass spectrometry. A very special 'thank you' goes to **Jasmin** for her technical and mental support. Most importantly, I would like to express my deepest gratitude to Kristin and Arnaud for

reviewing this manuscript and for sharing more than a desk with me in the last years! **Kristin**, you became a real friend to me, keep your positive energy and I am sure you will stay as great as you are! Thank you for your support and your kindness. **Arnaud**, we went through a lot together and I consider you a real friend – Merci pour ton aide sans limite, ton calme, ta patience et tes conseils avisés.

I would like to thank the group of the Metics, especially **Martin Sprick** for his input in our joined seminar, for sharing his knowledge in our journal club and for his support in the establishment of biochemical methods. A special 'thank you' goes to **Elisa Espinet**, **Corinna Klein** and **Massimo Saini** for help and discussion. I would also like to thank **Elisa Noll** for reviewing this manuscript and for helpful discussions.

Unfortunately I cannot name you all… Thank you to the whole A010 department for such a friendly atmosphere! A special 'thank you' goes to **Wiebke Nadler** for her eternal mental support and for reviewing this manuscript. Thank you to **Hind Medyouf** for strengthening the French community! I would also like to thank **Erika**, **Dagmar** and **Marina** for their organizational talents and for keeping our place running in any situations!

I would like to thank the Helmholtz International Graduate School for funding me during the first 3 years of my work and for supporting me during my entire PhD. A special 'thanks' goes to **Lindsay** for her advices.

The DKFZ wouldn't be such a great working place without its core facilities. I would like to particularly thank **Damian Krunic**, **Manuela Brom**, **Ann Atzberger**, **Claudia Fellbinger and Tobias Rubner** for technical support.

When I arrived in Heidelberg 10 years ago, I couldn't have imaged finding such great friends here. I would like to thank **Kendra**, **Annika**, **Maja**, **Kathrin**, **Vera** and **Johanna** for having been my first family in Germany and for sharing so much with me during the last years! A very special 'thank you' goes to our friend (and best babysitter ever!), **Dave**!

I wouldn't have made it to this point without an incredible family!
Maman, Papa et **Charlotte**, je ne peux vous dire à quel point votre amour et votre soutien m'ont aidée au quotidien ces dernières années. Merci de toujours croire en moi, même quand je n'y crois plus.
Alexandra, Andreas, ich könnte mir keine besseren Schwiegereltern wünschen, danke für Eure unermüdliche Unterstützung während all den Jahren…

Acknowledgements

A huge kiss goes to the tiniest of all my loves. **Johann**, si tu lis ceci un jour, sache que ton rire et ta frimousse m'ont portée de jour en jour depuis ta naissance et font de moi chaque jour une personne meilleure.

The biggest thank goes to the most incredible person I've ever met. Mein **Tomula**, ich kann in Worten nicht fassen was Du für mich in den letzten Jahren getan hast. Danke für Deine unendliche Geduld und Deine tägliche Unterstützung. Ich wünschte, ich könnte Dir einen Bruchteil davon zurück schenken. Danke dafür, dass ich bei Dir immer ich selbst sein kann, egal ob mit Tränen oder mit Lachen. Deine Liebe lässt mich täglich wachsen...